

University of Louisville

ThinkIR: The University of Louisville's Institutional Repository


Electronic Theses and Dissertations

8-2016

The role of O-GlcNAcase during heart failure.

Sujith Dassanayaka

Follow this and additional works at: <https://ir.library.louisville.edu/etd>

 Part of the [Circulatory and Respiratory Physiology Commons](#), [Medical Physiology Commons](#), and the [Systems and Integrative Physiology Commons](#)

Recommended Citation

Dassanayaka, Sujith, "The role of O-GlcNAcase during heart failure." (2016). *Electronic Theses and Dissertations*. Paper 2493.
<https://doi.org/10.18297/etd/2493>

This Doctoral Dissertation is brought to you for free and open access by ThinkIR: The University of Louisville's Institutional Repository. It has been accepted for inclusion in Electronic Theses and Dissertations by an authorized administrator of ThinkIR: The University of Louisville's Institutional Repository. This title appears here courtesy of the author, who has retained all other copyrights. For more information, please contact thinkir@louisville.edu.

THE ROLE OF O-GLCNACASE DURING HEART FAILURE

By

Sujith Dassanayaka

B.A., Transylvania University, 2006

M.S., University of Louisville, 2010

A Dissertation Submitted to the Faculty of the School of Medicine of the
University of Louisville in Partial Fulfillment of the Requirements for the Degree of

Doctor of Philosophy in Physiology and Biophysics

Department of Physiology

University of Louisville

Louisville, Kentucky

August, 2016

THE ROLE OF O-GLCNACASE DURING HEART FAILURE

By

Sujith Dassanayaka

B.A., Transylvania University, 2006

M.S., University of Louisville, 2010

A Dissertation Approved on

July 28, 2016

By the Following Dissertation Committee

Dissertation Advisor: Steven P. Jones, Ph.D.

Irving G. Joshua, Ph.D.

Dale A. Schuschke, Ph.D.

Claudio Maldonado, Ph.D.

Bradford G. Hill, Ph.D.

DEDICATION

This dissertation is dedicated to my loving mother, father, and uncle Ranjith. They instilled in me the importance of an education, an intense work ethic, and an unwavering attitude necessary to persevere against any obstacle. I am eternally grateful for their love, support, guidance, and belief in me.

ACKNOWLEDGEMENTS

The pursuit of this doctorate degree has been an arduous but fruitful journey that would have been next to impossible without the support, guidance, and mentorship of many individuals. I would like to briefly acknowledge the many important people that helped shape the physiologist/scientist I've become today. First and foremost I would like to acknowledge my mentor Dr. Steven P. Jones. His unique training regimen afforded me various opportunities for educational, technical, and professional development that I would not have received in any other environment. I am very grateful for his mentorship. Next I would like to highlight the importance of my co-mentors Drs. Joshua, Wead, Schushke, Maldonado and Hill. In addition to providing me a great educational experience, Drs. Joshua, Wead, Schushke, Hill, and Maldonado provided security, support, and encouragement throughout my time as a student.

I am grateful to my lab mates for making this journey enriching as well as enjoyable. The many past and present members of the lab greatly contributed to my development in addition to serving as a surrogate family. Drs Brainard and Readnower were instrumental in training me when I first joined the lab. Dr. Brainard taught me in vivo surgical models of heart failure; coronary artery ligation and transaortic constriction. Dr. Readnower introduced me to

mitochondrial function and adult cardiomyocyte isolations. Their training prepared me for the experiments that my Ph.D. training would entail. Drs. Zafir and Muthusamy provided invaluable training in molecular and cellular techniques as well as guidance in daily experiments. Ken Brittian's expertise in echocardiography was vital to my thesis and made understanding cardiac function all the more accessible to me. Ms. Bethany Long was instrumental in her efforts to train me in molecular techniques, breeding, and maintaining our colonies. I am thankful to Angelica DeMartino for her help with surgical models of heart failure that were essential to this work. Ms. Linda Harrison, our lab manager, made our days easier by taking care of the managerial duties and help to make a smoothly functioning lab. Finally, Deanna Husted and Monica Sivori's upbeat attitude and pleasant demeanor always helped make the workday brighter.

I am grateful to the several collaborators that I have been able to work with during my time as a student. Drs. Hill, Hong, and Wysoczynski were all invaluable mentors that enriched my training experience. I am also grateful to Drs. Cummins, Salabei, Sansbury, and Mehra who were available to provide advice and share their expertise when needed. I am grateful to Dr. James McCracken and Timothy Hoffman for their expertise in flow cytometry. I am thankful to Don Mosely for his eagerness to help with animal husbandry. I am also grateful to the resource research center and their support staff especially Eric Calle and Mandy Ryan.

I will be eternally grateful to the Department of Physiology. My success as a student is in part attributed to the department and the caring and friendly environment they provided me. I am especially grateful for the wonderful support I've received from Mrs. Denise Hughes, Mrs. Carol Noll, Mrs. Gisel Durry-Murphy, and Mrs. Jennifer Wells.

Finally, I would like to thank my family and friends that have been supportive during this period of my development.

ABSTRACT

THE ROLE OF O-GLCNACASE DURING HEART FAILURE

Sujith Dassanayaka

July 28, 2016

Global augmentation of protein O-GlcNAcylation occurs in response to a myriad of stressors and confers a survival advantage at the cellular level. This protective phenomenon has been demonstrated to mediate cardioprotection through various *in vitro* and *in vivo* studies during ischemia-reperfusion, myocardial infarction, and oxidative stress; however, relatively little is known of the regulation of protein O-GlcNAcylation. Protein O-GlcNAcylation is regulated by two antagonistic enzymes, namely, O-GlcNAc transferase (OGT) and O-GlcNAcase (OGA). Ablation of cardiomyocyte OGT, the enzyme that catalyzes the addition of O-GlcNAc to proteins, exacerbates cardiac dysfunction during infarct-induced heart failure (HF). However, little is known of the enzyme

mediating the removal of the O-GlcNAc modification, OGA, in the context of HF. The present study focused on this limitation in the field.

We characterized the temporal expression of OGA following myocardial infarction (MI) and found that OGA expression is decreased and remains suppressed for 4 wk post MI. Conversely, OGT expression is augmented early, but normalizes by 4 wk post MI. Despite the normalization of OGT expression, O-GlcNAcylation remains elevated, which may be due to chronic OGA suppression. Furthermore, we observed upregulation of miRNA-539 in HF. *In vitro* studies confirmed induction of miRNA-539 negatively regulated OGA expression. These data indicate that suppression of OGA could be mediated by miRNA-539.

Next, we developed a genetic model of cardiomyocyte specific OGA ablation to test whether ablation of OGA would augment O-GlcNAcylation and attenuate HF. Our model successfully suppressed OGA expression, augmented cardiac protein O-GlcNAcylation, and did not induce cardiac dysfunction; however, genetic ablation of OGA prior to coronary ligation hastened cardiac dysfunction within 1 wk compared to wild-type mice. Hearts from OGA KO mice were more dilated and less efficient, which suggests rejection of our hypothesis. These data indicate that OGA expression may be proadaptive during HF.

Because O-GlcNAcylation of mitochondrial complexes has been implicated to depress mitochondrial respiration we hypothesized that augmented O-GlcNAcylation may mediate mitochondrial dysfunction and may help explain the exacerbation in cardiac dysfunction we observed after 1 wk of HF. We virally augmented either OGT or OGA in cardiomyocytes to alter overall protein O-

GlcNAcylation. Neither overexpression of OGA nor OGT mediated mitochondrial dysfunction. Though induction of O-GlcNAcylation through hyperglycemia did suppress mitochondrial reserve capacity. This depression in mitochondrial function was recapitulated with an osmotic control. We concluded that modulation of O-GlcNAc alone did not cause mitochondrial dysfunction.

These data indicate that suppression of OGA occurs during HF and may be mediated by posttranscriptional regulation by miR-539. In addition, ablation of OGA expression can hasten HF. Furthermore, the exacerbation in cardiac dysfunction is not likely due to O-GlcNAc-mediated mitochondrial dysfunction. These data indicate that chronic augmentation of O-GlcNAcylation may be detrimental in HF. More specifically they indicate that dynamic cycling of O-GlcNAcylation may be more beneficial in HF than permanently driving O-GlcNAc levels in one direction.

TABLE OF CONTENTS

	PAGE
DEDICATION	iii
ACKNOWLEDGEMENTS	iv
ABSTRACT	vii
LIST OF TABLES	xi
LIST OF FIGURES	xii
CHAPTER I BACKGROUND AND LITERATURE REVIEW	1
CHAPTER II HYPOTHESIS AND SPECIFIC AIMS	24
CHAPTER III MATERIALS AND METHODS	26
CHAPTER IV RESULTS	43
CHAPTER V DISCUSSION	85
CHAPTER VI SUMMARY AND FUTURE DIRECTIONS	99
REFERENCES	105
CURRICULUM VITAE	118

LIST OF TABLES

	PAGE
Table 1. Genotyping primer sequences	39
Table 2. miRNA expression in the failing heart	51

LIST OF FIGURES

	PAGE
Figure 1. Hexosamine Biosynthetic Pathway	7
Figure 2. Protein O-GlcNAcylation is augmented in human HF	45
Figure 3. Myocardial infarction induces cardiac dysfunction	46
Figure 4. OGA expression is suppressed at 5 d and 28 d post MI	47
Figure 5. miRNA-539 is upregulated in the failing heart	50
Figure 6. miRNA-539 regulates OGA expression	53
Figure 7. Inhibition of miR-539 rescues OGA expression	55
Figure 8. Negative regulatory effect of miR-539 in human cells	57
Figure 9. Hypoxia-reoxygenation induces miR-539 expression	59
Figure 10. Inducible OGA knockout breeding strategy	61
Figure 11. MerCreMer transgenic mice do not exhibit cardiac dysfunction	62
Figure 12. OGA ablation depresses OGA expression in the heart	64
Figure 13. Cardiac OGA ablation does not alter cardiac function	65
Figure 14. Cardiac geometry is altered in OGA knockout hearts	67
Figure 15. OGA deletion hastens cardiac dysfunction 1 wk post MI	68
Figure 16. OGA deletion does not alter cardiac function 4 wk post MI	69
Figure 17. Ablation of OGA does not affect infarct size	70
Figure 18. Extracellular flux allows measurement of mitochondrial function	72

Figure 19.	OGT or OGA does not affect bioenergetic reserve	73
Figure 20.	Inhibition of OGA negligibly affects mitochondrial function	75
Figure 21.	Inhibition of OGA increases State 3 respiration	77
Figure 22.	High glucose depresses cardiomyocyte bioenergetic reserve	79
Figure 23.	High glucose depresses State 3 and 4 _o respiration	82
Figure 24.	OGA does not rescue suppression of bioenergetic reserve	84
Figure 25.	Aim 1 summary	87
Figure 26.	Aim 2 summary	90
Figure 27.	Aim 3 Summary	93
Figure 28.	Summary Figure	104

CHAPTER I

BACKGROUND AND LITERATURE

REVIEW

In every year since the turn of the twentieth century, except 1918, cardiovascular disease (CVD) has claimed more lives than any other major cause of death in the United States¹. Roughly 2,200 Americans die of CVD each day, which accumulates to 803,000 CVD-related deaths a year¹. More than one-third of all global deaths in 2013 were attributed to CVD¹. CVD is also the leading cause of death worldwide accounting for 17.3 million deaths per year in 2013¹. CVD is essentially a worldwide pandemic.

CVD encompasses a variety of diseases including, but not limited to, diseases of arteries, high blood pressure, HF (HF), stroke, and coronary heart

disease. Within these subsections of CVD, coronary heart disease accounts for 46% of all CVD-related deaths in the United States¹. Impediments to coronary artery flow can lead to myocardial infarction, which is the primary antecedent for HF. Following an infarction, the significant loss of cardiomyocytes is replaced with akinetic scar tissue, rather than contracting cardiomyocytes. Such 'wound healing' satisfies the short-term goal of retaining ventricular integrity; however, the chronic implications include progressive fibrosis, stiffness, and dilation of the ventricle. The central element of HF is the heart's inability to pump sufficient blood to meet the metabolic demands of the body.

Although improvements in acute management of HF have improved outcomes, efforts to halt the inexorable deterioration of cardiac function are largely futile. The current clinical approach focuses on disease management rather than curing HF – because there is presently no cure. Primary treatment consists of angiotensin-converting enzyme inhibitors, beta-blockers, and mineralocorticoids antagonists. And, although a new class of agents (i.e. neprilysin inhibitor) has shown promise in a Phase 3 clinical trial, collectively, these drugs only delay the progression of HF. Given the general stagnation in the progress of clinical treatment of HF, the need to further elucidate the pathobiology of HF is self-evident.

Heart failure and metabolism

In the healthy heart, 95% of cardiac ATP is derived from oxidative phosphorylation in the mitochondria². The remaining 5% of ATP is derived from glycolysis and the citric acid cycle². From the pool of cardiac ATP, 60-70% is designated as fuel for contraction². The rest is designated to the functioning of various ion pumps, including the Ca²⁺-ATPase in the sarcoplasmic reticulum². The cardiac energy pool consists of ATP (5 μmol/g wet weight) and phosphocreatine (PCr; 8 μmol/g wet weight)². PCr serves as an ATP transporter because the high energy bond in ATP can be transferred to creatine by mitochondrial creatine kinase to form PCr. This small transport molecule can readily diffuse through the mitochondrial membrane into the cytosol and can be used to generate ATP from ADP. The continuous mechanical work generated by the heart requires a high rate of ATP hydrolysis (0.5 μmol/g wet weight per second)². As a result, the ATP pool in the heart can be exhausted within seconds. Thus, any alteration in cardiac ATP production can dramatically affect the contractile function of the heart.

Despite the progression of HF, the metabolic demands of the heart are not reduced. The heart still requires high rates of ATP turnover necessary for contraction; however, these ATP demands become largely unmet following myocardial infarction and cardiac metabolism is impaired in patients with dilated cardiomyopathy³. Myocardial phosphocreatine-to-ATP (PCr:ATP) ratios were measured noninvasively with ³¹P-MR spectroscopy and demonstrated that HF patients had lower PCr:ATP ratios than normal healthy patients³. In addition,

decreased PCr:ATP ratios were associated with increased mortality and lower ejection fractions in patients with dilated cardiomyopathy³. Essentially, cardiac metabolic remodeling may play a key role in the pathophysiology of HF.

In HF cardiac metabolism becomes altered and substrate utilization changes. Normally the adult heart relies on fatty acid oxidation (FAO) for generation of 70-90% of cardiac ATP pool². The remaining 10-30% of ATP is derived primarily from glycolysis and lactate. Small amounts of ketone bodies and amino acids also contribute to ATP production. Substrate utilization changes in HF^{2, 4-6}. Studies on HF have reported reduction in expression of FA transporters in the presence of systolic cardiac dysfunction⁷. Similarly, FA oxidation rate and expression of FA enzymes were suppressed in early stages of compensated LV hypertrophy^{8, 9}. FA uptake and oxidation is reduced in HF. Studies on glucose oxidation are less consistent. Most evidence suggests that glucose oxidation is unchanged in compensated hypertrophy but decreased in HF; however, several non-ATP generating pathways of glucose metabolism become enhanced during HF².

Accessory pathways of glucose utilization

Glucose functions not only as a ubiquitous source of energy but also confers significant capacity for cellular signaling. Upon entering a cell, glucose is phosphorylated to glucose-6-phosphate. During glycolysis, it is further metabolized to fructose-6-phosphate permitting entry into a host of accessory pathways of glucose metabolism, including, glycogen synthesis, the Pentose

Phosphate Pathway (PPP), and the Hexosamine Biosynthetic Pathway (HBP). These pathways are upregulated in HF². This thesis focuses heavily on the end product of the HBP pathway and its role in HF.

Hexosamine biosynthetic pathway

Approximately 5% of intracellular glucose enters the HBP¹⁰. Four enzymatic reactions convert fructose-6-phosphate to uridine diphosphate-N-acetylglucosamine (UDP-GlcNAc), the monosaccharide donor for the post-translational O-GlcNAc modification on nuclear and cytoplasmic proteins. The first reaction is the rate-limiting conversion of fructose-6-phosphate to glucosamine-6-phosphate by L-glutamine: fructose-6-phosphate amidotransferase (GFAT)^{10, 11}. The second reaction is the conversion of glucosamine-6-phosphate to N-acetylglucosamine-6-phosphate through glucosamine-6-phosphate acetyl-transferase (Emeg32; Gnpnat1)¹² using acetyl-CoA. The penultimate reaction converts N-acetylglucosamine-6-P to N-acetylglucosamine-1-P with phosphoglucomutase 3 (Pgm3). Interestingly, deletion of either Emeg32¹² or Pgm3¹³ is embryonic lethal. Finally, pyrophosphorylase catalyzes the conjugation of a uridine nucleotide to form UDP-GlcNAc, which serves as the monosaccharide donor for O-GlcNAcylation. As shown in Figure 1¹⁴, nutrient-derived glucose, glutamine, acetyl-CoA, and glucosamine all feed into the HBP at different points linking it with most major metabolic processes. Because the production of UDP-GlcNAc requires nutrients derived from other metabolic pathways, O-GlcNAcylation may serve as a nutrient or metabolic sensor¹⁵⁻¹⁹. However, the β -O-linkage of N-acetylglucosamine (O-

GlcNAc) to proteins has been predominantly implicated in altering expression, translation, and function of the target proteins. Recently, O-GlcNAc has emerged as key player in the primary pathophysiology of many cardiovascular diseases.

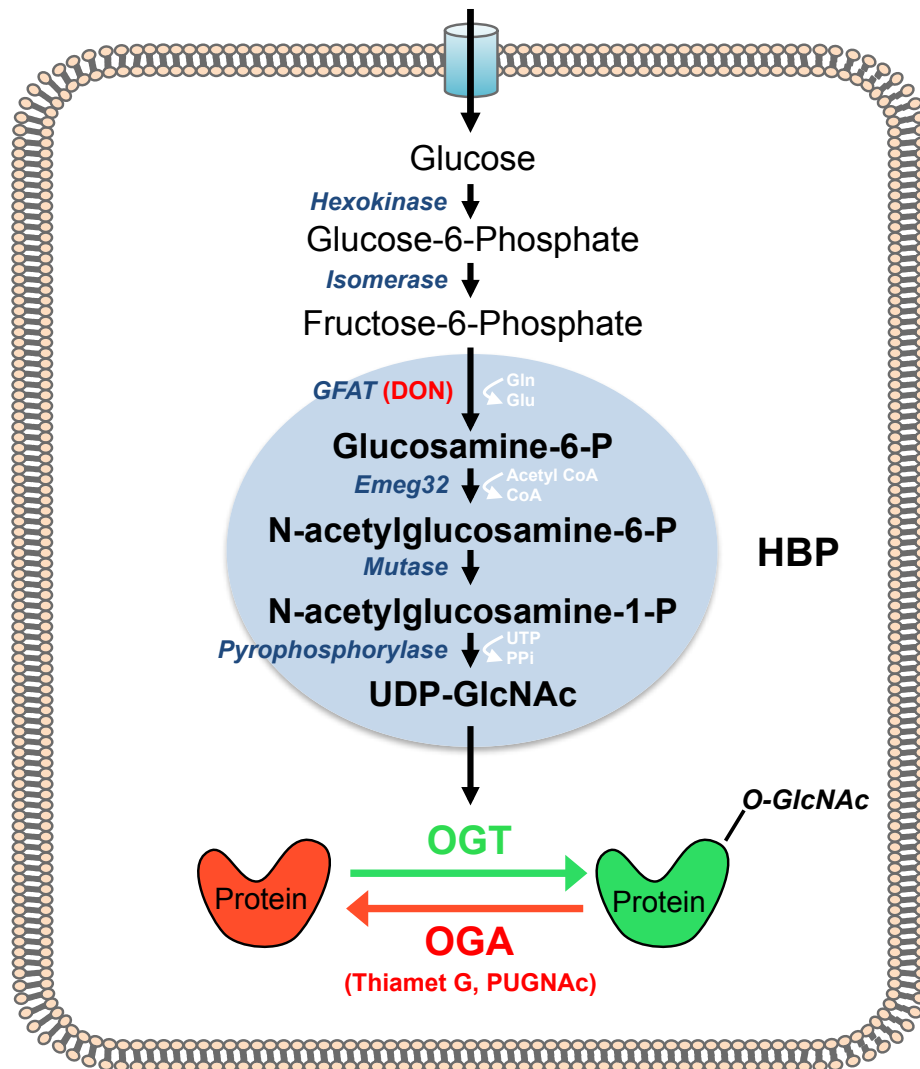


Figure 1. Hexosamine biosynthetic pathway (HBP). Glucose becomes phosphorylated upon entering the cell and can become committed to the HBP (reactions in blue oval). The culmination of the HBP is the formation of UDP-GlcNAc. OGT adds the O-GlcNAc moiety to proteins and OGA removes it. Effective inhibitors of the enzymes in the pathway are listed in parenthesis.

Regulation of O-GlcNAc: GFAT, OGT, and OGA

GFAT

Flux through the HBP can be altered based on the availability of nutrients and activity of enzymes. The first and rate-limiting enzyme of the HBP is GFAT¹⁰, which is highly conserved and exists in two different isoforms, GFAT1 and GFAT2²⁰. Although all tissues express GFAT, the specific isoform expressed varies. GFAT1 is expressed in the pancreas, placenta, testes, and skeletal muscle^{21, 22}. GFAT2 is expressed in the heart and the central nervous system. It can be regulated transcriptionally, post-transcriptionally, and through negative feedback inhibition by UDP-GlcNAc^{11, 23-25}. GFAT uses glutamine as a substrate for the formation of glucosamine-6-phosphate¹⁰. GFAT antagonists, such as O-diazoacetyl-L-serine (azaserine) and 6-diazo-5-oxonorleucine (DON), irreversibly inhibit GFAT, resulting in reduced flow of glucose through the HBP; however, a primary issue with such analogs of glutamine is that they are general amidotransferase inhibitors. The rate-limiting nature of GFAT can be bypassed by exogenously administered or naturally occurring glucosamine. Given the conceptual difficulty in targeting GFAT via a glutamine analog approach and the fact that the ultimate product, UDP-GlcNAc, is essential for traditional complex glycosylation as well as other sugar nucleotide synthesis, GFAT seems to be a poor target to specifically reduce O-GlcNAcylation.

OGT

Ultimately, two highly conserved enzymes, OGT and OGA, directly regulate O-GlcNAcylation of proteins. The X-linked gene, OGT, catalyzes the

addition of a single GlcNAc moiety to serine/threonine residues on proteins²⁶⁻²⁹. In addition to glycosylation, OGT can function in a proteolytic capacity. OGT is expressed ubiquitously but is found to be most abundant in glucose-sensing cells of the brain and pancreas. Alternate splicing of the message produces three isoforms of OGT: nucleocytoplasmic OGT (ncOGT), mitochondrial OGT (mOGT), and short OGT (sOGT)^{26, 29}. The predominant isoform of OGT is nucleocytoplasmic in localization. Interestingly, a gene with functional relationship to OGT, EGF repeat-specific O-GlcNAc transferase (Eogt), was identified in flies and later in mammals. Eogt O-GlcNAcylates EGF-repeats, may be sequestered in the ER, and, unlike OGT, may be restricted to a specific consensus sequence^{30, 31}.

The mechanism of substrate specificity of OGT has yet to be determined; however, recent advances in the study of its structural and kinetic properties yield important insights. OGT consists of an N-terminal domain with tetratricopeptide repeats (TPR) and an intervening domain flanked by two glycotransferase catalytic domains^{32, 33}. The 34 amino acid TPR motif produces a structure with two antiparallel α -helices^{34, 35}. Multiple tandem arrays of TPRs generate a right-handed helical structure with potential to mediate protein-protein interactions. The different isoforms of OGT vary only in the number of TPR regions. As determined by X-ray crystallography, the N-terminal region of human OGT has a canonical superhelical fold typified by TPRs and a groove³⁶. Further studies with bacterial OGT demonstrated that the TPRs and the catalytic domain are juxtaposed such that the superhelical groove extends into the active site^{37, 38}.

Through binding with the continuous groove, protein substrates may influence substrate specificity in the catalytic center³⁹. This notion was consistent with *in vitro* studies that identified the role of TPR in modifying O-GlcNAcylation of proteins⁴⁰.

The interactions between OGT and protein substrates require the presence of UDP-GlcNAc. Kinetic studies by the Walker group indicated that OGT employs an ordered bi-bi kinetic mechanism where UDP-GlcNAc binds first followed by the substrate⁴¹. The interaction between UDP-GlcNAc and OGT induces a conformational change between TPR 12 and 13 that is hypothesized to allow protein substrate entry into the catalytic domain active site. Post-translational modifications involving tyrosine kinases, nitrosylation of cysteine residues, and O-GlcNAc modification may also regulate OGT activity. Yet, unlike most kinases, there is no known consensus sequence for OGT. Thus, the splice variants themselves, interacting proteins, and potentially the concentrations of UDP-GlcNAc may largely regulate substrate selection.

The Walker laboratory also identified, through a high-throughput screen, a number of potential OGT inhibitors⁴². Two compounds, TT04 and TT40, characterized with an oxobenzoxazole core were found to have irreversible action through modifying the catalytic base at the active site⁴³; however, these compounds demonstrated low water solubility, which limited their application⁴⁴. TT04 has been successfully used in the Jones lab as an OGT inhibitor in neonatal rat cardiomyocytes, though the effective dose range appears relatively narrow⁴⁵. Recent work by Vocadlo led to the development of an O-GlcNAc

substrate analog named 5-thioglucosamine (5SGlcNAc)⁴⁶. The acetylated 5SGlcNAc readily crosses the cell membrane due to its hydrophobic nature, becomes converted to UDP-5sGlcNAc and ultimately binds to the active site of OGT competitively inhibiting its function. Preliminary cell culture treatment with the inhibitor resulted in marked reduction in overall O-GlcNAcylation and did not affect cell viability.

Genetic deletion and translational silencing techniques have also been employed to reduce activity of OGT. Neonatal cardiomyocytes from loxP-flanked OGT mice were infected with adenoviral Cre recombinase (to knockout OGT) or transfected with short interfering RNA directed against OGT; both approaches decreased global O-GlcNAcylation and sensitized cardiomyocytes to post-hypoxic death⁴⁵. Accordingly, there are several biological methods to suppress OGT activity; however, the efficacy of such traditional pharmacologic inhibitors requires further validation and may require the development of new compounds.

OGA

OGA catalyzes the removal of the O-GlcNAc modification from proteins³². It resides primarily in the cytoplasm but can be found in nuclei and, potentially, mitochondria. The structure of OGA consists of two main domains: an N-terminal domain with glycoside hydrolase activity and a C-terminal histone acetyltransferase (HAT) domain. These domains flank a region containing a caspase-3 cleavage site⁴⁷. There are two confirmed splice variants of OGA. The full-length protein variant is predominately found in the cytosol whereas the

shorter variant, which lacks the C-terminal domain, resides in the nucleus⁴⁸. The shorter form of OGA also lacks apparent HAT activity.

Human OGA employs a two-step catalytic mechanism and the transient formation of a bicyclic oxazoline intermediate. The highly conserved active site has two adjacent aspartate residues^{39, 49}. They are proposed to play a key role in the cleavage of O-GlcNAc from protein substrates. The first aspartate residue acts as a base to attack the 2-acetamido group of the anomeric carbon. The second aspartate acts as an acid to permit the departure of the leaving group.

Accessibility to the sugar moiety and restricted conformational freedom of the modified protein dictate OGA substrate specificity³⁹. Recent work with the mutagenesis of β -N-acetylglucosaminidase from *Oceanicola granulosus*, an enzyme homologous to human OGA in sequence (37%) and function, revealed that peptide binding on the surface of human OGA is important for its function⁵⁰. Further studies with the *Clostridium perfringens* OGA homologue demonstrated the importance of conformational restraint when deletion of hydrogen bonding within glycopeptides resulted in decreased affinity for human OGA⁵⁰. These studies extend the hypothesis that accessibility to the sugar is important and that conformational change in protein substrates serves to impair OGA processing³⁹.

Several OGA inhibitors have been developed to study the biological roles of O-GlcNAc. O-(2-acetamido-2-deoxy-D-glucopyranosylidene)amino N-phenyl carbamate (PUGNAc), GlcNAcstatin, and Thiamet G are three inhibitors that limit OGA activity⁴⁴. PUGNAc acts as a transition state analog but is unstable in aqueous solutions. GlcNAcstatins, following a similar structure to PUGNAc, were

developed to have higher selectivity to human OGA⁵¹. These proved to penetrate the cell and increase global O-GlcNAcylation 2-3 fold but at the cost of low solubility in aqueous solutions⁵¹. Yuzwa et al. mimicked electrostatic interactions that occur once the bicyclic oxazoline intermediate forms during the reaction mechanism of OGA to produce another inhibitor called Thiamet G. Currently, it is the most potent inhibitor of OGA and is exceptionally stable in aqueous solutions⁵².

In addition to traditional pharmacologic approaches, Ngoh et al. demonstrated successful inhibition of OGA through RNA interference. Neonatal rat cardiomyocytes (NRCMs) transfected with short interfering RNA directed against OGA resulted in significantly augmented O-GlcNAc levels when compared to addition of a scrambled non-silencing control sequence. Primed with increased O-GlcNAcylation, these myocytes were less susceptible to post-hypoxic cell death⁵³. Compared to OGT inhibitors, OGA inhibitors are generally more reliable and better characterized.

O-GlcNAcylation and phosphorylation

Because it shares some similarities with phosphorylation, O-GlcNAcylation, and its impact on signaling, can become exceptionally complicated. Both O-GlcNAcylation and phosphorylation modifications occur on serine and threonine residues, are dynamically added and removed, and alter function of proteins⁵⁴. Although hundreds of genes regulate phosphorylation, only two known mammalian genes encode enzymes for the addition and removal of

O-GlcNAc. Part of the complexity arises within sites of occupancy for O-GlcNAc and O-phosphate. Site mapping studies have revealed evidence for at least three types of interplay between these signaling mechanisms⁵⁵. The first is competitive site occupancy where O-GlcNAc and O-phosphate compete for the same threonine or serine moiety at the same site⁵⁶. The second is alternative occupancy at adjacent sites. Here, occupancy of O-GlcNAc and O-phosphate at adjacent sites can influence the turnover or function of proteins. A third type of interaction involves O-GlcNAc and O-phosphate at the same sites, on adjacent sites, or on distant sites. Although O-GlcNAc and phosphorylation are often described as having a Yin-Yang relationship⁵⁷, it is difficult to imagine such a relationship as universal and obligatory.

O-GlcNAc acts as an alarm or stress signal

The O-GlcNAc post-translational modification may sense and trigger a pro-adaptive response to cellular stressors. Some of the earliest evidence to support such a contention involved the association between hyperglycemia and O-GlcNAcylation and/or OGT⁵⁸. Although these can be retrospectively viewed as 'stress' studies, the first *bona fide* investigation of O-GlcNAc as a stress signal came in 2004⁵⁹. Zachara et al. found that O-GlcNAcylation increased in response to various forms of stress, including heat, oxidative, osmotic, ultraviolet light, and others⁵⁹. O-GlcNAcylation increased in a roughly dose-dependent manner in response to these stressors in various cell lines. More importantly, augmenting O-GlcNAc levels promoted cell survival, whereas depressing O-GlcNAc levels

reduced survival⁵⁹. Such insights offered the clarion call for new investigations into a previously unrecognized role for O-GlcNAcylation in cell survival.

The role of O-GlcNAc in the cardiovascular system

Acute cardioprotection

The O-GlcNAc modification confers protection to subsequent lethal insults, which has been reviewed extensively, elsewhere. Briefly, in response to myocardial ischemia-reperfusion injury – which is characterized by calcium overload, oxidative stress, and ER stress – global levels of O-GlcNAcylation are augmented. Temporal changes in O-GlcNAcylation have been observed *in vitro* and *in vivo* studies of cardiomyocyte survival. In *in vitro* studies, O-GlcNAc levels decrease during hypoxia then increase during reoxygenation in isolated, perfused hearts subjected to simulated ischemia-reperfusion⁶⁰. This same effect occurs during hypoxia-reoxygenation of NRCMs⁶¹. Interestingly, *in vivo* myocardial ischemia-reperfusion studies demonstrate similar findings⁶². The elevation in O-GlcNAc before and after ischemia functions to reduce cell death⁶⁰ and, antecedent elevation of O-GlcNAcylation promotes myocardial tissue viability in other models of tissue injury. Regulation of the HBP and enzymatic regulators of O-GlcNAcylation may provide potential targets for therapeutic intervention in cardiovascular disease.

O-GlcNAc modulates vascular activity

Sustained alteration of cardiovascular reactivity can result in hypertension, a primary risk factor for cardiovascular disease. Deranged vascular activity, endothelial reactivity, and hypersensitivity to vasoconstrictors are all hallmarks of hypertension and vascular dysfunction. Interestingly, the development of these hallmark characteristics appears to coincide with augmented O-GlcNAcylation. Lima et al. described increased O-GlcNAcylation in the vasculature of hypertensive rats^{63, 64}, which had impaired endothelium-dependent relaxation and enhanced sensitivity to vasoconstrictors. Augmenting O-GlcNAcylation with PUGNAc was sufficient to recapitulate these vascular effects in normoglycemic conditions, indicating a potential role for O-GlcNAc in the development of hypertension.

Furthermore, Lima et al. correlated a link between O-GlcNAcylation and endothelin-1 (ET-1), a major player in the development of vascular dysfunction⁶⁵. ET-1 is responsible for inducing vasoconstriction and triggering a host of transcription factors that lead to inflammation, oxidative stress, and eventually tissue death⁶⁵. The authors found that protein O-GlcNAcylation increases following incubation with ET-1 and alters vascular reactivity, and, when OGT is inhibited in the presence of ET-1, the effect of ET-1 on O-GlcNAc and vascular reactivity is abrogated. Moreover, blocking the ET_A receptor with atrasentan, resulted in decreased O-GlcNAcylation. ET-1 treatment depresses OGA expression and activity, which could result in the observed increase in O-

GlcNAcylation. Thus, a complex interplay exists between ET-1 and the induction of O-GlcNAcylation.

Conversely, data from the Oparil lab supports a role of O-GlcNAc in preventing vascular dysfunction. First, they demonstrated that the induction of O-GlcNAcylation inhibits acute inflammatory responses to endoluminal injury⁶⁶. Further studies showed that pretreatment of aortic rings with Thiamet G and glucosamine lead to increased global O-GlcNAcylation and prevented TNF α induced hypo-contraction and endothelial dysfunction⁶⁷. This inhibition of TNF α 's effects may be the result of O-GlcNAcylation of the p65 subunit of NF κ B⁶⁸. As in the myocardium, the vasculature may host divergent responses to O-GlcNAcylation, which may largely relate to duration of the stimulus.

O-GlcNAc in the failing heart

Nowhere has the rebirth of metabolic investigation in the cardiovascular system been more evident than in HF. Metabolic changes during HF result in changes in substrate utilization and the reversion to a fetal metabolic profile. The heart suppresses fatty acid oxidation and augments its reliance on carbohydrate oxidation^{69, 70}. Flux through accessory pathways of glucose metabolism such as the HBP become enhanced and result in augmented protein O-GlcNAcylation. Watson et al. reported increased O-GlcNAcylation and OGT expression during HF in mice. In this infarct-induced HF model, OGT expression was elevated and OGA expression was reduced⁷¹. In a loss of function study, cardiac-specific deletion of OGT and consequent reduction in cardiac O-GlcNAcylation

significantly exacerbated infarct-induced HF⁷¹. Specifically, survival was somewhat reduced, ventricular dysfunction was significantly depressed, and apoptosis was augmented. These results demonstrate that the pro-adaptive increase in O-GlcNAc is required in the failing heart. Interestingly, cardiomyocyte OGT deletion did not result in any acute signs of HF in otherwise naïve (non-infarcted) mice.

O-GlcNAc and cardiac hypertrophy

In response to MI or hypertension, cardiac hypertrophy is essential process to preserve cardiac function. Unsurprisingly, O-GlcNAc signaling has been implicated in cardiomyocyte hypertrophy. In models of pressure-overload hypertrophy, UDP-GlcNAc concentrations are greatly increased⁷². Accordingly, levels of O-GlcNAc and GFAT increased in Brown-Norway rats as their hearts with age-related cardiac hypertrophy⁷³. This observation suggests that HBP and/or O-GlcNAc may be involved in the development of hypertrophy.

To identify directly the role of O-GlcNAcylation in hypertrophy, Facundo et al. determined that NFAT activation during cardiomyocyte hypertrophy required O-GlcNAcylation. O-GlcNAc-dependent activation of NFAT resulted in hypertrophy whereas depressing O-GlcNAcylation blunted cardiomyocyte NFAT activation and hypertrophy⁷⁴. Because others showed that NFAT could be a target of O-GlcNAc in other model systems⁷⁵, and that NFAT is phosphorylated when excluded from the nucleus (i.e. not activated⁷⁶), it is tempting to speculate that cardiomyocyte hypertrophy is driven by direct O-GlcNAcylation of NFAT.

O-GlcNAc and diabetes

Diabetes mellitus, characterized by elevated blood glucose levels, represents a primary, independent risk factor for cardiovascular disease. Given the simple association of hyperglycemia with diabetes and elevated O-GlcNAcylation^{10, 58, 77-83}, it is not surprising that protein O-GlcNAcylation has been linked to diabetes. Indeed, several reports indicate elevated O-GlcNAcylation in diabetic models^{58, 60, 77, 79-81, 83}. Although some may question this relationship in individual tissues or cell types – particularly insulin sensitive tissues – evidence supports a general relationship between diabetes and O-GlcNAcylation. Interesting proof-of-concept studies demonstrated a relationship between the HBP and insulin resistance *in vitro*. Specifically, overexpression of GFAT1 in rat fibroblasts leads to decreased insulin sensitivity⁸⁴, and transgenic overexpression of GFAT resulted in insulin resistance⁸⁵. Marshall et al. rescued hyperglycemia-induced insulin resistance through GFAT inhibition. Similarly, overexpression of OGT in muscle and adipose tissue leads to insulin resistance and hyperleptinemia^{17, 18} while inhibiting O-GlcNAcase with PUGNAc (to increase O-GlcNAcylation) leads to insulin resistance in cell culture⁸⁶. Such findings support a role for the HBP and O-GlcNAcylation in promoting, or at least participating in, the pathogenesis of insulin resistance and diabetes.

Other groups have published varying results regarding the role of O-GlcNAc in triggering diabetes⁸⁷. Treatment with PUGNAc, in addition to increasing O-GlcNAcylation, has been found to induce proteins involved in ubiquitin-proteasome degradation and insulin signaling pathways⁸⁸. Specifically,

PUGNAc appears to increase ubiquitination of proteins and decrease not only Akt phosphorylation but also the protein itself⁸⁸. Similarly, recent studies from the Buse lab contend that elevating O-GlcNAc alone may be insufficient to induce diabetes^{89, 90}. The Vocadlo group used a more selective OGA inhibitor than PUGNAc (i.e. NButGT) to determine a correlation between insulin resistance and O-GlcNAcylation. NButGT rapidly increased O-GlcNAcylation without the added effect of causing insulin resistance in 3T3-L1 adipocytes⁹¹. Neither inducing O-GlcNAcylation through overexpression of OGA nor ablating O-GlcNAcylation through knockout of OGT appeared to be engender insulin resistance⁹²; however, Dentin et al. showed overexpression of OGA in a diabetic mouse model rescues glucose tolerance and insulin sensitivity⁹³. Taken together, these results suggest that global O-GlcNAcylation may not necessarily cause insulin resistance on its own. Thus, the causative role of the HBP and O-GlcNAc in diabetes may not be as clear as initially thought.

O-GlcNAc in diabetic cardiac dysfunction

Similar to the basic cell studies tying O-GlcNAc to diabetic pathogenesis, several groups have suggested an association between increased O-GlcNAcylation and cardiac dysfunction. At a reductionist level, cells grown in hyperglycemic conditions demonstrate reduced ATP production as a potential result of altered mitochondrial proteins⁸⁰. Increased O-GlcNAcylation, secondary to hyperglycemia, may depress function of mitochondrial electron transport complexes I, III, and IV in NRCMs which may be attenuated by overexpression of

OGA. Nevertheless, it still remains unclear whether all of the necessary components (i.e. OGT, UDP-GlcNAc, appropriate binding partners) to produce O-GlcNAcylation are present in the mitochondria, and, although such studies are exciting, further work is required to fully understand how O-GlcNAc may regulate mitochondrial function.

Not only may O-GlcNAc alter basic aspects of mitochondrial function, it may also affect cardiac contractile function through altering calcium handling. Cardiomyocytes subjected to high concentrations of extracellular glucose, glucosamine, or PUGNAc exhibited delayed calcium transients^{74, 79, 80, 94}. Overexpression of OGT in cardiomyocytes similarly delayed calcium transients while OGA overexpression rescued calcium transients. The interaction between phospholamban and SERCA2a may also be modified by O-GlcNAcylation⁹⁵. O-GlcNAcylation at Ser16 on phospholamban, a reported manifestation in diabetes, results in reduction in phosphorylation of phospholamban and a decrease in its association with SERCA2a, thereby decreasing the pump's activity⁹⁵. Such studies suggest the increased O-GlcNAcylation during hyperglycemia/diabetes may be part of the cause of the pathology, either at the mitochondrial level and/or the level of calcium handling. Yet, it remains unclear how cardiomyocytes, which (according to conventional wisdom) normally require insulin for most glucose uptake, might exhibit increased glucose uptake during diabetes, at least to a level sufficient to drive flux, and consequently O-GlcNAcylation, through the HBP. On an even larger scale, some investigators contend that myocardial insulin

resistance serves as a pro-adaptive, defensive response against nutrient excess⁹⁶.

Summary

O-GlcNAcylation plays a vital role in cardiac and vascular function, especially during disease. Although O-GlcNAcylation uniformly promotes cardiomyocyte survival in the context of acute cell injury, the role of O-GlcNAc in the vasculature or in the chronically failing/diabetic heart is less clear-cut. Nevertheless, modulation of O-GlcNAcylation is ripe with tremendous therapeutic potential. In the case of acute cardioprotection, therapeutic augmentation of O-GlcNAc levels is a clinically feasible option. One such strategy would be to limit de-O-GlcNAcylation through pharmacological inhibition of OGA. Another method would be to prime cardiomyocytes through genetically enhancing O-GlcNAcylation. Either approach could be used in cases such as heart transplant or coronary artery bypass grafting – both of which involve predictable stress/ischemic events in the heart. The implementation of targeted O-GlcNAcylation, though difficult to imagine at this point, may provide a therapeutic benefit to the cardiovascular system prior to or following acute cardiovascular injury. These strategies may provide protection during ischemic events in the heart resulting in improved survival and cardiac function.

In the meantime, laboratory efforts should be directed toward understanding O-GlcNAc biology. There are many questions to be resolved regarding the role of O-GlcNAcylation in the pathology of diseases. Previous

studies have demonstrated that protein O-GlcNAcylation increases in response to stress. Two highly conserved enzymes regulate cellular O-GlcNAc levels, though, we have virtually no understanding of their transcriptional or posttranscriptional regulation. Another facet of O-GlcNAc biology is that O-GlcNAcylation of proteins is transient and acute augmentation of O-GlcNAc signaling is cytoprotective. However in the context of disease (ie. HF and diabetes) O-GlcNAc levels become chronically elevated. Much of the detrimental effects on mitochondrial function in metabolic disorders such as diabetes, where flux through the HBP is elevated, have been attributed to dysregulated protein O-GlcNAcylation. The question remains whether prolonged augmentation of O-GlcNAcylation is protective or maladaptive.

This project addresses these queries through elucidating the role of OGA/O-GlcNAc in HF. It will determine the temporal changes in expression of the machinery necessary to regulate O-GlcNAcylation: OGT and OGA. The project will identify a novel posttranscriptional regulator of OGA in response to myocardial stress. In addition, through ablation of cardiac OGA, we will demonstrate the effect of prolonged O-GlcNAcylation on cardiac function alone and then in the context of HF. These studies will provide insight into the role that prolonged O-GlcNAc plays in HF. Finally, this project will shed light on the long purported link between O-GlcNAcylation and mitochondrial function.

CHAPTER II

HYPOTHESIS AND SPECIFIC AIMS

Current treatments for HF are largely palliative. As a result, the prognosis for patients with HF remains grim. New approaches to understand basic pathophysiology of the heart could create new treatment options. Although metabolic changes clearly occur in HF, we lack sufficient understanding of some of the peripheral aspects of metabolism; that is, HF is not simply an ATP-deficient pathology. Accordingly, this project will identify the role of a unique accessory pathway associated with glucose metabolism, which is distally regulated by OGA, in the failing heart.

Recent studies in our laboratory have identified the significant induction of a stress signal, O-GlcNAc, following myocardial infarction (MI). Furthermore, our laboratory described the role of OGT in the failing heart and found that it was necessary for the heart's post-MI response. Using a somewhat complementary – though mechanistically more advanced – approach, the present proposal will unequivocally determine the role of OGA (the enzyme that removes the O-GlcNAc modification). We posit that genetic abrogation of OGA activity could attenuate the severity of HF.

Overarching Hypothesis: OGA suppression favors O-GlcNAcylation and attenuates HF through preservation of mitochondrial function.

Specific Aim 1. Establish the temporal changes of OGA in HF.

- A) Identify temporal changes of OGA expression in the failing heart.
- B) Identify regulators of OGA expression in the failing heart.

Specific Aim 2. Determine the role of OGA in HF.

- A) Characterize inducible, cardiomyocyte-specific OGA deficient mouse.
- B) Perform HF studies in the setting of OGA deletion.

Specific Aim 3. Assess the contribution of OGA to cardiomyocyte mitochondrial function.

- A) Interrogate changes in mitochondrial respiration following alteration of OGA expression or activity.

CHAPTER III

MATERIALS AND METHODS

All de-identified human samples were obtained with informed consent and in accord with the institutional review board of the University of Louisville. All human HF samples (in collaboration with Dr. Sumanth Prabhu) were collected from males, age 50-58 years; were classified NYHA IIIb-IV; had elevated BNP levels; and had ejection fractions below 25%. Control samples were purchased from Integrated Laboratory Services – Biotech (ILSbio; Chestertown, MD). All animals were used in compliance with the Guide for the Care and Use of Laboratory Animals issued by the National Institutes of Health. The experimental protocols in this study have been reviewed and approved by the University of Louisville Institutional Animal Care and Use Committee.

Tamoxifen treatment: 4-hydroxytamoxifen (25 mg, Sigma, St. Louis, MO) was added to 1 mL of warmed (37°C) 100% ethanol. The mixture was vortexed and sonicated until fully dissolved. Then the mixture was added to 9 mL peanut oil (Sigma, St. Louis, MO) and was vortexed and sonicated until dissolved. A bolus of 4-hydroxytamoxifen (20 mg/kg) was injected intraperitoneally on alternating

sides for 5 d. Residual 4-hydroxytamoxifen was allowed to “wash out” for 5 d prior to experimentation.

Non-reperfused myocardial infarction (MI) surgery: Initial HF studies were conducted in three-month-old wild-type C57BL6J mice for Aim 1. In Aim 2 we used three-month-old *i-cmOGA^{+/-}* mice and wild-type littermates and subjected them to MI surgery following 4-hydroxytamoxifen treatment. Mice were anesthetized with ketamine (50 mg/kg, intraperitoneal) and pentobarbital (50 mg/kg, intraperitoneal), orally intubated with polyethylene-60 tubing, and ventilated (Harvard Apparatus Rodent Ventilator, model 845) with oxygen supplementation. The left anterior coronary was visualized through an intercostal incision and a 7-0 silk suture was looped around the coronary. The suture was tied. Successful occlusion of the coronary artery was assessed visibly through pallor. The chest was sutured with 4-0 silk suture and the skin was sutured with 4-0 polyester suture. Analgesia (ketoprofen, 5 mg/kg, subcutaneous) was given before mice recovered from anesthesia and at 24 h and 48 h of the postoperative period. Mice were extubated upon recovery of spontaneous breathing and were allowed to recover in warm, clean cages supplemented with oxygen. At the end of each study, mice were euthanized and the hearts were rapidly excised and weighed. The hearts were then immediately frozen in liquid nitrogen and stored at -80°C, or, perfused and fixed for immunohistochemical analyses.

Histopathology: Histology was performed using previously published methods⁷¹. Briefly, formalin-fixed, paraffin embedded hearts from sham and MI mice were sectioned, deparaffinized, and rehydrated. Masson's trichrome (Richard-Allan Scientific, Masson's trichrome kit, Fisher Scientific, Ottawa, Ontario) was used to detect collagen. Cardiac collagen content was determined as the percentage of collagen in long-axis sections of the LV.

Echocardiography: Transthoracic echocardiography of the left ventricle was performed as previously described⁹⁷⁻¹⁰³ with adjustments for the Vevo 770 echocardiography machine. Body temperature was maintained (36.5°C-37.5°C) using a rectal thermometer interfaced with a servo-controlled heat lamp. Mice were anesthetized with 2% isoflurane, maintained under anesthesia with 1.5% isoflurane, and examined. Mice were placed chest up on an examination board interfaced with the Vevo 770. The board was outfitted with EKG electrodes for all limbs. Next, depilatory cream was applied to the mouse's chest and wiped clean to remove all hair in the area of interest. The 707-B (30 MHz) scan head was used to obtain 2D images (100 fps) of the parasternal long axis. M-modes were taken from the same images. The probe was then rotated to acquire a short axis view of the heart. Beginning at the level of the papillary muscles and moving apically, serial 2D images were taken every millimeter. All measurements were taken by utilizing the Vevo 770's rail system to maintain probe placement and allow for minute adjustments of position. Left ventricular inner diameter during diastole (LVIDd) and left ventricular inner diameter during systole (LVIDs) and

heart rate (HR) were determined from M-modes. Left ventricular fractional shortening (%FS) was calculated as: $((LVIDd-LVIDs)/LVIDd) \times 100\%$. Applying Simpson's rule of discs to the serially acquired, short-axis images provided diastolic and systolic volumes. Stroke volume (SV) was calculated as: Diastolic volume - Systolic Volume. Ejection Fraction was calculated as: $(SV/Diastolic\ Volume) \times 100\%$. Cardiac output was determined by: $SV \times HR$.

miRNA microarray and real-time PCR: Total RNA from the 5- and 28-day sham and infarcted mouse hearts ($n = 4/\text{group/time point}$) was isolated using TRIzol reagent (Invitrogen). Rodent miRNA microarray kit (Applied Biosystems) was used according to the manufacturer's protocol. In brief, 1 μg of total RNA was reverse-transcribed with Megaplex RT primers (Megaplex RT Rodent Pool A), followed by a real-time PCR with TaqMan Rodent MicroRNA Array performed on an Applied Biosystems 7900HT System. SDS software version 2.3 and DataAssist version 3.0 (Applied Biosystems) were used to obtain the comparative threshold cycle (C_t) value. U6 small nuclear RNA included in the TaqMan Rodent MicroRNA Array was used as an endogenous control. Quantitative RT-PCR (qRT-PCR) analyses were carried out using TaqMan miRNA assays (Applied Biosystems) according to the manual. Relative expression of miR-539 was calculated using the $\Delta\Delta C_T$ method normalized to the expression of U6 small nuclear RNA (Applied Biosystems). Relative levels of OGA and OGT mRNA were examined with specific primers (OGA: forward, 5'-TGGAAGACCTTGGGTTATGG-3' and reverse, 5'-

TGCTCAGCTTCTTCCACTGA-3'; GT, orward, '-
CCTGGGTCGCTTGGAAGA-3' and reverse, 5'-TGGTTGCGTCTCAATTGCTTT-
3') using Fast SYBR Green (Applied Biosystems) and normalized to levels of 18
S mRNA. All qRT-PCRs were performed in duplicate.

In situ hybridization: MicroRNA-539 *in situ* hybridization was performed using the protocol described by Obernosterer *et al*¹⁰⁴. In brief, frozen sections of sham and infarcted mouse hearts (5 and 28 days) were prepared as mentioned earlier, washed in PBS for 10 min, placed in acetylation solution (98% diethyl pyrocarbonate-treated water, 1.3% triethanolamine, 0.175% HCl, 12% acetic anhydride) for 20 min and digested by Proteinase K (25 µg/ml) for 5 min at room temperature, washed in PBS for 5 min, and prehybridized (50% formamide, 25% 20× SSC, 10% 50× Denhardt's, 1.25% 20 mg/ml of yeast tRNA, 5% 10 mg/ml of salmon sperm DNA, 0.4 g of blocking reagents in 20 ml of solution and 8.75% diethyl pyrocarbonate-treated water) at 50 °C for 4 h. The digoxigenin-labeled mmu-miR-539 LNA probe (Exiqon, Woburn, MA). Probes (1 nM) were denatured with denaturing hybridization solution (50% formamide, 25% 20× saline-sodium citrate (SSC), 10% 50× Denhardt's, 1.25% 20 mg/ml of yeast tRNA, 5% 10 mg/ml of salmon sperm DNA, 0.4 g of blocking reagents in 20 ml of solution, 2.5% of 10% CHAPS, 0.5 of 20% Tween, and 5.75% diethyl pyrocarbonate-treated water) at 95 °C for 5 min, then added to the slides and hybridized at 50 °C for overnight. The slides were washed in 5× SSC for 5 min followed by 0.2× SSC for 60 min at 60 °C. After blocking for 1 h (2% fetal bovine serum), the sections were

incubated with anti-digoxigenin antibody (Roche Applied Science; 1:2000) overnight at 4 °C. The bound antibody was detected by AP substrate, nitro blue tetrazolium chloride/5-bromo-4-chloro-3-indolyl phosphate, toluidine salt for color development for 24–48 h at room temperature in the dark, and imaged using a NS-F12 camera mounted on a Nikon Eclipse Ni microscope.

NRCM and HEK293 cell culture: NRCMs were isolated from 1–2-day-old Sprague-Dawley rats according to the protocol as previously described¹⁰⁵. The isolated cardiomyocytes were cultured in DMEM containing 10% fetal bovine serum, penicillin/streptomycin, and vitamin B₁₂ in the presence of anti-mitotic BrdU (0.1 mM) for 4 days to inhibit fibroblast growth and subsequently grown in the absence of BrdU. HEK293 cells were grown in DMEM containing 10% fetal bovine serum and penicillin/streptomycin. 293FT cells cultured in DMEM Glutamax (Invitrogen) containing 10% fetal bovine serum, penicillin/streptomycin, and Geneticin (Invitrogen) were used for the lentivirus preparation.

Luciferase reporter assay: For luciferase assay, we transiently co-transfected (Lipofectamine 2000, Invitrogen) pLenti6/V5-miR-539 or pLenti6/V5-scrambled (250 ng) overexpressing constructs with luciferase reporter plasmid containing wild-type OGA-3'UTR (Genecopoeia, Inc.) or miR-539 binding seed mutant OGA-3'UTR (250 ng) in 60–70% confluent HEK293 cells grown in a 12-well plate. *Renilla* reporter plasmid (10 ng) was used as transfection control. At 48 h post-transfection, cells were lysed and assayed for luciferase activity using a dual

luciferase assay kit (Promega).

miRNA-539 construct and lentivirus preparation: The precursor miRNA-539 was amplified from mouse genomic DNA using forward (5'-CACGTGTGAGGAGTGGTGAT-3') and reverse (5'-CCTTGTGCCAGGTAAGG-3') primers containing EcoRI and XhoI restriction sites, respectively. Scrambled sequence amplified from pEZX-MR04 (GeneCopoeia, Inc.) using forward (5'-ACACCCTGTTTATTGATGCTGA-3') and reverse (5'-CCTGTTATTCTCTGCTAACGCC-3') primers was used as a control. The amplified precursor miRNA-539 and scrambled control were cloned into pLenti6/V5 plasmid and verified by sequencing. The integrity of miRNA-539 and scrambled control stem loop structure was analyzed using mfold version 2.3. 3 µg of pLenti6/V5-miR-539 was mixed with 9 µg of ViraPower Packaging Mix (Invitrogen) and transfected in 293FT cells using Lipofectamine 2000 transfection reagent according to the manufacturer's instruction. The pseudolentiviral particles released in the medium were concentrated using Lenti-X Concentrator (Clontech Laboratories, Inc.) and titrated in NRCMs by qPCR using SV40 forward, 5'-GCTCCCCAGCAGGCAGAAGTATG-3' and reverse, 5'-TGGGGAGCCTGGGGACTTTCCAC-3' primers. pLenti6/V5-mCherry was used as a transduction control.

Functional study of miRNA-539: We examined the effect of miR-539 on OGA and OGT by transducing NRCMs and HEK293 cells with miR-539 lentivirus or

scrambled or mCherry control lentiviruses. The cells were maintained in their regular growth medium for 2 days and selected with blasticidine for 5 days. Alternatively, cells were transfected with mirVana™ miR-539 inhibitor or a negative control Oligonucleotides (10 nmol/liter) using Lipofectamine™ RNAiMAX (Invitrogen) after 5 days of lentivirus treatment. Overexpression of miR-539 expression was verified by qRT-PCR using miRNA assay as described above and the loss or gain of OGA expression followed by miR-539 mimic/inhibitor was analyzed by Western blotting.

***In vitro* hypoxia-reoxygenation injury:** To determine whether additional insults, such as hypoxia-reoxygenation alter miR-539 levels, NRCMs were subjected to hypoxia-reoxygenation as described. In brief, cells were subjected to 3 h hypoxia in Esumi lethal ischemia medium for glucose and nutrient deprivation (containing 117 mmol/liter of NaCl, 12 mmol/liter of KCl, 0.9 mmol/liter of CaCl₂, 0.49 mmol/liter of MgCl₂, 4 mmol/liter of HEPES, 20 mmol/liter of sodium lactate, and 5.6 mmol/liter of L-glucose; pH 6.2) in a sealed humidified hypoxic chamber (Billups-Rothenberg, Inc.) flushed with 5% CO₂ and 95% N₂, and maintained at 37 °C. After 3 h, the cells were switched to Esumi control medium (containing 137 mmol/liter of NaCl, 3.8 mmol/liter of KCl, 0.9 mmol/liter of CaCl₂, 0.49 mmol/liter of MgCl₂, 4 mmol/liter of HEPES, and 5.6 mmol/liter of D-glucose, pH 7.4) and allowed to reoxygenate for 3, 6, and 12 h in the modular incubator. Cells grown in the Esumi control medium for the same durations were used as normoxic controls. The expression of miR-539 and OGA protein level was

analyzed as described above.

Protein isolation: NRCM or HEK292 cellular protein content was harvested using a cell scraper in buffer containing: HEPES (5 mmol/L), EDTA (1 mmol/L), EGTA (1 mmol/L), KCl (50 mmol/L), mannitol (200 mmol/L) and sucrose (68 mmol/L, pH = 7.4 with KOH). The following reagents were freshly added to the buffer: DTT (1 mmol/L), protease inhibitor (0.0001%), Triton X-100 (0.4%), NP-40 (0.4%), sodium orthovanadate (1 mmol/L), sodium fluoride (1 mmol/L), alloxan (OGT inhibitor, 1 mmol/L) and O-(2-Acetamido-2-deoxy-D-glucopyranosylideneamino) N-phenylcarbamate (i.e., PUGNAc, which is an OGA inhibitor, 1 μ mol/L) were added to the buffer in order to avoid artificial O-GlcNAc addition or removal, respectively, to the proteins *in vitro*. NRCM lysates were sonicated twice at 4°C for 25 sec each, with 30 min separating each sonication. After the second sonication, the NRCM lysates were centrifuged at 16,000xg for 5 min. The supernatant was collected, snap frozen, and stored at -80°C until used.

Protein isolation from heart tissue: Heart tissue was minced, weighed, and placed in buffer containing: Tris-HCl (50 mmol/L, pH 7.4), NaCl (150 mmol/L), deoxycholic sodium salt (0.01 mmol/L), EDTA (1 mmol/L), sodium orthovanadate (1 mmol/L), sodium fluoride (1 mmol/L), PUGNAc (0.001 mmol/L), alloxan monohydrate (0.001 mmol/L). Protease Inhibitor 556 μ l/L (P8340, Sigma-Aldrich) and NP-40 (10%) were freshly added to the buffer. To this solution, 1.4 mm

diameter stainless steel beads were added at a ratio of 3:1 (mass of bead:mass of tissue) in 1.5 mL tubes. Tubes were transferred to a Bullet Blender and subjected to bead-homogenization at 4°C. Lysates were centrifuged at 14,000xg at 4°C for 5 min. Supernatant was saved and precleared with sepharose G (GE Healthcare) to limit the interaction of the secondary antibody (anti-mouse) with endogenous immunoglobulins. Heart lysates were frozen in liquid nitrogen and stored at -80°C until used.

Protein quantification: NRCMs, HEK293, and heart lysate protein concentration were determined by Bradford assay with Bio-Rad protein assay dye reagent (Bio-Rad Laboratories) using different concentrations of bovine serum albumin as standards. Protein concentrations were measured with a Thermo Multiskan Spectrum spectrophotometer.

Immunoblotting: NRCM, HEK293, or whole heart protein samples were subjected to electrophoresis in SDS-PAGE gels (4-12%, Invitrogen) and transferred to PVDF membrane (Immobilon-P, EMD Millipore, Billerica, MA) at 4°C. For O-GlcNAc immunoblotting membranes were allowed to dry at room temperature for 1 hr. Then the blot was probed with primary antibody against: O-GlcNAc: CTD 110.6 (1:1000; Covance) or RL2 (1:1000, Affinity Bioreagents) in PBS-casein (Bio-Rad Laboratories) overnight at 4°C. Membranes were washed three times with 1x PBS. Membranes were incubated at room temperature with secondary antibody goat anti-mouse IgG-HRP (1:4000, sc-2005; Santa Cruz

Biotechnology) in PBS-casein. Membranes were again washed three times with 1x PBS and then imaged. All other western blotting followed standard protocols. Briefly, membranes were blocked at room temperature using Tris-buffered saline pH 7.5 (TBS) containing nonfat milk (5%), washed with TBS containing Tween-20 (TBS-T, 0.1%), and probed with primary antibody. Antibodies for OGT (SQ-17 - 1:2000, Sigma-Aldrich), OGA (NCOAT – 1:1000, Santa Cruz Biotechnology), GATA-4 (14353 – 1:1000, Cell Signaling Technology), and α -tubulin (1:2000, Sigma-Aldrich) were made in TBS containing nonfat milk (1%). After overnight incubation at 4°C, blots were washed in TBS containing Tween-20 (TBS-T, 0.1%). The blots were blocked for 15 min in TBS-T containing 1% milk, washed, and then incubated with goat anti-rabbit IgG-HRP (sc-2004; Santa Cruz Biotechnology or 7074; Cell Signaling Technology) or goat anti-mouse IgG-HRP (Santa Cruz Biotechnology), in 1:2000 dilution (for OGT, OGA, GATA-4, α -smooth muscle actin, and α -tubulin). After washing three times with TBS-T, the membrane was saturated with SuperSignal West Pico Chemiluminescent Substrate (Thermo Fisher Scientific) and imaged on a Fuji LAS-3000 bio-imaging analyzer. To confirm the linear range of the signal, multiple exposures from every experiment were performed. Levels of proteins in each lane were normalized to loading protein content (α -tubulin) or to Ponceau stain and expressed as relative to control (set as 100%).

Reverse transcriptase PCR and real-time PCR: The total RNA from OGA KO and WT hearts was extracted with Trizol reagent (Invitrogen, Carlsbad, CA).

Total RNA levels were quantified using the ratio of absorbance at 260 nm to 280 nm (A₂₆₀/A₂₈₀ ratio) with the NanoDrop™ 1000 Spectrophotometer (Thermo Fisher Scientific). To check for organic contaminants like phenol and other aromatic compounds (Trizol, for example), the total RNA was verified by the absorbance ratio of 260 nm to 230 nm (A₂₆₀/A₂₃₀). We limited the use of RNA to samples with 260/230 ratio greater than 1.8. Total RNA (1 µg) was then subjected to transcription in a final volume of 20 µL for 30 min to synthesize cDNA using iScript™ cDNA synthesis kit (Bio-Rad Laboratories, Hercules, CA). The relative levels of mRNA transcripts were quantified by real-time PCR using SYBR® Green (Thermo Fisher Scientific) on a real-time PCR system (ABI 7900 HT, Applied Biosciences). All primers were made using NCBI Primer Blast except HPRT primers (PPM03559E-200, QIAGEN). The data were normalized to mouse HPRT mRNA threshold cycle (C_T) values by using the $\Delta\Delta C_T$ comparative method.

Generation of inducible, cardiac-specific OGA deficient mice: We received OGA-loxP flanked mice as a generous gift from the Hanover lab. Progeny from these mice were then bred with either the α -MHC MerCreMer (MCM) or α -MHC Cre transgenic mouse lines to generate inducible or constitutive cardiac-specific OGA ablated mice respectively. Inducible, cardiomyocyte-specific *Oga* deficient (i-cm*Oga*^{+/-}) mice and their wild-type (MCM positive) littermates were bred based on strategy (Figure X). All mice used in this study were on a C57BL/6J background.

Genotyping of transgenic mice: At 3-4 weeks of age, mice were ear tagged, and tail snips were taken. Total DNA was isolated from tail snips using the Qiagen DNeasy Tissue Kit. The DNA was stored at -20°C until PCR is performed. PCR was performed using the Taq PCR Core Kit from Qiagen. Mixes were created as follows: tube 1 contained 1 µl DNTP, 1ul of 20 µmol/L forward primer 1 µl of 20 µmol/L reverse primer, 10 µL Enzyme Q, and 7 µL water per sample. Tube 2 contained 5 µl 10X buffer, 0.5 µL Taq, and 14.5 µL water per sample. 20 µL of each tube were added to a PCR tube containing 10 µL of purified DNA. PCR was performed at the following conditions: 1 cycle of 94°C for 3 min, 35 cycles of 94°C for 30 sec, 61°C for 1 min and 72°C for 1 min, 1 cycle of 72°C for 2 min then held at 4°C ad infinitum. PCR samples were then run on a 1.2% agarose gel with SYBR Safe stain (Invitrogen). Gels were visualized under UV light using a Fuji LAS-3000 imaging system. All primer sequences used for genotyping are listed in Table 1.

Primer Name	Primer Sequence 5'-3'
OGA UTR1F	ACC GCA CAC TCT CCA TCG CCA TAA
OGA UTR4R	CCC GCT TCC TGT TTA TCC GCA CTG
OGA R7	CAC CGC CTC CTC CTC CGA CAA ATC
Neo F	TGC TCC TGC CGA GAA AGT ATC CAT CAT GGC
Neo R	CGC CAA GCT CTT CAG CAA TAT CAC GGG TAG
MCM F	GTC TGA CTA GGT GTC CCT TCT
MCM R	CGT CCT CCT GCT GGT ATA G

Table 1. Genotyping Primers

NRCM culture for extracellular flux analysis:

NRCMs were isolated as previously described. NRCMs were plated at a density of 850000 cells/ml in six-well plates for protein isolation or 75000 cells per well in Seahorse plates for bioenergetic assay. For the first 4 days following isolation, NRCMs were cultured in medium containing BrdU (bromodeoxyuridine;0.1 mM), 5% FBS, penicillin (100units/ml), streptomycin (100mg/ml) and vitamin B12 (2 µg/ml). On day 4 (post-isolation), NRCM medium was changed to Dulbecco's Modified Eagle's medium (DMEM) supplemented with 4 mM glutamine, 1 mM pyruvate and the corresponding treatment (5 mM D-glucose, 33 mM D-glucose or 5 mM D-glucose + 28 mM mannitol). A 5 mM D-glucose + 28 mM mannitol treatment served as the osmotic control. Cells were cultured in their respective treatment for 48 h prior to protein or bioenergetics assays.

Gene transfer and OGA inhibition: For gene transfer experiments, NRCMs were serum-starved overnight and then transduced with 100 multiplicity of infection (MOI) of replication deficient adenoviruses carrying OGT gene (Ad-OGT), OGA gene (Ad-OGA) or null virus (Ad-Null) in medium containing 5 % FBS for 5 h. After 5 h, the medium was replenished with medium lacking virus. Bioenergetics profiling and protein isolation occurred 48 h post- transduction. To pharmacologically augment O-GlcNAc levels, we used Thiamet G (TMG; Cayman Chemicals), which inhibits OGA and increases protein O-GlcNAcylation. NRCMs were treated with 1 μ M TMG or vehicle (DMSO). Bioenergetics profiling of intact NRCMs was conducted 48 h after TMG treatment. Bioenergetics profiling of permeabilized NRCMs was conducted 24 h after TMG treatment.

Bioenergetic profiling of intact, adherent cells: The bioenergetics of intact, adherent NRCMs that were seeded at 75000 cells per well was measured using a Seahorse Bioscience XF24 Flux Analyzer (Seahorse Biosciences). For these experiments, the treatment medium was replaced with 675 μ l of assay medium: unbuffered DMEM supplemented with glucose ((5 or 33 mM; or appropriate concentration of mannitol osmotic control), 4mM glutamine and 1mM pyruvate) and plates were placed in a non-CO₂ supplemented incubator 1 h before assay. Following microplate insertion, the XF24 automated protocol consisted of a 10min delay followed by baseline oxygen consumption rate (OCR) and extracellular acidification rate (ECAR) measurements (3 \times (3 min mixing, 2 min wait and 3 min measure)). To interrogate mitochondrial function, the following

compounds were injected following three baseline measurements: Port A, oligomycin; Port B, FCCP; and Port C, antimycin A (AA). After each injection, one measurement was recorded, with each having a 3 min mixing, 2 min wait and 3 min measure cycle. Stocks (1 mM) of oligomycin (Sigma), FCCP (Sigma) and AA (Sigma) were prepared in 100% DMSO(Sigma). Prior to assay, stocks were diluted in assay medium to yield 0.01 mM oligomycin, 0.01 mM FCCP and 0.1 mM AA, which, after injection, yielded final concentrations of 1.0 μ M oligomycin, 1.0 μ M FCCP and 10.0 μ M AA. All experiments were conducted at 37 ° C. Parameters of mitochondrial function were calculated as previously described. Protein concentration measured following XF analysis was not significantly different between groups.

Bioenergetic profiling of permeabilized, adherent cells: Bioenergetic profiling for electron transport chain activity was performed as recently described. Prior to bioenergetic profiling, NRCMs were changed to mannitol and sucrose (MAS) medium {220mM mannitol, 70mM sucrose, 5mM MOPS (3-(*N*-morpholino)propansulfonic acid) and 4% fatty-acid free BSA, pH 7.2). NRCMs were permeabilized following a Port A injection of 25 μ g/ml saponin. Complex II-specific substrate (10 mM succinate, 1 μ M rotenone (Rot) and 1 mM ADP) was also contained in Port A to support cellular respiration. Following State 3 rate measurements, oligomycin (1 μ g/ml) was injected from Port B; following State 4o measurement, AA (10 μ M) and Rot (1 μ M) were injected from Port C to inhibit mitochondrial oxygen consumption. Parameters of mitochondrial function were

calculated essentially as described. Protein concentration measured following XF analysis was not significantly different between groups.

Cell fractionation: NRCMs ($n=3$) were fractionated to assess O-GlcNAcylation of mitochondrial proteins following treatment with 5 or 33 mM glucose, osmotic control (5 mM glucose + 28 mM mannitol), TMG, Ad-Null or Ad-OGA. Cardiomyocytes were trypsinized with 0.25 % trypsin–EDTA (Thermo Fisher) for 5 min at 37°C. Trypsin was neutralized and cells were counted. Cardiomyocyte fractionation was performed with a standard Cell Fractionation Kit (Abcam).

Statistical analysis: Results are shown as mean \pm SD. The statistical analysis (GraphPad 5.0d) was conducted using student's t test or by one-way ANOVA followed by Newman-Keuls Multiple Comparison Test, when appropriate. Differences were considered statistically significant if $p < 0.05$.

CHAPTER IV

RESULTS

Protein O-GlcNAcylation is augmented in human HF patients

Transplant-listed patients with end-stage HF occasionally receive left ventricular assist devices (LVADs) as a bridge to transplantation due to limited availability of donor hearts. We assessed cardiac O-GlcNAc levels in patients' myocardial samples to determine whether O-GlcNAcylation was altered in failing human hearts (Figure 2). Specifically, apical cores removed during LVAD implantation were saved; this tissue served as our HF (HF) group. Cardiac tissue from severe HF patients prior to LVAD implantation (HF) demonstrated augmented protein O-GlcNAcylation when compared with patients without heart disease (Control; C) (Figure 2, $p < 0.05$). These data combined with our published data are consistent with the notion that increased protein O-GlcNAcylation is a relevant, chronic feature in human HF.

Expression of OGT, OGA are temporally altered after MI

Wild-type C57BL6J mice were subjected to Sham or MI for 5 d or 28 d and cardiac function was assessed via echocardiography. Cardiac dysfunction was exhibited within 5 d of MI and after 28 d of MI compared with Sham mice (Figure

3). Fractional shortening, ejection fraction, and cardiac output were all significantly diminished in infarcted mice 5 and 28 d post MI (Figure 3, $p < 0.05$).

Because protein O-GlcNAcylation is augmented during human HF, it was necessary to identify temporal changes in protein expression of OGT and OGA during HF. We assessed expression of OGT and OGA, and protein O-GlcNAcylation in hearts 5 d and 28 d post MI. After 5 d of MI, OGT protein and mRNA were upregulated compared to 5 d Sham (Figure 4, $p < 0.05$). After 28 d MI OGT mRNA was still upregulated; however, protein expression was not different between Sham and MI groups. OGA protein and mRNA expression remained suppressed throughout the 28 d period (Figure 4). Protein O-GlcNAcylation was upregulated after 5 d MI and remained augmented after 28 d MI (Figure 4, $p < 0.05$). These data suggest that suppression of OGA could drive augmentation of protein O-GlcNAcylation in HF. How OGA suppression occurs remains unknown. Regulators (transcriptional or posttranscriptional) of OGA expression have yet to be discovered.

Human cardiac O-GlcNAc levels

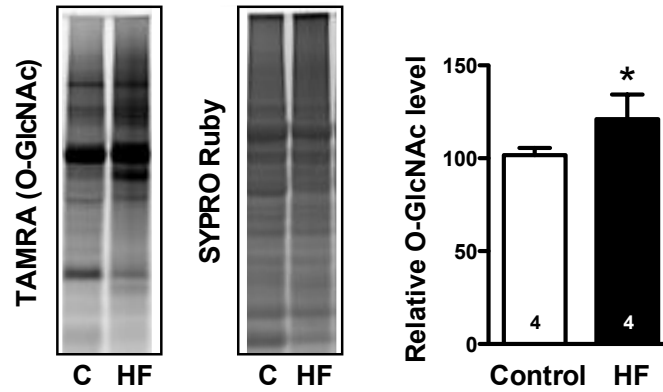


Figure 2. Protein O-GlcNAcylation is augmented in human heart failure. Human O-GlcNAcylation was measured from cardiac biopsies of disease free patients (Control; C) and heart failure (HF) patients. * $p < 0.05$ vs. control human heart group.

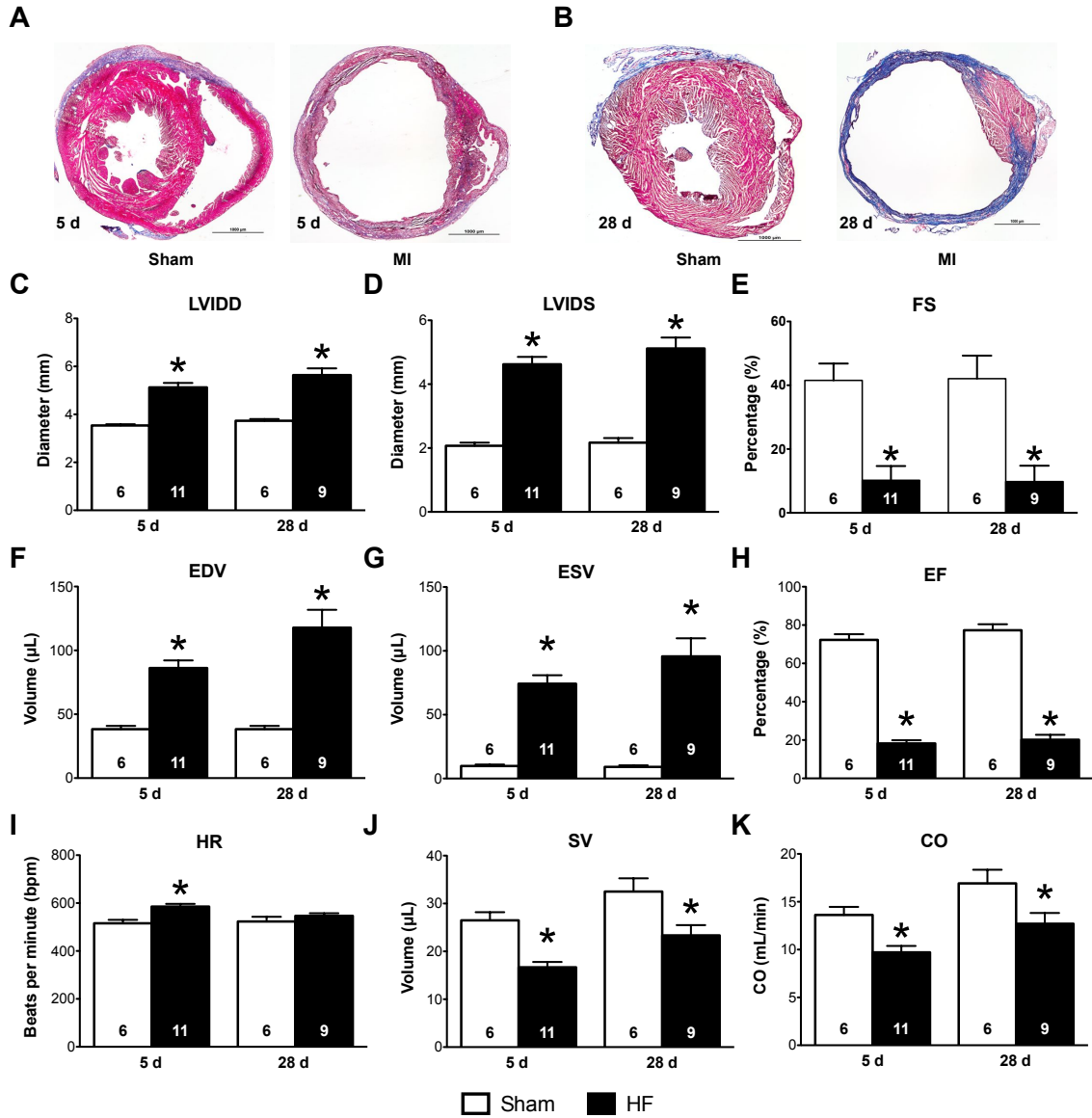


Figure 3. Myocardial infarction induces cardiac dysfunction 5 and 28 d post coronary ligation. Masson's trichrome staining shows collagen fibers (blue) and healthy myocardium (red) in sham and infarcted mouse hearts 5 d and 28 d post MI (A,B). Infarcted hearts exhibit decreased left ventricular wall thickness with increased collagen deposition and loss of myocardium compared with their respective sham hearts (A,B). Magnification at $\times 2$; scale bar = 1000 μm . Mice subjected to MI had severely dilated left ventricles (C,D), reduced fractional shortening (FS)(E), reduced ejection fraction (EF)(H), and reduced stroke volume (SV)(J). Cardiac output (CO) was significantly diminished at both 5 and 28 days (K). LVIDD, left ventricular internal diameter – diastole; LVIDS, left ventricular internal diameter – systole. * indicates a $p < 0.05$.

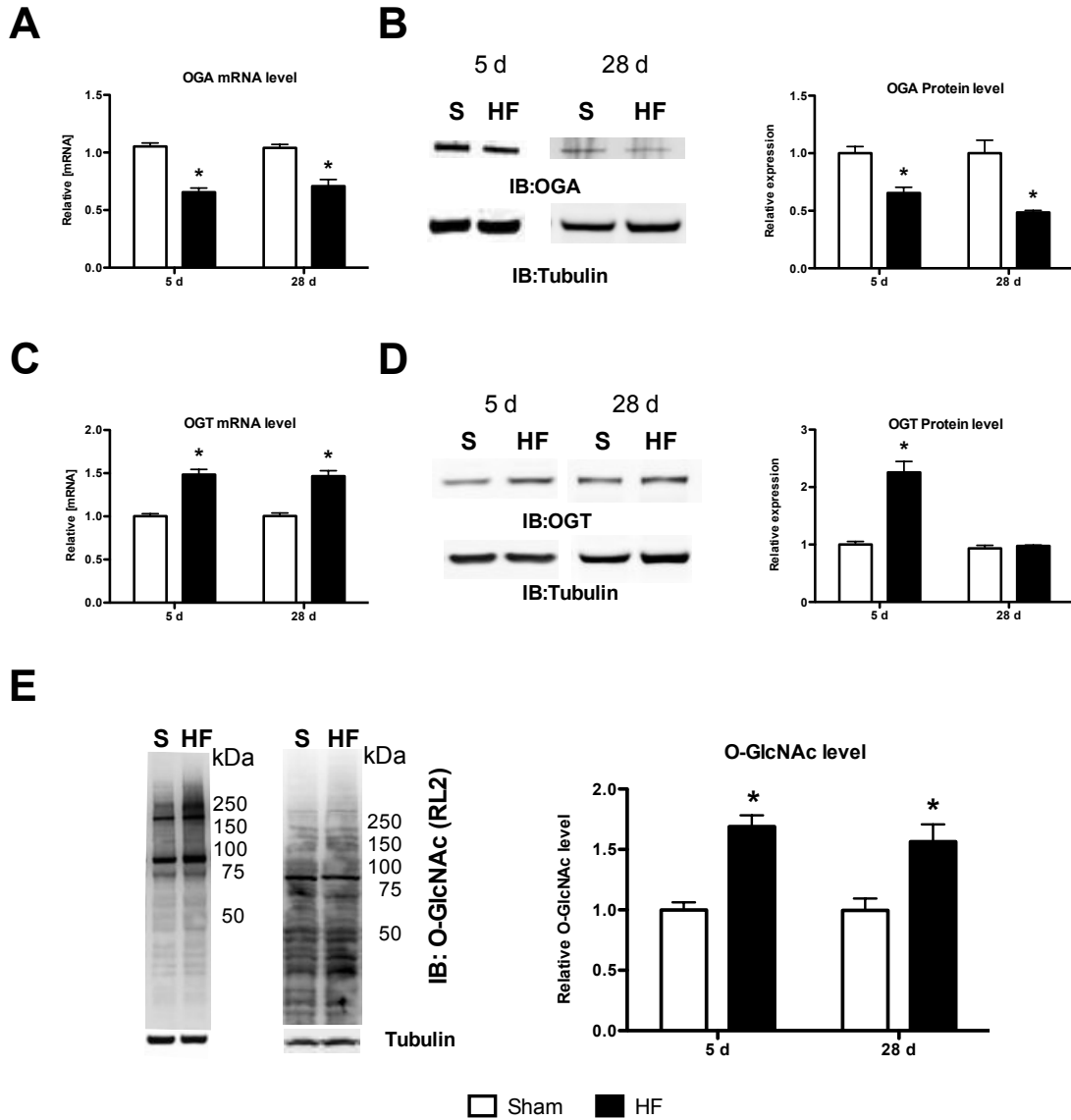


Figure 4. Down-regulation of OGA expression and increased protein O-GlcNAcylation in the failing heart. OGA expression was measured by qRT-PCR and normalized to the expression of 18 S rRNA, which shows significant down-regulation in the failing heart compared with the sham heart at 5 and 28 days (A). Western blot analysis from the 5- and 28-day failing heart shows significant down-regulation of OGA at the protein level (B). QRT-PCR analysis shows significant up-regulation of OGT in the failing heart compared with sham heart at 5 and 28 days (C). Western blot analysis shows and increased OGT protein level in 5-day failing heart but not at 28 days (D). Significant increase in protein O-GlcNAcylation compared with sham heart (E). Data are expressed as the mean \pm S.D. (n = 4/group). IB, immunoblot.

miRNA-539 is upregulated in the failing heart

Alteration of O-GlcNAc levels is not limited to heart failure. It occurs in diseases such as diabetes, cancer, and neurodegenerative disorders. In order to better understand the pathophysiology of disease it is necessary to determine the underlying mechanisms that regulate the O-GlcNAc machinery (OGT and OGA). Because OGA expression was suppressed following MI we proceeded to study the possible regulatory mechanisms of OGA expression. These possible regulatory mechanisms included miRNAs.

We assessed global miRNA expression in both 5 d and 28 d failing hearts compared with respective sham hearts. This profiling analysis revealed several miRNAs are differentially expressed in HF (Table 2). We performed target prediction analysis (TargetScan and MiRanda algorithms) and found a potential binding site in the OGA-3'UTR for miRNA-539. This binding site is conserved among mouse, rat, and human (Figure 5). Next we performed qRT-PCR to determine whether miRNA was upregulated in the failing myocardium. miRNA-539 was increased at both 5 d and 28 d post MI hearts compared with respective sham hearts. (Figure 5). Next, we determined in which region of the failing heart miRNA-539 was localized. We performed *in situ* hybridization analysis using a miRNA-539 LNA probe and demonstrated that miRNA-539 expression was upregulated in remote zone (non-infarcted) of the failing heart (Figure 5). Additionally, histomorphological analysis revealed perinuclear localization of miRNA-539 in cardiomyocytes (Figure 5). In summary, we found the first

potential negative regulator of OGA whose expression coincides with suppression of OGA protein during HF.

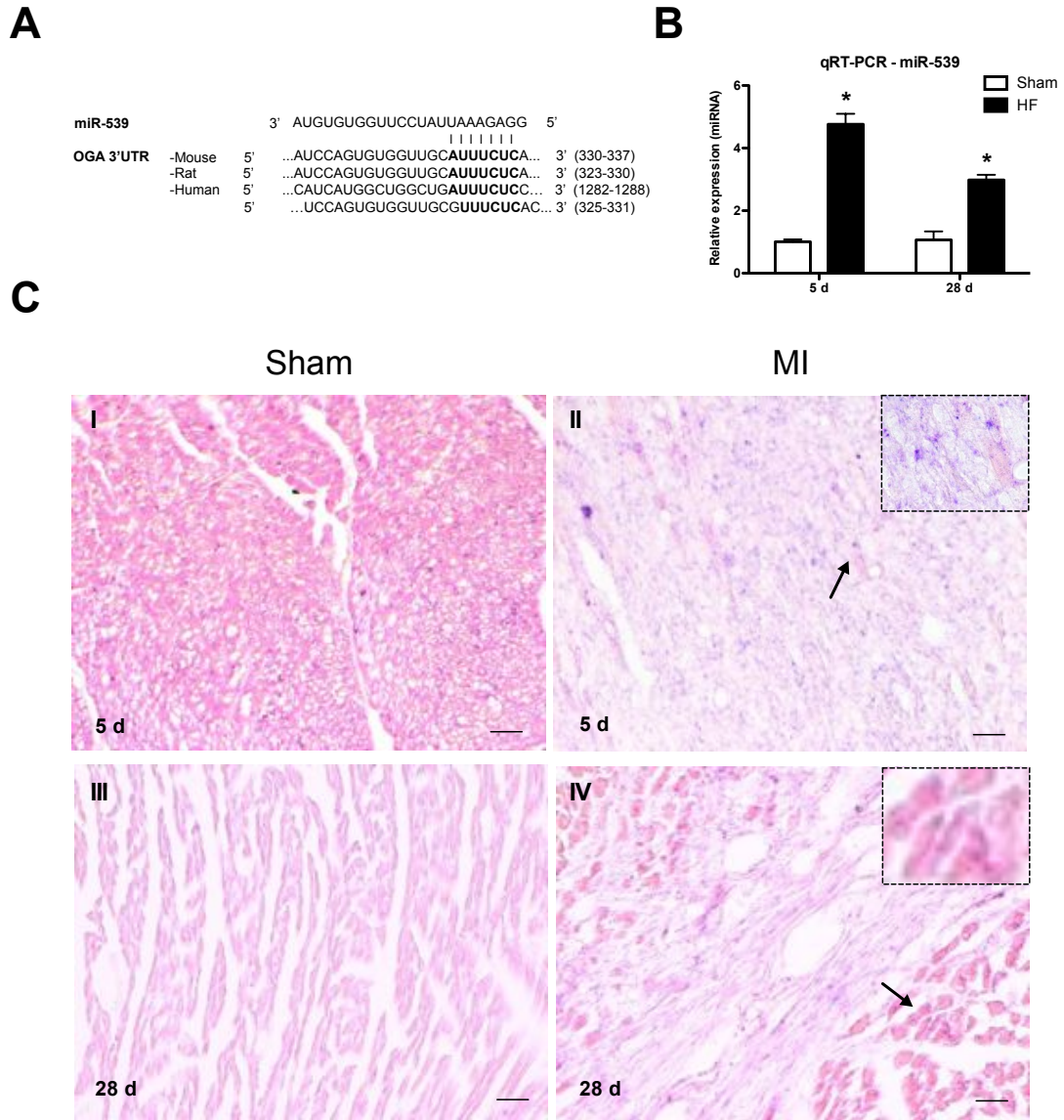


Figure 5. Up-regulation of miR-539 in the failing heart. MiR-539 binding sites in the OGA-3'UTR are conserved among mouse, rat, and human. TargetScan 6.2, where human OGA-3'UTR has two putative miR-539 binding sites (A). Expression of miR-539 was measured by qRT-PCR and normalized to the expression of U6 in each sample. The failing heart shows significant up-regulation of miR-539 in 5 and 28 d compared with sham heart (B). Probing of miR-539 LNA in the cryosections using in situ hybridization shows increased miR-539 expression (in purple) in the remote zone of the failing heart (II and IV) compared with the sham heart (I and III) (C). Histological observation also reveals perinuclear localization of miR-539 in the cardiomyocytes (insets). Low magnification images were taken at $\times 20$; insets are at $\times 60$ magnification. Scale bar = $10 \mu\text{m}$. * indicates a $p < 0.05$.

miRNA	5 d MI		28 d MI		miRNA	5 d MI		28 d MI	
	Mean	SD	Mean	SD		Mean	SD	Mean	SD
mmu-let-7g	0.54	0.04	0.48	0.01	mmu-miR-30e	0.64	0.12	0.34	0.01
mmu-miR-126-5p	0.73	0.05	0.48	0.01	mmu-miR-31	3.19	0.16	1.93	0.01
mmu-miR-127	5.89	0.34	3.87	0.01	mmu-miR-328	0.62	0.05	0.48	0.01
mmu-miR-128a	0.86	0.15	0.69	0.01	mmu-miR-335-3p	2.30	0.18	1.93	0.01
mmu-miR-133a	0.58	0.14	0.48	0.00	mmu-miR-337-3p	4.31	0.32	3.86	0.01
mmu-miR-133b	0.52	0.06	0.49	0.00	mmu-miR-337-5p	5.40	0.79	3.89	0.01
mmu-miR-135a	0.49	0.04	0.48	0.01	mmu-miR-342-3p	1.21	1.38	0.96	0.01
mmu-miR-135b	0.40	0.09	0.24	0.01	mmu-miR-345-5p	0.62	0.12	0.48	0.01
mmu-miR-139-5p	0.52	0.04	0.48	0.01	mmu-miR-34a	0.66	0.05	0.48	0.02
mmu-miR-140	1.77	0.14	1.95	0.01	mmu-miR-34b-3p	1.68	0.16	1.94	0.01
mmu-miR-142-3p	4.23	1.18	3.24	0.59	mmu-miR-351	2.91	0.17	1.94	0.03
mmu-miR-142-5p	3.80	0.25	3.23	0.01	mmu-miR-361	0.88	0.05	0.48	0.01
mmu-miR-143	0.64	0.05	0.48	0.00	mmu-miR-362-3p	2.49	0.67	1.36	0.58
mmu-miR-145	0.65	0.04	0.48	0.01	mmu-miR-376a	13.82	1.94	6.51	0.02
mmu-miR-148b	0.70	0.13	0.69	0.01	mmu-miR-376b	3.45	1.56	3.86	0.03
mmu-miR-150	0.64	0.04	0.49	0.02	mmu-miR-376c	4.34	0.28	3.89	0.01
mmu-miR-150b	2.36	0.15	1.94	0.01	mmu-miR-382	4.47	0.48	7.96	0.01
mmu-miR-181a	1.15	0.10	0.48	0.01	mmu-miR-384-5p	0.60	0.17	0.34	0.02
mmu-miR-184	4.88	2.54	4.59	0.96	mmu-miR-409-3p	7.78	3.22	7.71	0.58
mmu-miR-187	0.77	0.13	0.48	0.01	mmu-miR-410	6.91	0.36	3.92	0.01
mmu-miR-18a	4.24	1.11	2.76	0.02	mmu-miR-411	4.62	1.30	3.88	0.01
mmu-miR-194	0.61	0.15	0.48	0.58	mmu-miR-434-3p	4.00	1.12	2.74	0.58
mmu-miR-199a-3p	5.23	0.30	3.92	0.01	mmu-miR-434-5p	3.35	0.99	2.73	0.01
mmu-miR-200b	0.20	0.15	0.94	0.03	mmu-miR-486	0.46	0.04	0.49	0.01
mmu-miR-203	0.56	0.05	0.48	0.01	mmu-miR-487b	4.05	1.04	2.73	0.58
mmu-miR-204	0.57	0.14	0.49	0.01	mmu-miR-495	3.96	0.23	3.93	0.01
mmu-miR-208	0.88	0.13	0.68	0.01	mmu-miR-499	0.55	0.04	0.48	0.01
mmu-miR-21	4.59	0.39	3.95	0.01	mmu-miR-500	2.82	0.73	2.77	0.01
mmu-miR-214	4.22	1.36	2.75	0.58	mmu-miR-503	3.54	0.33	3.85	0.01
mmu-miR-215	0.66	0.04	0.48	0.02	mmu-miR-539	6.98	2.82	5.50	0.01
mmu-miR-223	3.17	0.86	1.93	0.02	mmu-miR-542-5p	0.66	0.04	0.48	0.03
mmu-miR-224	2.40	0.15	1.93	0.01	mmu-miR-543	1.79	0.16	1.94	0.00
mmu-miR-26a	0.61	0.05	0.48	0.04	mmu-miR-652	1.71	0.14	1.95	0.01
mmu-miR-296-5p	5.46	0.82	3.92	0.02	mmu-miR-667	4.73	0.27	3.82	0.01
mmu-miR-29b	1.07	0.14	0.70	0.58	mmu-miR-674	2.18	0.60	1.93	0.58
mmu-miR-30a	0.61	0.04	0.48	0.01	mmu-miR-685	1.52	0.42	1.93	0.02
mmu-miR-30b	0.56	0.04	0.49	0.02	mmu-miR-7a	2.64	0.81	1.94	0.00
mmu-miR-30c	0.52	0.11	0.34	0.58					

Table 2: MiRNA expression in the failing heart. Table shows summary of several miRNAs differentially expressed in 5 d and 28 d infarcted mouse heart by miRNA microarray analysis. miR-539 (red font) is significantly upregulated at both 5 d and 28 d in the failing hearts compared to sham hearts.

MiRNA-539 targets the OGA-3'UTR region

Next, we queried whether miRNA-539 directly targets the OGA-3'UTR. First we made a reporter plasmid with luciferase upstream to the wild-type OGA-3'UTR to serve as our control. Then we made a reporter plasmid with luciferase upstream of a miRNA-539 binding site mutant. We co-transfected these plasmids with scrambled control or miRNA-539 expression plasmids in HEK293 cells. Co-transfection of the wild-type OGA-3'UTR with miRNA-539 significantly reduced luciferase activity compared with the scrambled control ($p < 0.05$, Figure 6B). Luciferase activity was not affected with co-transfection of mutated OGA-3'UTR with miRNA-539. These findings suggest that miRNA-539 binds to the predicted OGA-3'UTR indicating a possible role in the regulation of OGA.

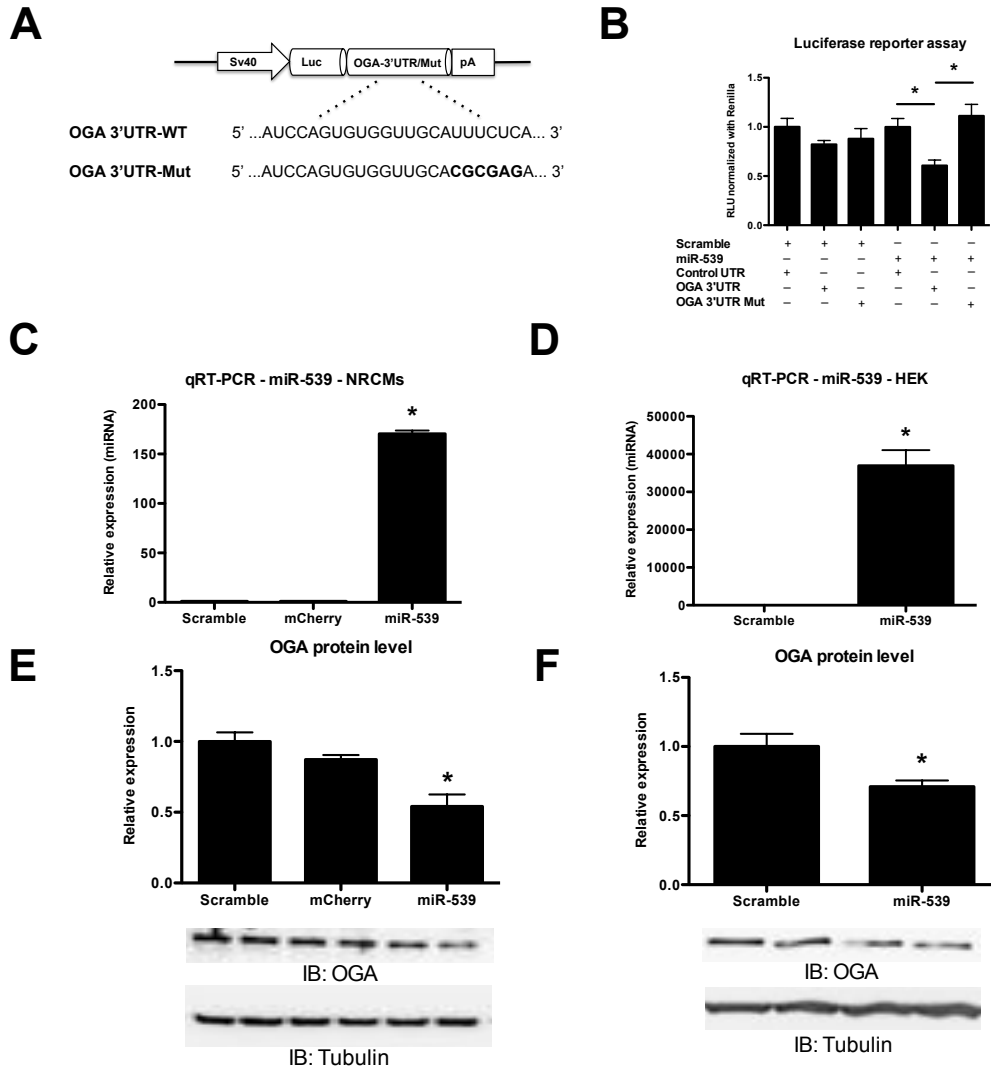


Figure 6. miR-539 regulates OGA expression. Reporter plasmid containing luciferase upstream to the OGA-3'UTR was obtained from Genecopoeia and the miR-539 binding site seed sequence (AUUUCUC) was mutated (ACGCGAG) by site-directed mutagenesis using mutated forward and reverse primers (A). Luciferase activity was measured after 48 h from HEK293 lysates co-transfected with OGA-3'UTR or miR-539 binding site mutant with scrambled or miRNA-539 expression plasmids (B). Luciferase activity was normalized with internal Renilla control. Significant down-regulation of luciferase activity was determined by miR-539 when co-transfected with OGA-3'UTR, whereas the miR-539 binding site mutation was unaffected. QPCR analysis shows significant level of miR-539 expression in NRCMs and HEK293 cells transduced with lentivirus encoding miR-539 ($n = 3/\text{group}$) compared with mCherry-transduced cells (C,D). Western blot analysis and respective quantitative analysis shows around 40 and 30% reduction of OGA expression in miR-539 overexpressing NRCMs and HEK293 cells, respectively, compared with scrambled controls ($n = 3/\text{group}$) (E,F). IB, immunoblot. * indicates a $p < 0.05$.

miRNA-539 suppress OGA expression *in vitro*

Because we verified that miRNA-539 binds OGA-3'UTR, we then queried whether this interaction would affect OGA expression. We designed a lentivirus to overexpress miR-539 in neonatal rat cardiomyocytes (NRCMs) and human HEK293 cells. Transduction of NRCMs and HEK293 cells resulted in 170-fold and 35,000-fold respective increase in miR-539 compared with a scrambled control lentivirus (Figure 6 C,D). This upregulation of miRNA-539 resulted in a reduction of OGA protein expression by 40% in NRCMs and 30% in HEK293 compared with mCherry-transduced NRCMs or scrambled control respectively (Figure 6 E,F). Inhibition of miRNA-539 rescued OGA expression in NRCMs and HEK293 overexpressing miRNA-539 (Figure 7).

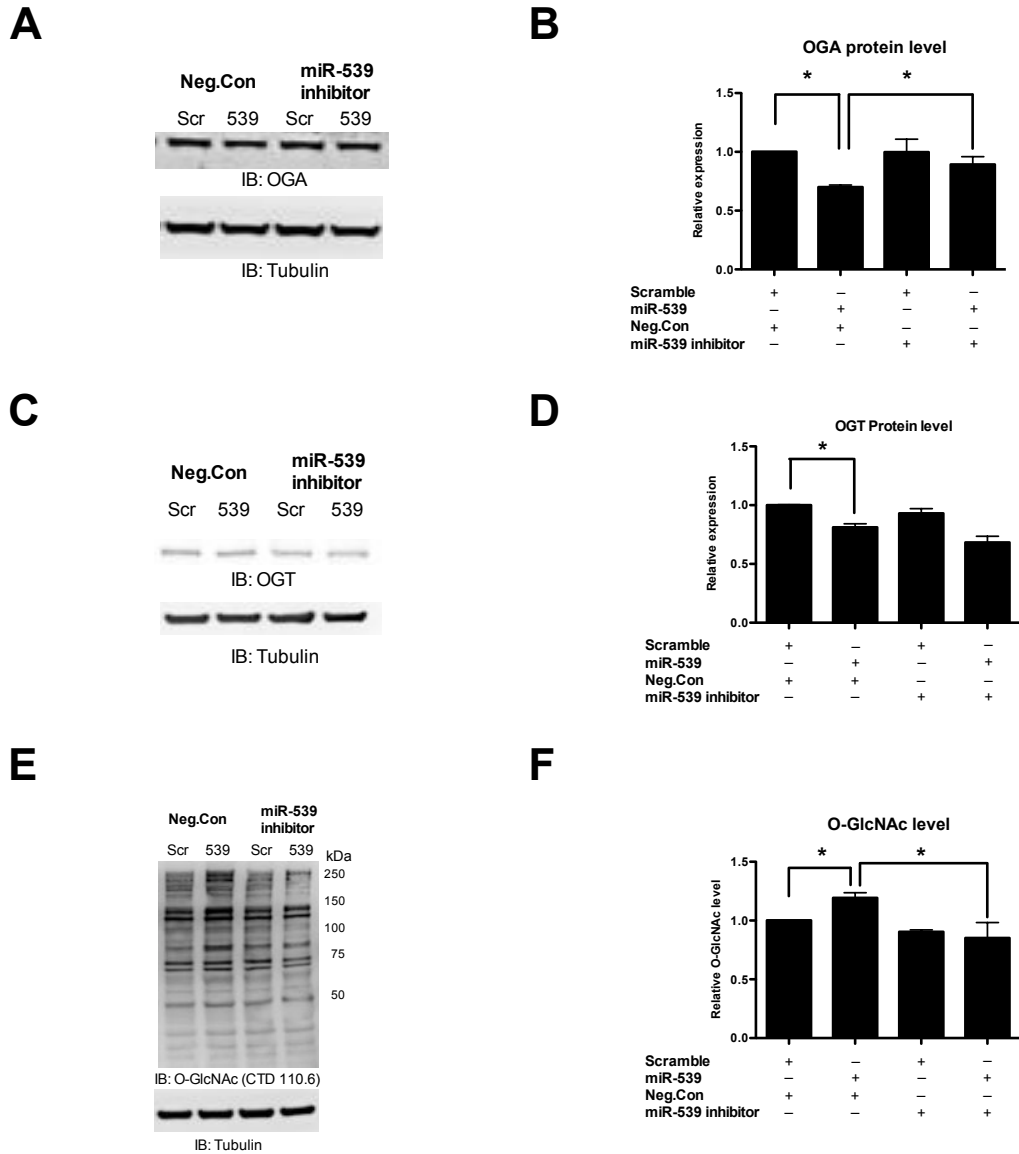


Figure 7. Inhibition of miR-539 rescues OGA expression and O-GlcNAcylation in NRCMs. Western blot analysis shows a significant reduction of OGA and OGT levels transduced with miRNA-539 upon negative control treatment, whereas anti-miR-539 transfection rescued the OGA expression toward the normal level (n = 3/group) (A-D). Western blot analysis shows a significant increase in protein O-GlcNAcylation by miR-539 overexpression, and inhibition of miR-539 brought the O-GlcNAc level to normal (n = 3/group) (E,F). IB, immunoblot. * indicates a p < 0.05.

Because induction of miRNA-539 was sufficient to reduce OGA protein levels, we assessed whether this reduction mediated a change in protein O-GlcNAcylation. Overexpression of miRNA-539 significantly increased O-GlcNAc levels ($p < 0.05$, Figure 8) compared with scrambled control. Inhibition of miRNA-539 equilibrated O-GlcNAc to control levels (Figure 8). MiRNA-539 is negative regulator of OGA and consequently induces protein O-GlcNAcylation.

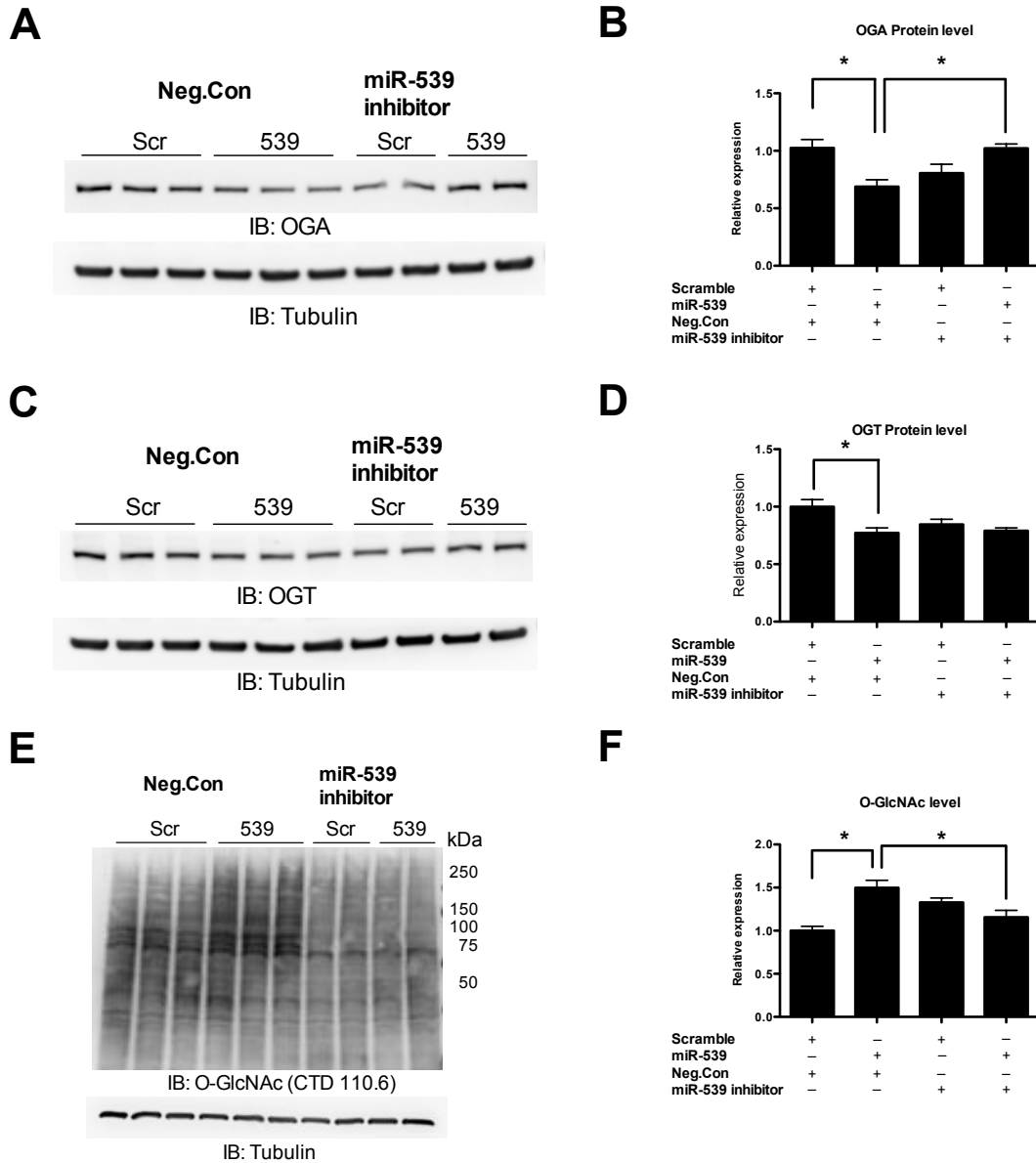


Figure 8. Negative regulatory effect of miR-539 on OGA expression in human, non-cardiac cell types. Western blot analysis shows a significant reduction of OGA and OGT levels in HEK293 cells transfected with miR-539; anti-miR-539 transfection rescued OGA expression toward the basal level ($n = 3/\text{group}$) (A-D). Western blot analysis shows a significant increase in protein O-GlcNAcylation by miR-539 overexpression, and inhibition of miR-539 returned O-GlcNAc levels to normal ($n = 3/\text{group}$) (E,F). IB, immunoblot. * indicates a $p < 0.05$.

Hypoxia-reoxygenation increases miR-539 and suppresses OGA expression

Despite demonstrating that miRNA-539 is upregulated in the failing heart, the miRNA-539-mediated regulation of OGA we observed was conducted in an *in vitro* setting devoid of a pathological insult. As such, we wanted to test whether a similar pathological stimulus would elicit miRNA-539 upregulation *in vitro*. We chose hypoxia-reoxygenation to serve as a pathological proxy for MI in NRCMs. NRCMs were subjected to 3 h of hypoxia and 3, 6, and 12 h of reoxygenation. MiRNA-539 and OGA protein expression were assessed at each time point. MiRNA-539 was augmented after 3 h of hypoxia, which was concomitant with suppression of OGA protein at 6 and 12 h after reoxygenation ($p < 0.05$, Figure 9). Thus, the induction of miRNA-539 and subsequent suppression of OGA occurs following hypoxic conditions.

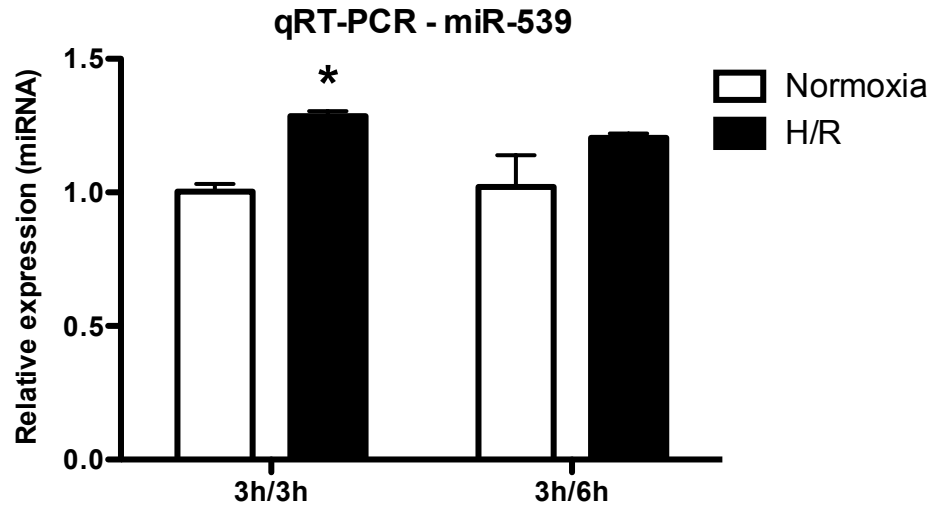
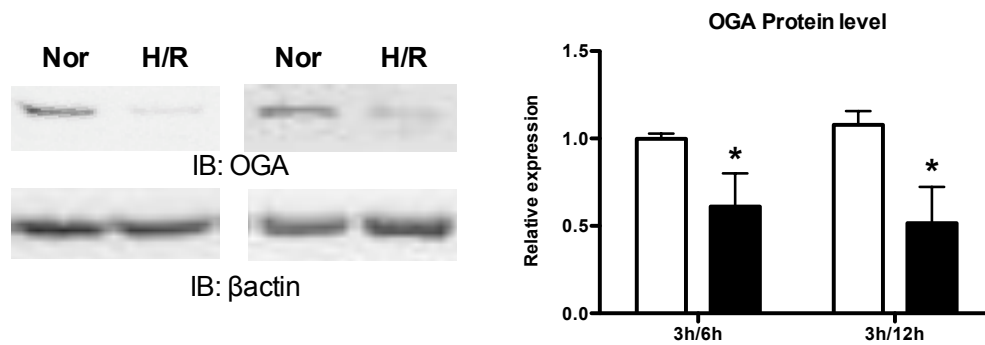
A**B**

Figure 9. Hypoxia-reoxygenation induces miR-539 expression followed by a decrease in OGA expression. NRCMs subjected to 3 h of hypoxia were reoxygenated for 3, 6, and 12 h. qRT-PCR analysis shows a significant increase in miR-539 expression at 3 h reoxygenation (A). Western blot analysis shows a significant decrease in OGA protein level at both 6 and 12 h of reoxygenation ($n = 4/\text{group}$) (B). IB, immunoblot. * indicates a $p < 0.05$.

Generation of an inducible cardiomyocyte-specific OGA knockout mouse

We have shown that suppression of OGA occurs through 4 wk of HF and that may be sufficient to augment protein O-GlcNAcylation. In addition, negative transcriptional regulators of OGA are upregulated to mediate suppression of OGA. Hence, suppression of OGA may be a proadaptive process in HF. We hypothesized that ablation of OGA may favor O-GlcNAcylation and attenuate HF. To test this hypothesis, it was necessary to generate a model where we could ablate cardiomyocyte OGA and augment O-GlcNAcylation.

We developed both a constitutive and inducible model of OGA ablation through breeding of a MHC cre or Mer Cre Mer mice with OGA floxed mice. The constitutive OGA knockout resulted in suppression of cardiac OGA mRNA and protein (data not shown) compared to WT mice. Despite generating a successful constitutive KO, we were not able to generate sufficient cohorts to execute a HF study. As such, we focused on an inducible cardiomyocyte specific model of OGA ablation. To generate the inducible OGA knockout, we crossed an OGA floxed mouse with an alpha MHC driven Mer-Cre-Mer mouse (Figure 10). This cross led to the production of an inducible cardiomyocyte-specific knockout of OGA following the administration of tamoxifen. To verify successful cardiac depletion of OGA, we harvested hearts 5 d post tamoxifen treatment and assessed OGA expression. OGA mRNA and protein levels were significantly reduced and cardiac O-GlcNAcylation was enhanced in the OGA ablated hearts (Figure 11 and 12). To demonstrate that OGA deletion was specific to the heart, we isolated protein from skeletal muscle, kidney, and lung. OGA expression was

unaltered in these tissues (Figure 12). Thus, we generated an inducible cardiomyocyte-specific KO of OGA.

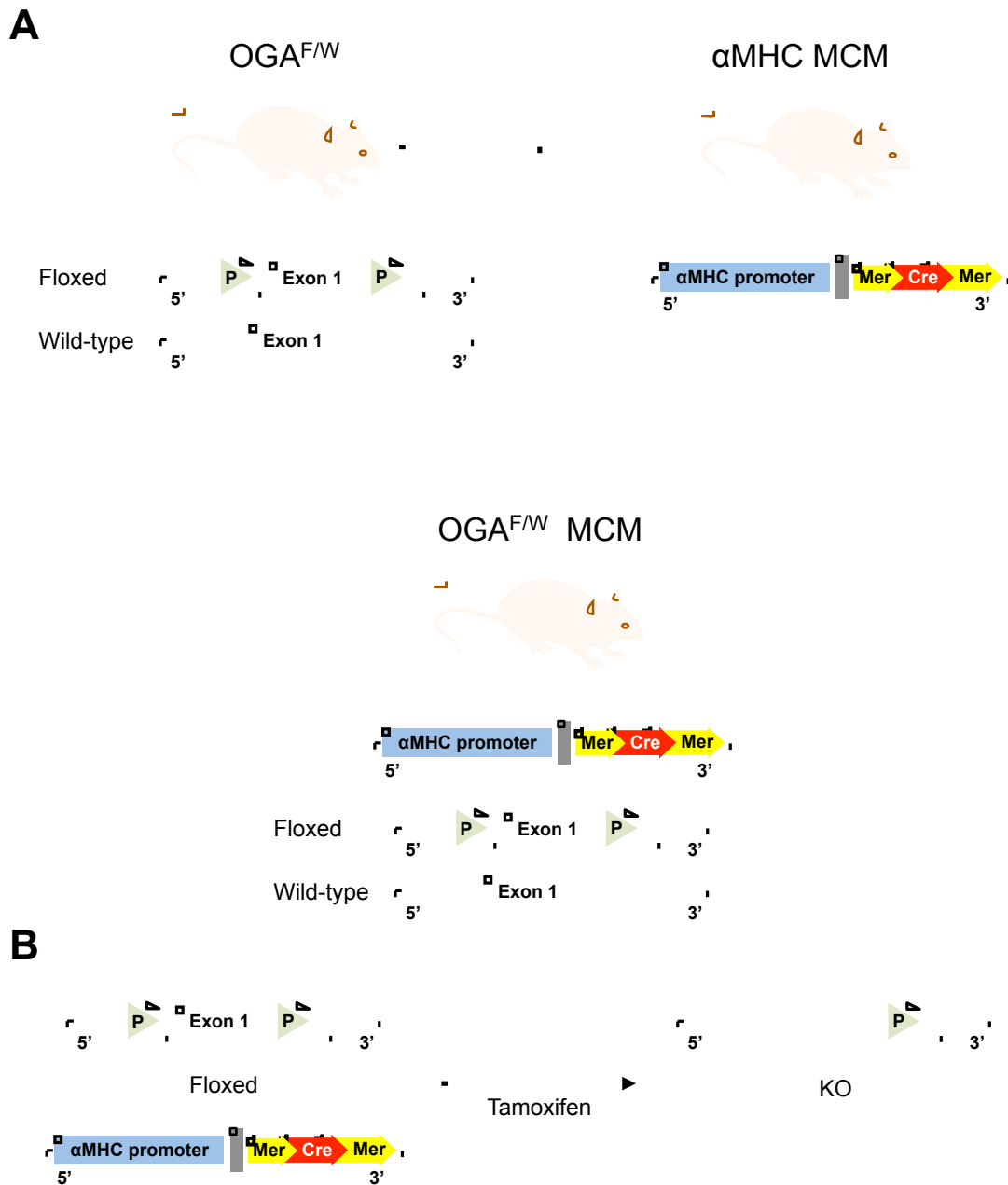


Figure 10. Scheme generation of inducible cardiomyocyte specific OGA ablation in mice. A) OGA floxed mice were cross with αMHC driven cre recombinase mouse to generate inducible OGA KO. (B) Induction of tamoxifen results in deletion of OGA containing exon.

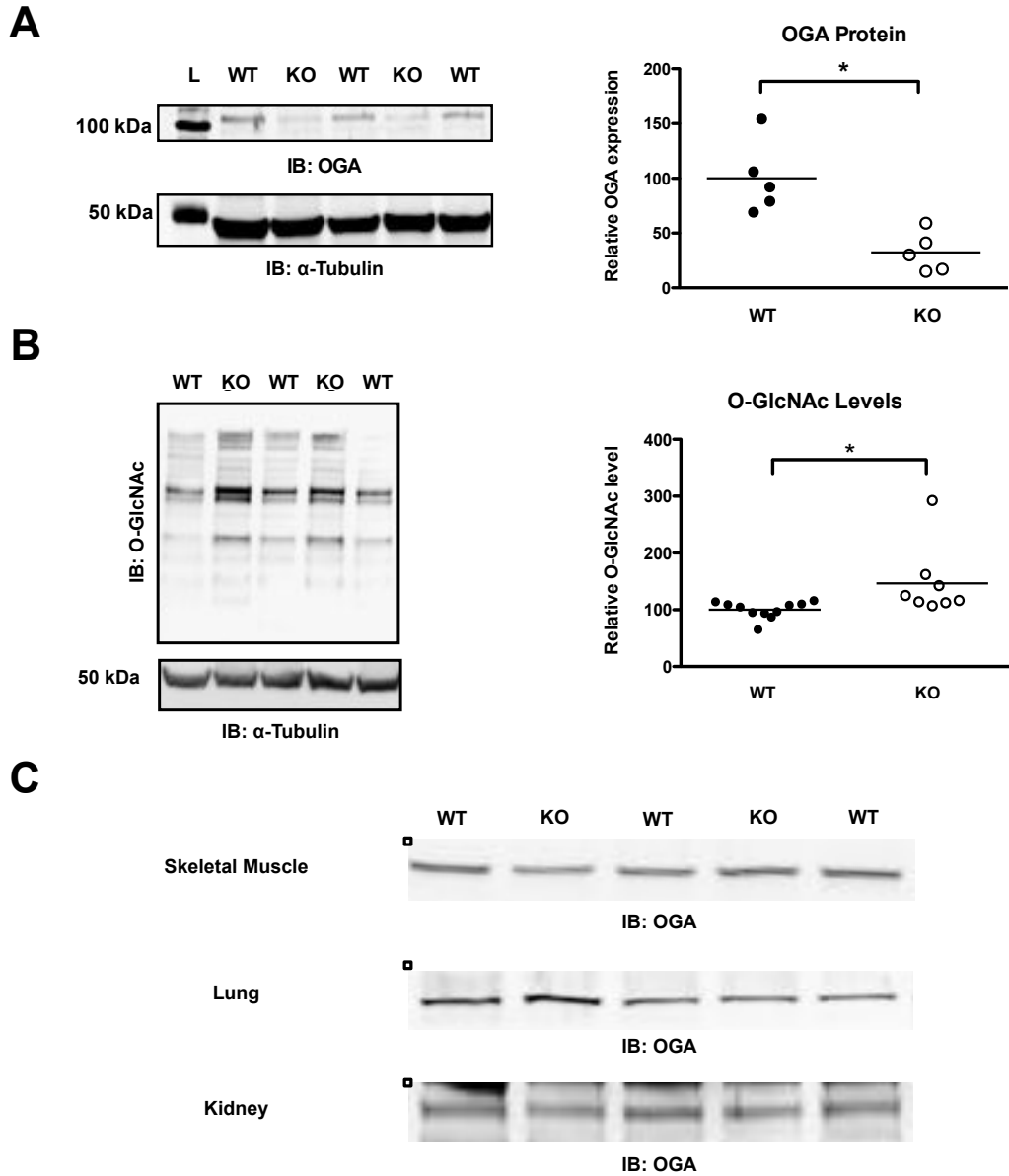


Figure 11. OGA ablation depresses OGA expression in the heart. Surgically naïve WT and OGA KO mice were harvest 5 d post tamoxifen. Immunoblot of cardiac OGA protein expression (A). Immunoblot of cardiac protein O-GlcNAcylation (B). Immunoblots of OGA protein in skeletal muscle, lung, and kidney from WT and OGA KO mice (C). * indicates a $p < 0.05$.

Next, we queried whether cardiomyocyte OGA deletion was sufficient to alter cardiac function. First, we verified that the MCM gene alone was insufficient to induce cardiac dysfunction (Figure 12). Then, we subjected OGA^{F/W}MCM⁺ positive and OGA^{W/W} (wild-type), MCM⁺ mice to echocardiography at baseline (prior to tamoxifen) and up to 8 weeks post tamoxifen treatment. Parameters of cardiac function remained unaltered despite ablation of OGA (Figure 13). Neither induction of MCM alone nor ablation of OGA was sufficient to induce cardiac dysfunction in surgically naïve mice.

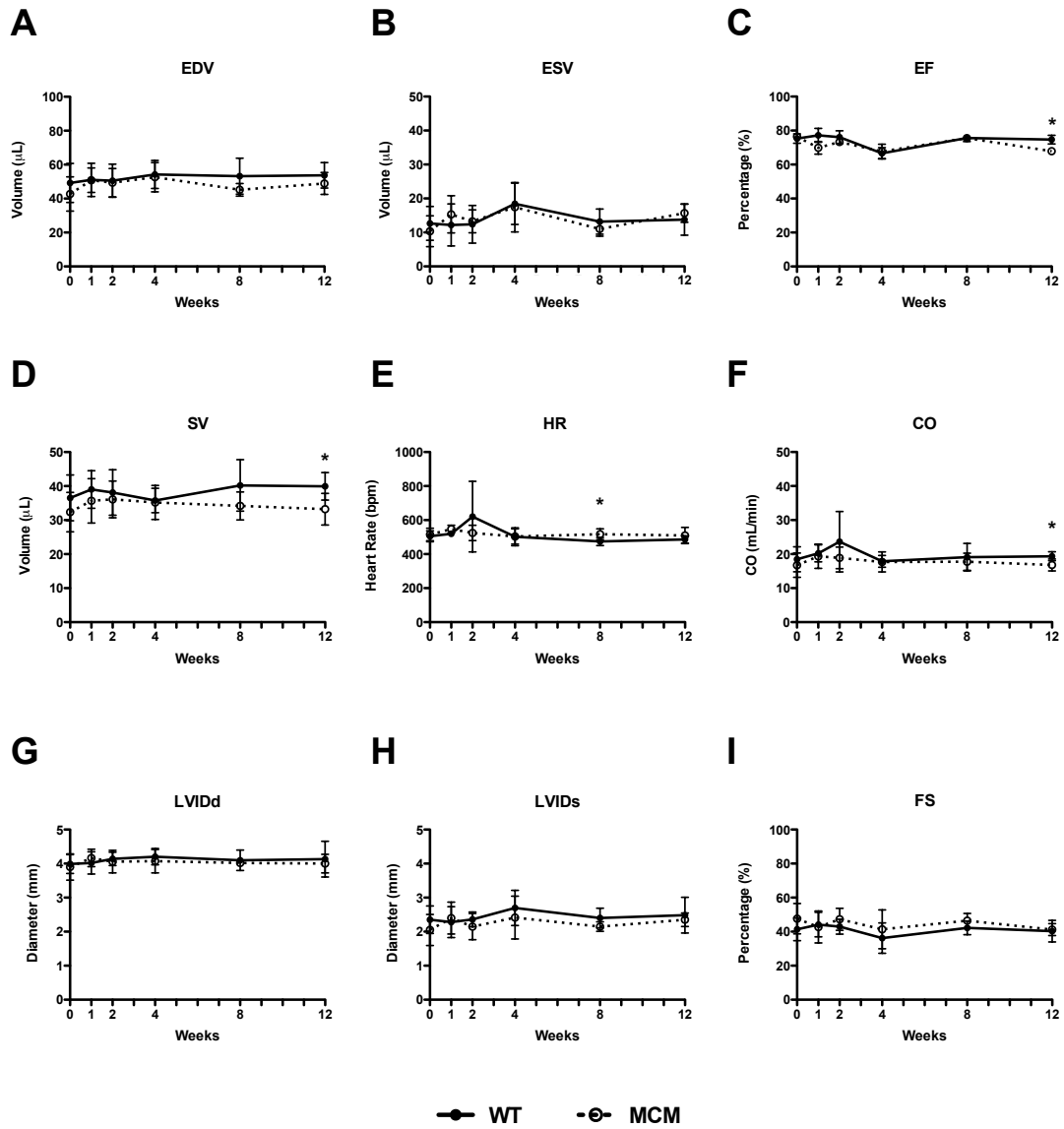
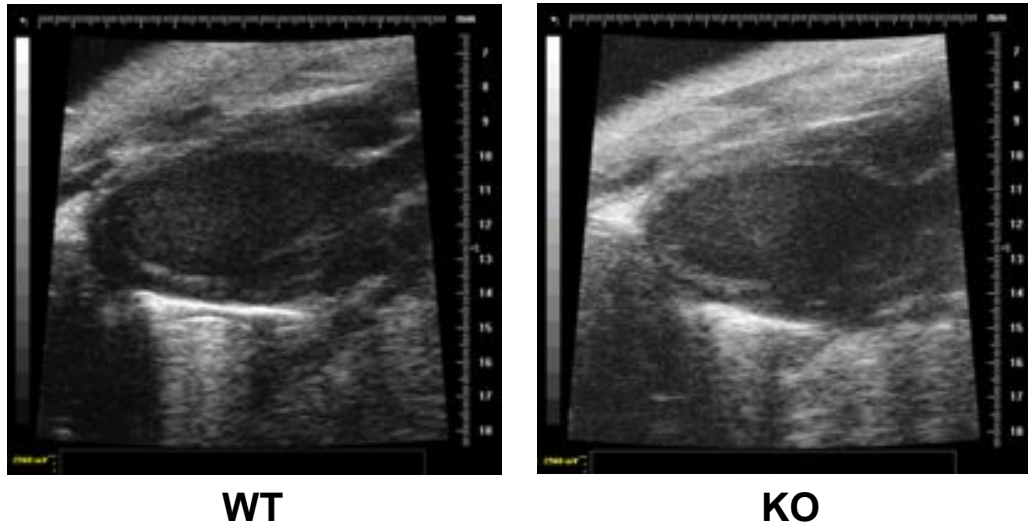


Figure 12. MerCreMer does not induce cardiac dysfunction. WT and MCM+ mice were subjected to echocardiography at baseline, and 1, 2, 4, and 8 wk post tamoxifen injection. EDV; end-diastolic volume. ESV; end-systolic volume. EF; Ejection fraction. SV; stroke volume. HR; heart rate. CO; cardiac output. LVIDd; left ventricular inner diastolic diameter. LVIDs; left ventricular systolic inner diameter. FS; fractional shortening. * indicates a $p < 0.05$.

A



B

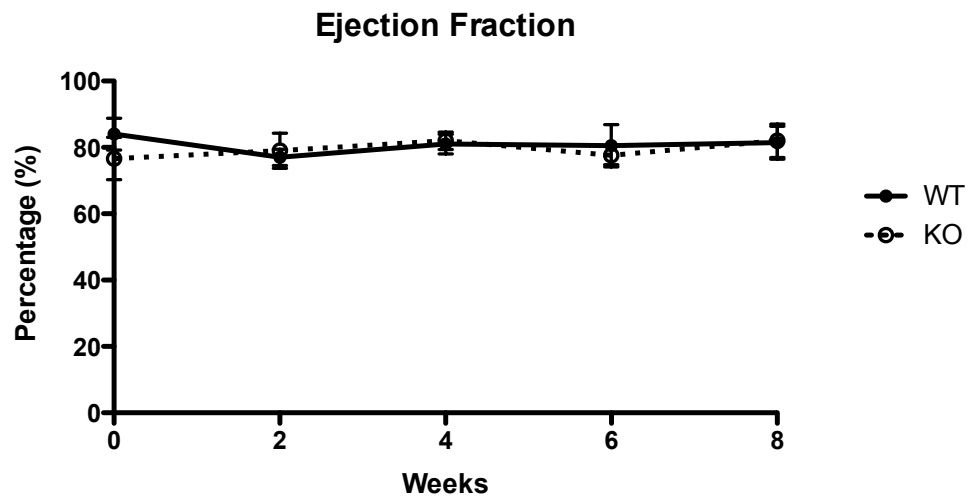


Figure 13. OGA KO does not induce cardiac dysfunction. Surgically Naïve WT and OGA KO mice were subjected to echocardiography at baseline, 2, 4, 6, and 8 wk post tamoxifen injection. Representative frames from B-mode imaging of WT and OGA KO hearts 8 week post tamoxifen (A). Ejection fraction (EF) (B). n=4 WT; n=3 OGA KO.

We then tested the hypothesis that ablation of OGA would attenuate HF.

We subjected mice to inducible OGA deletion and performed MI. Mice were

subjected to echocardiography 1 and 4 wk post MI. Surprisingly, cardiac dimensions were altered in infarcted OGA KO hearts; they were more dilated than the WT (Figure 14). Moreover, OGA ablation hastened cardiac dysfunction when compared with WT control (Figure 15, $p < 0.05$). However, after 4 wk there was no difference in cardiac function between OGA KO and WT (Figure 16). OGA suppression and augmentation of O-GlcNAcylation were preserved 4 wk post MI in OGA KO hearts compared to WT hearts (Figure 16, $p < 0.05$). We assessed infarct size after 24 h of MI to determine whether the hastening of HF could be attributed to differences in infarct size between the two groups; however, we found no discernable difference in infarct size (Figure 17). Ablation of OGA prior to MI hastens HF within one week.

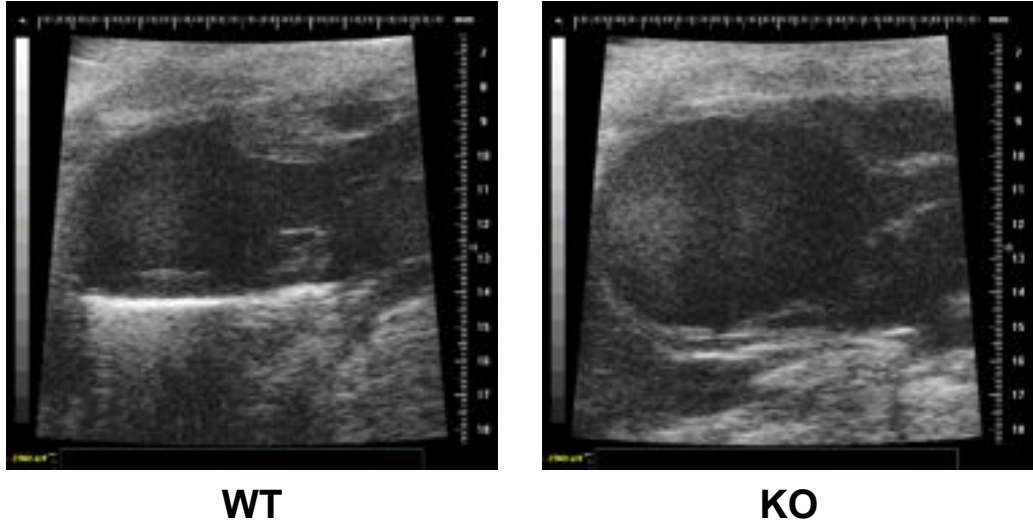


Figure 14. Cardiac dimensions are altered in infarcted OGA KO hearts. Representative frames from B-mode imaging of WT and OGA KO hearts 1 week post MI.

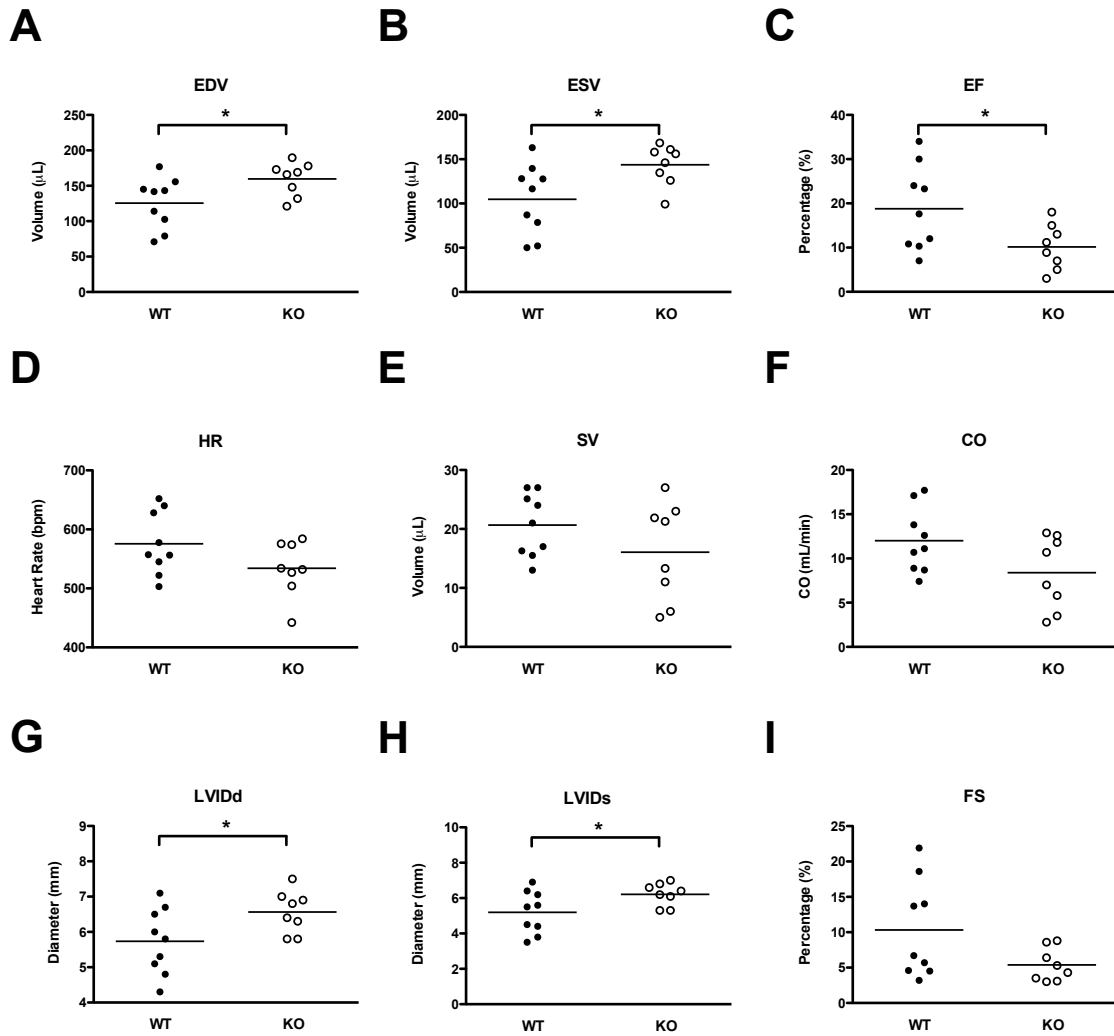


Figure 15. OGA KO exacerbates infarct-induced cardiac dysfunction. OGA KO and WT mice were subjected to tamoxifen treatment to induced OGA deletion. Mice were subjected to MI 5 d post tamoxifen and subjected to echocardiography after 1 wk. EDV; end-diastolic volume. ESV; end-systolic volume. EF; Ejection fraction. SV; stroke volume. HR; heart rate. CO; cardiac output. LVIDd; left ventricular inner diastolic diameter. LVIDs; left ventricular inner systolic diameter. FS; fractional shortening. * indicates a p<0.05.

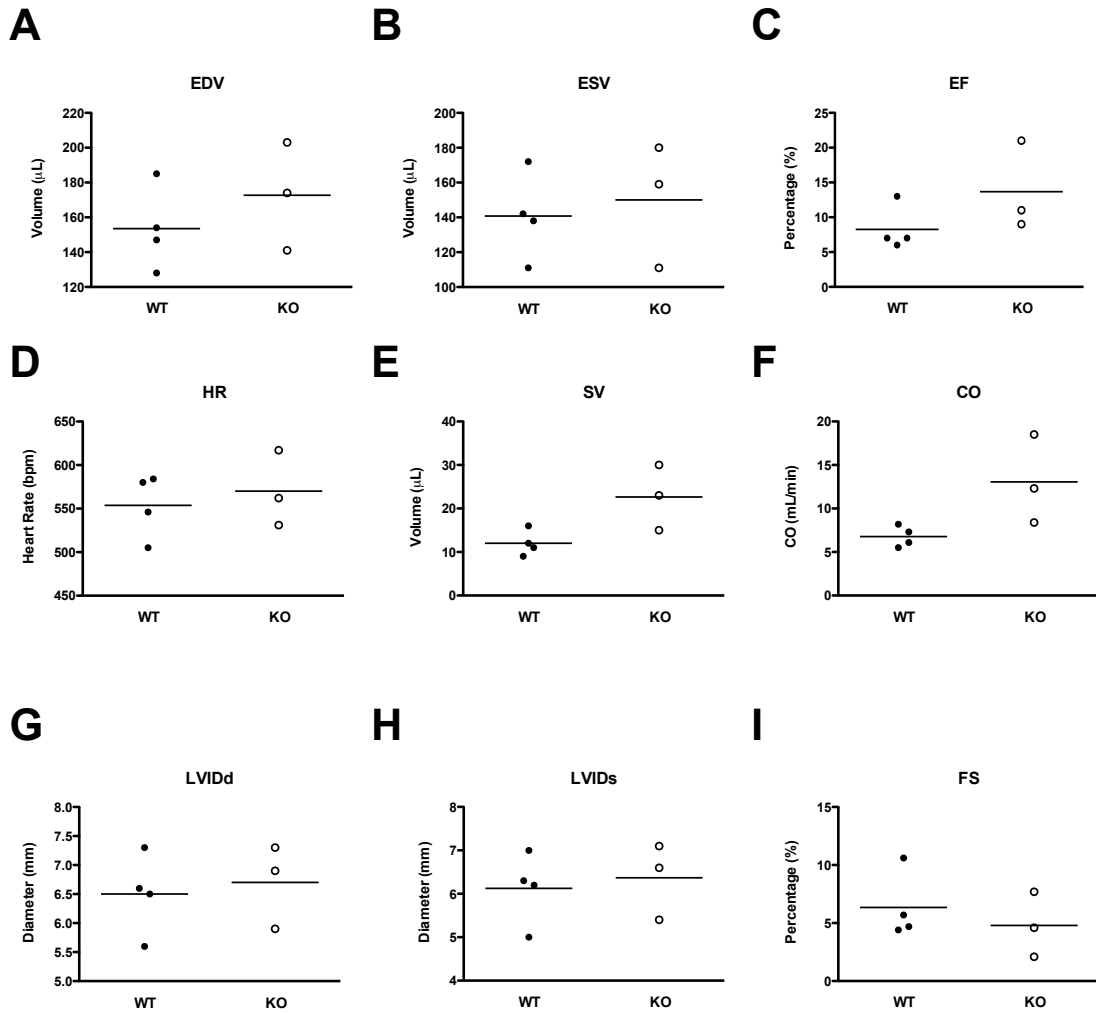


Figure 16. OGA deletion does not alter cardiac function at 4 wk post MI. OGA KO and WT mice were subjected to tamoxifen treatment to induced OGA deletion. Mice were subjected to MI 5 d post tamoxifen and subjected to echocardiography after 4 wk. EDV; end-diastolic volume. ESV; end-systolic volume. EF; Ejection fraction. SV; stroke volume. HR; heart rate. CO; cardiac output. LVIDd; left ventricular inner diastolic diameter. LVIDs; left ventricular systolic inner diameter. FS; fractional shortening. * indicates a $p < 0.05$.

24 h infarct analysis

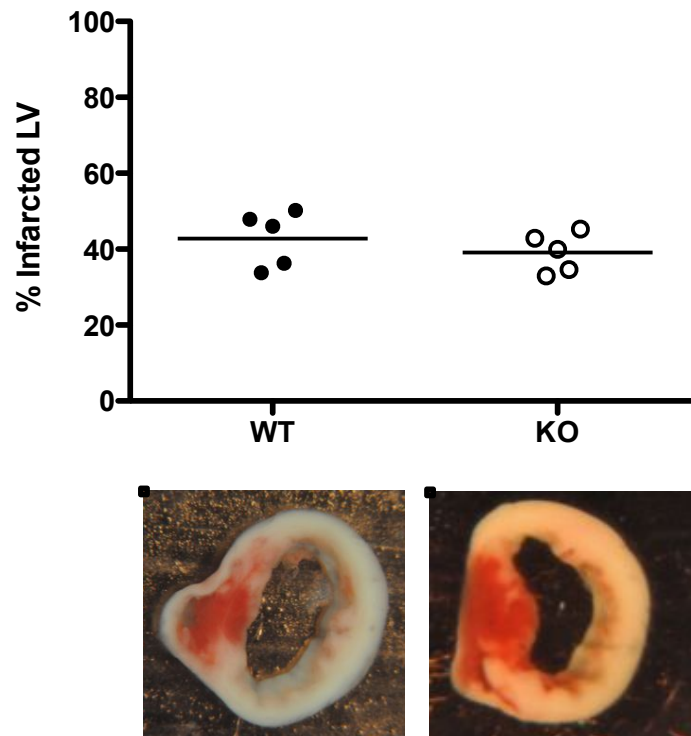
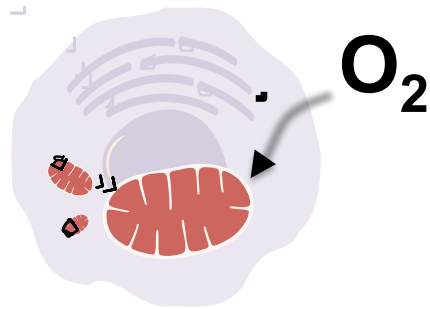


Figure 17. Cardiac OGA KO does not affect infarct area. WT and OGA KO mice were subjected to MI for 24 h. Hearts were harvested and stained with TTC. Infarct area was measured.

OGA or OGT overexpression does not alter bioenergetic reserve

In the previous *in vivo* studies, we demonstrated that ablation of OGA hastened cardiac dysfunction following 1 wk of MI. We suspected that this hastening in the decline of cardiac function could be due to suppression of mitochondrial function. Because augmented O-GlcNAcylation has been associated with mitochondrial dysfunction, we queried whether modulation of O-GlcNAcylation through altering expression or activity of OGA and OGT would affect mitochondrial respiration. Therefore, we used extracellular flux analysis to assess parameters of mitochondrial function in NRCMs (Figure 18). NRCMs were transduced with adenovirus containing either OGT or OGA genes prior to euglycemic glucose treatment for 48 h (Figure 19). Transduction resulted in a corresponding increase in OGT and OGA protein expression (Figure 19A) and commensurate changes in protein O-GlcNAcylation (Figure 19B). Overexpression of either OGT (n=5) or OGA (n=5) induced a small but statistically significant depression in basal respiration (Figure 19C,D), and OGA overexpression decreased proton leak (Figure 19; $p < 0.05$). Overexpression of neither OGT nor OGA affected maximal respiration or reserve capacity (Figure 19E,F). Thus, neither promoting nor antagonizing O-GlcNAcylation via genetic means was sufficient to cause substantial mitochondrial dysfunction.

A



B

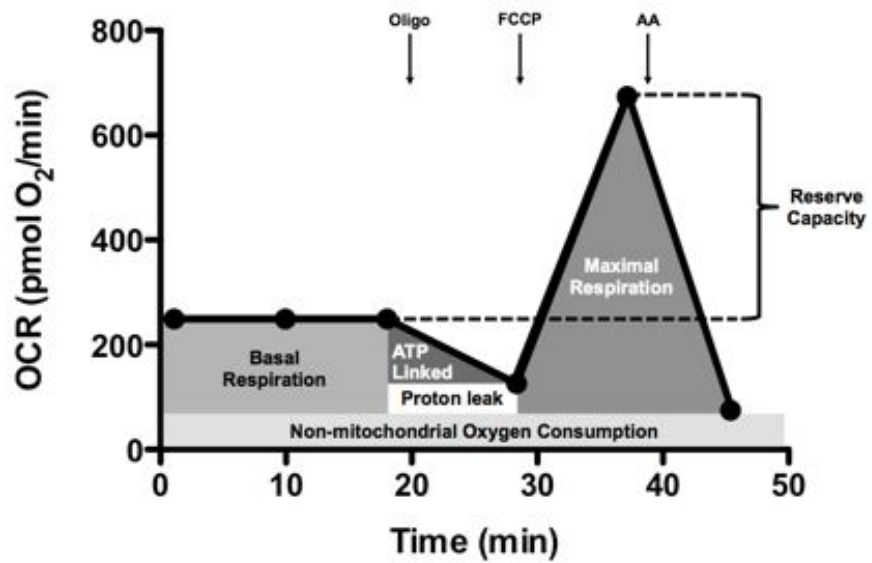


Figure 18. Extracellular flux analysis (XF). A) XF measures cell oxygen consumption. B) Parameters of mitochondrial function assessed during XF analysis. Adapted from *Sansbury et al. Chem Biol Interact. 2011.*

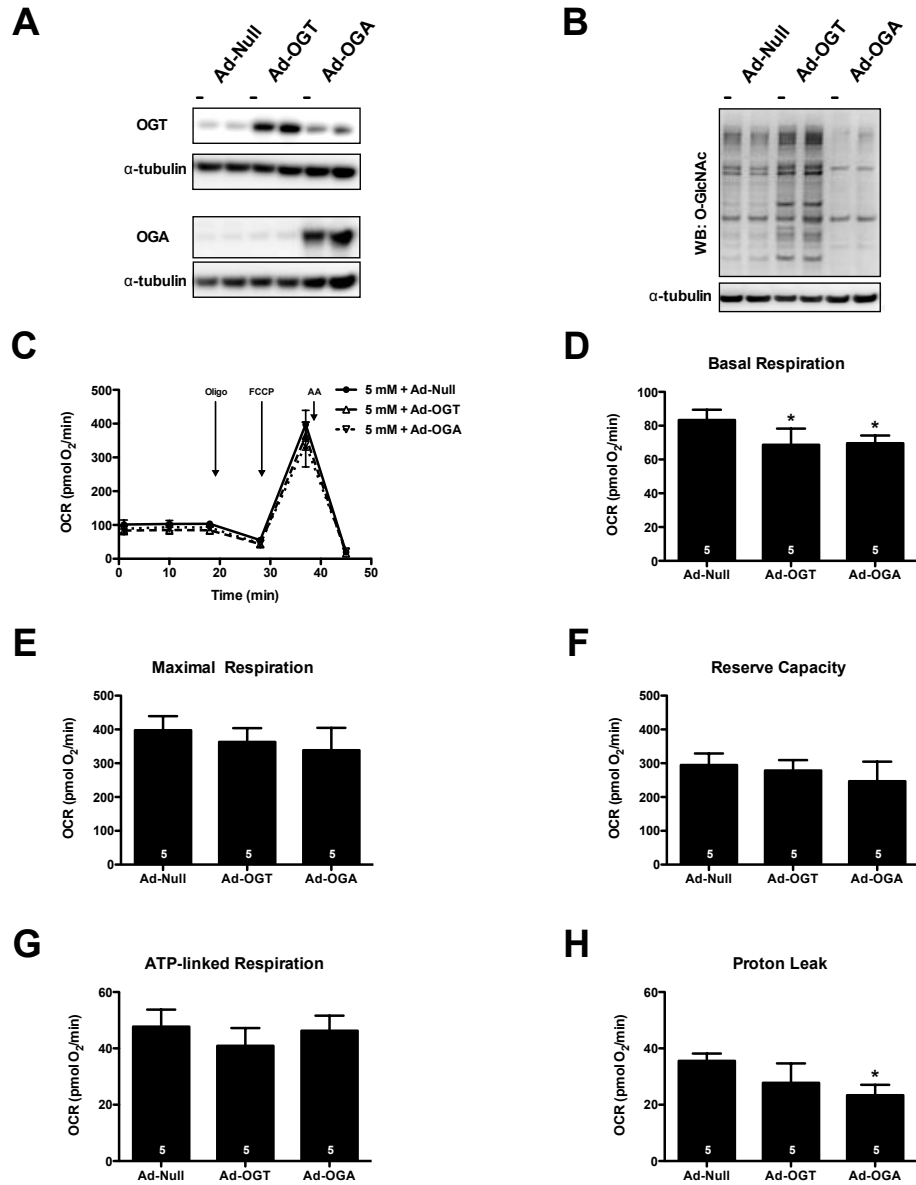


Figure 19. Overexpression of OGT or OGA does not affect bioenergetic reserve. NRCMs were subjected to adenoviral overexpression of OGT and OGA. A) Immunoblot for OGT and OGA protein expression following adenoviral treatment. B) Immunoblot for protein O-GlcNAcylation demonstrated an induction of O-GlcNAc in response to Ad-OGT and a reduction in response to Ad-OGA. C) Mitochondrial function assay of NRCMs 48 h post-transfection. Parameters of mitochondrial function were calculated from part C) including: D) Basal respiration, E) Maximal respiration, F) Reserve capacity, G) ATP-linked respiration, and H) Proton leak. As indicated in bars n=5 independent experiments, * indicates p<0.05, vs. Ad-Null

Inhibition OGA does not affect oxygen consumption in NRCMs

To further investigate whether protein O-GlcNAcylation could be responsible for the bioenergetic derangement, we used a potent pharmacologic inhibitor of OGA, Thiamet G (TMG), to increase robustly whole cell protein O-GlcNAcylation (Figure 20A, B). To determine whether mitochondrial proteins were indeed O-GlcNAcylated we isolated mitochondrial fractions from vehicle and TMG treated NRCMs. We observed O-GlcNAcylated mitochondrial proteins, but there was no net significant increase in protein O-GlcNAcylation, with the exception of one band (n=3, Figure 20C). Regardless, XF analysis in the intact cell preparations indicated that TMG did not significantly affect basal respiration, maximal respiration, or reserve capacity (Figure 20, D-F). TMG treatment slightly but significantly decreased ATP-linked respiration (Figure 20H); however, proton leak (Figure 20I) and non-mitochondrial OCR (data not shown) were not different. Thus, inhibition of OGA (via TMG) increased O-GlcNAcylation but did not suppress mitochondrial reserve capacity.

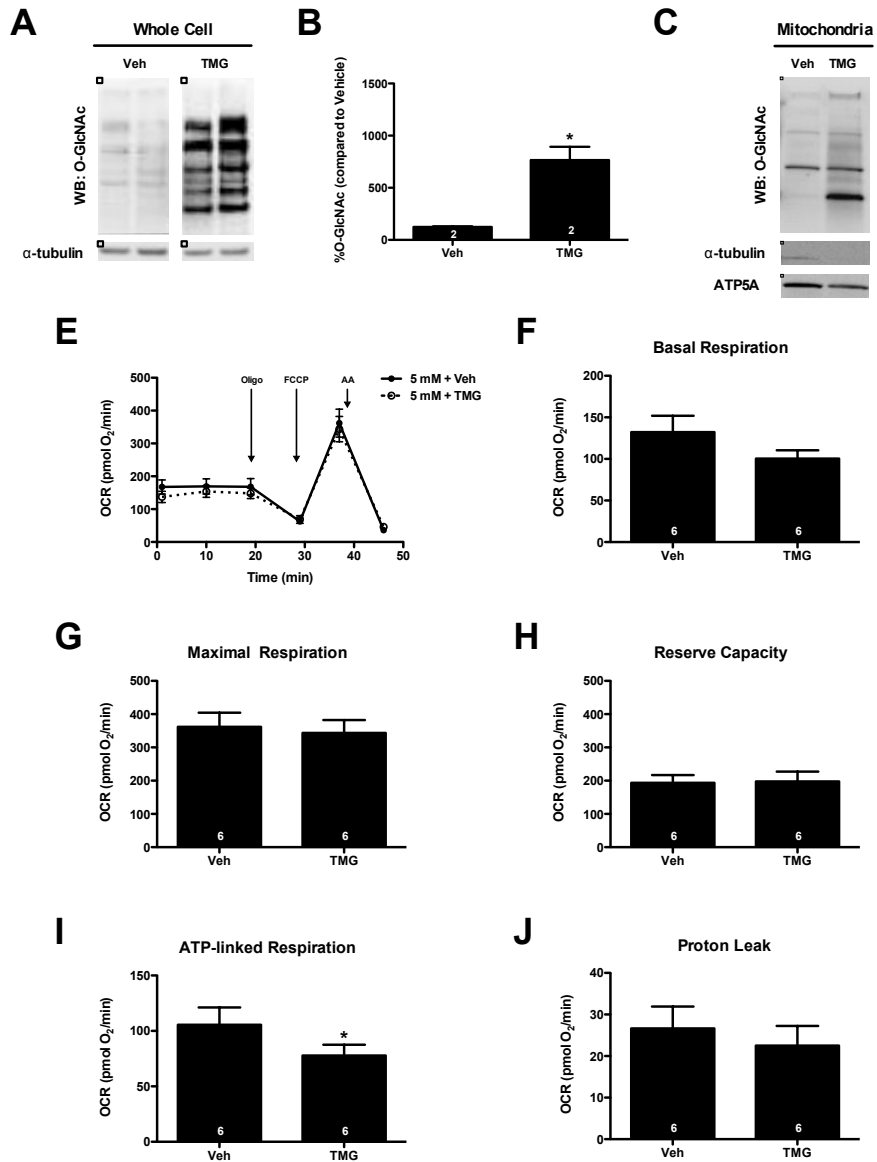


Figure 20. Inhibition of OGA has negligible effects on mitochondrial function. NRCMs were treated with TMG (1 μ M) for 48 h to induce protein O-GlcNAcylation. A) Immunoblot for whole cell protein O-GlcNAcylation. B) Densitometric measurement of O-GlcNAcylation. C) Immunoblot for mitochondrial protein O-GlcNAcylation following treatment with 1 μ M TMG. D) Mitochondrial function assay of NRCMs following 48 h treatment with TMG. Parameters of mitochondrial function were measured from D) including E) Basal respiration, F) Maximal respiration, G) Reserve capacity, H) ATP-linked respiration and I) Proton leak. As indicated in bars n=6 independent experiments, * indicates p<0.05

Inhibition of OGA increases Complex II-dependent State 3 respiration without affecting Complex I, III, or IV respiration

Hu et. al demonstrated impaired mitochondrial complex respiration upon induction of protein O-GlcNAcylation through hyperglycemia¹⁰⁶. As such, we wanted to verify whether augmented O-GlcNAcylation may affect mitochondrial function. We determined whether increasing O-GlcNAcylation with TMG (which inhibits OGA) might affect Complex II-dependent oxygen consumption in the permeabilized cell assay. Inhibition of OGA significantly increased protein O-GlcNAcylation and Complex II-dependent State 3 and 4_o respiration (Figure 21F,G); however, OGA inhibition did not significantly change respiration stimulated by provision of pyruvate and malate (Complex I), and it did not affect Complex III+IV-dependent OCR (Figure 21 A-C). Thus, pharmacologically augmenting protein O-GlcNAcylation is not sufficient to depress mitochondrial function, and may actually increase Complex II-dependent mitochondrial respiration under euglycemic conditions.

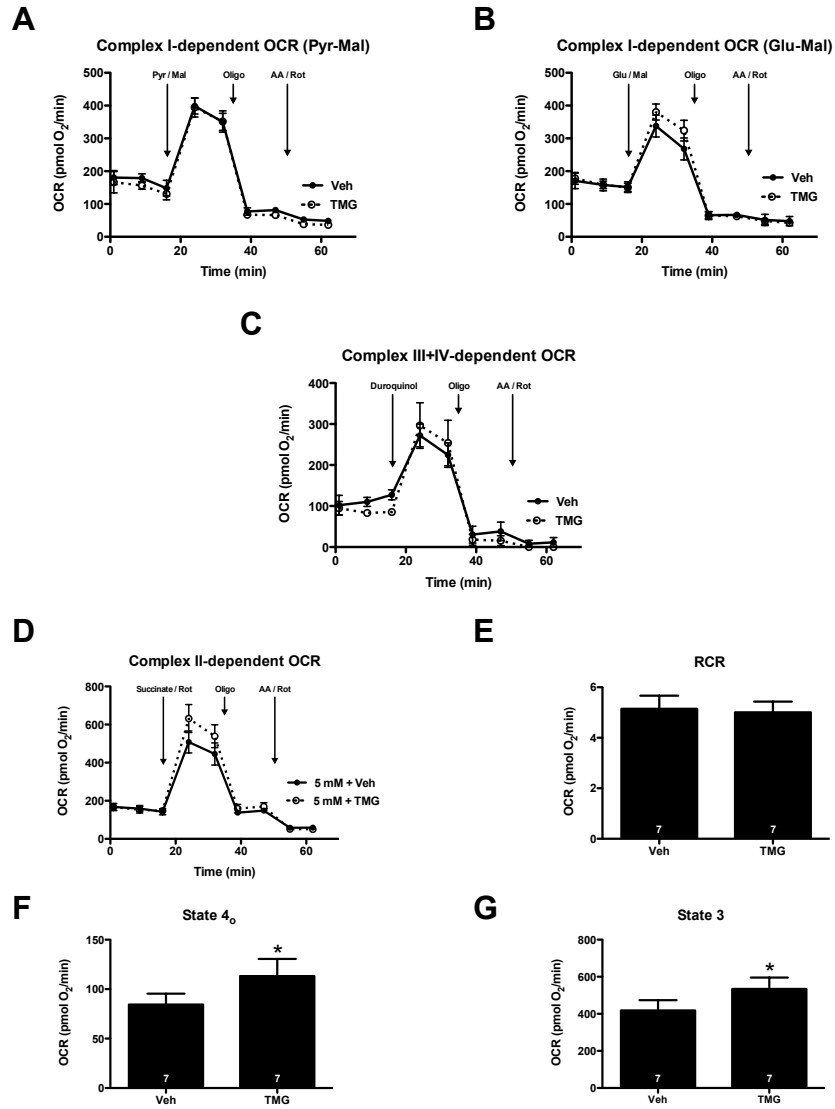


Figure 21. Inhibition of OGA increases Complex II-dependent State 3 respiration. NRCMs were treated for 24 h with 1 μ M TMG to induce protein O-GlcNAcylation. During XF analysis NRCMs were permeabilized and provided with succinate (to support Complex II-dependent respiration) as well as Rot (to inhibit Complex I activity). A) XF assay of Complex II-dependent respiration: following three baseline OCR measurements in MAS buffer, the permeabilization agent, saponin, and succinate+Rot were injected. After two measurements, oligomycin (Oligo) and AA + Rot (AA / Rot) were injected sequentially, with two measurements recorded after each injection. B) State 3 OCR: The AA + Rot rate was subtracted from the succinate-stimulated rate to determine the State 3 rates. C) State 4_o OCR: The AA + Rot rate was subtracted from the oligomycin rate to obtain State 4_o rates. D) RCR: State 3 / State 4_o. As indicated in bars n=7 independent experiments, * indicates a p < 0.05

High glucose increases protein O-GlcNAcylation

Thus far, the evidence indicating a role for O-GlcNAcylation and mitochondrial dysfunction was determined in the context of hyperglycemia attributable to a diabetic state. Indeed flux through the HBP is enhanced in diabetes leading to enhanced protein O-GlcNAcylation. Hence, we wanted to verify if enhanced O-GlcNAcylation as a result of hyperglycemia would affect cardiomyocyte mitochondrial function. To determine whether high glucose promotes protein O-GlcNAcylation, NRCMs were cultured for 48 h in medium supplemented with 0, 5, 10, 20, or 33 mM glucose (the osmotic control group was 5 mM glucose + 28 mM mannitol), and O-GlcNAc levels were assessed via immunoblotting (Figure 22A). Quantification of protein O-GlcNAc levels in whole cells demonstrated that the 33 mM glucose treatment resulted in a significant increase in O-GlcNAcylation when compared to 5 mM glucose (Figure 22B); however, when we isolated the mitochondrial fraction from similarly treated cells and probed for mitochondrial protein O-GlcNAcylation, we observed a much smaller effect (Figure 22C). Because we confirmed that high glucose induced protein O-GlcNAcylation in our system (similar to others^{79, 106}), we next queried whether high glucose compromises mitochondrial function.

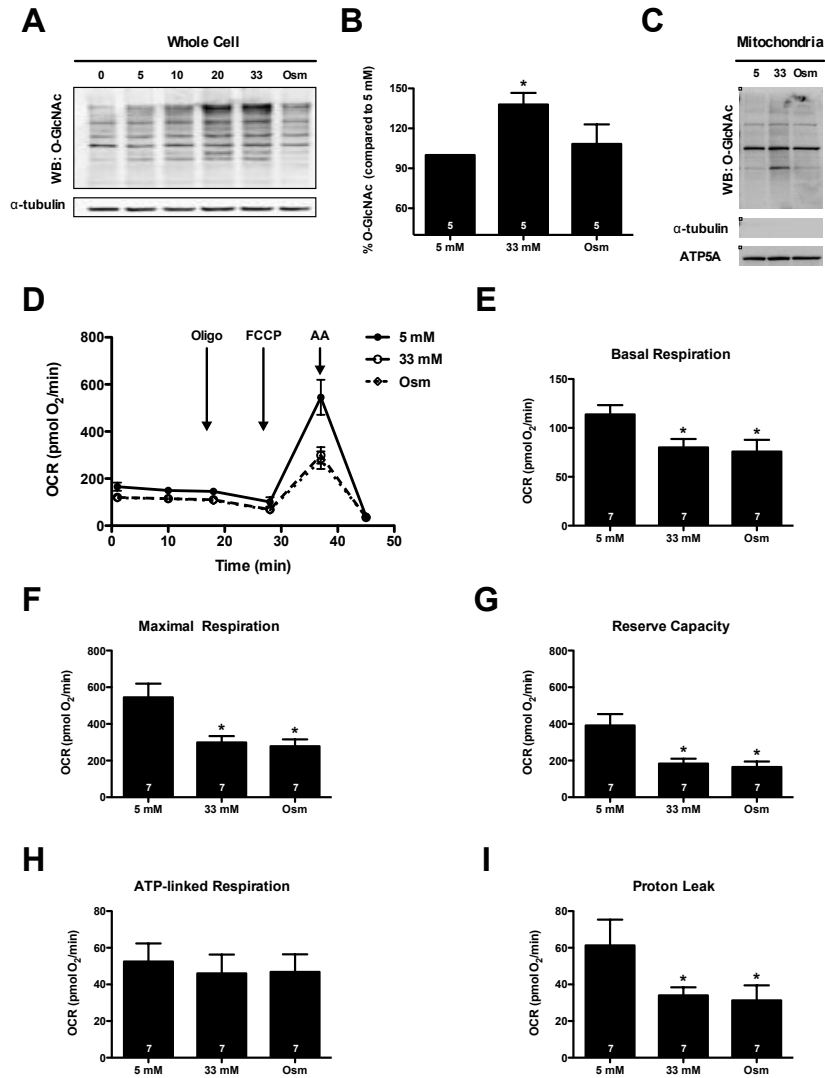


Figure 22. High glucose depresses the bioenergetic reserve capacity of cardiomyocytes

A) Immunoblot of whole cell protein O-GlcNAcylation following 0, 5, 10, 20, and 33 mM glucose treatment. An osmotic control (Osm, 5 mM glucose + 28 mM mannitol) was also used. B) Densitometric measurement of O-GlcNAcylation in relation to 5 mM control demonstrated a significant induction of protein O-GlcNAcylation following 33 mM glucose. C) Immunoblotting for mitochondrial protein O-GlcNAcylation. NRCMs were fractionated to isolate mitochondrial protein following treatment with 5 mM glucose, 33 mM glucose, and the osmotic control. D) Representative XF assay and diagram of how mitochondrial measurements were calculated. E) Mitochondrial function assay following 48 h of high glucose treatment. From part E) parameters of mitochondrial function were assessed (as described in D); F) Basal respiration; G) Maximal respiration; H) Reserve capacity; I) ATP-linked respiration; and J) Proton leak. As indicated in bars n=7 independent experiments, * indicates $p < 0.05$, vs. 5 mM.

High glucose depresses mitochondrial bioenergetic reserve capacity

We performed XF analysis of NRCMs to determine whether high glucose-mediated increases in O-GlcNAc could affect mitochondrial bioenergetics in the intact cell. Protein concentration measured following XF analysis was not significantly different between groups. High glucose (33 mM, n=7) depressed basal respiration (Figure 22E; $p<0.05$), maximal respiration (Figure 22F; $p<0.05$), reserve capacity (Figure 22G; $p<0.05$), and proton leak (Figure 22I; $p<0.05$) compared to the normal glucose control (5 mM, n=7). ATP-linked respiration remained unaltered following hyperglycemic treatment (Figure 22H). To address the contribution of an osmotic influence in the depression of mitochondrial function, we used an osmotic control (5 mM glucose + 28 mM mannitol, n=7), which recapitulated the depression ($p<0.05$) in basal respiration, maximal respiration, reserve capacity, and proton leak (Figure 22E-I). We also queried whether the osmotic stress also augmented O-GlcNAc levels (similar to the high glucose treatment) and found that the osmotic control (see lane "Osm" in Figure 22A) did not affect O-GlcNAc levels. Similarly, mitochondrial O-GlcNAcylation was largely unaffected by the osmotic control treatment (Figure 22C). Collectively, these findings indicate that the high glucose-induced suppression of basal respiration, maximal respiration, and reserve capacity were associated with an increase in osmolarity and not the high glucose-induced increase in O-GlcNAcylation (Figure 22A). Interestingly, much of the basal differences in OCR were attributable to reductions in proton leak, which was reduced in both the high glucose and osmotic control groups ($p<0.05$) (Figure 22I) compared to the

normal glucose group. Despite this apparent improvement in mitochondrial coupling, cells that were treated with high glucose or exposed to osmotic stress showed diminished mitochondrial reserve capacity. Thus, we suggest that osmotic stress caused by high glucose mediates loss of mitochondrial reserve capacity.

High glucose suppresses Complex II-dependent respiration

We demonstrated that inhibition of OGA alone enhanced Complex II-dependent State 4_o and State 3 respiration under euglycemic conditions. We wanted to test whether hyperglycemia-induced protein O-GlcNAcylation would recapitulate this effect. We subjected cardiomyocytes to euglycemia or hyperglycemia for 48 h and then examined mitochondrial activity in permeabilized cells. We found Complex II-dependent respiration was depressed by high glucose (Figure 23). Succinate-supported State 3 and State 4_o respiration was approximately 40% lower in cardiomyocytes incubated in high glucose ($p < 0.05$; Figure 23A-C). Similar to findings in intact cells, an osmotic control recapitulated the high glucose-induced suppression of State 3 respiration ($p < 0.05$; Figure 23B). No change in RCR was found after high glucose treatment or in the osmotic control (Figure 23D). These data are consistent with intact cell data, suggesting that high osmolarity mediates depression in mitochondrial function.

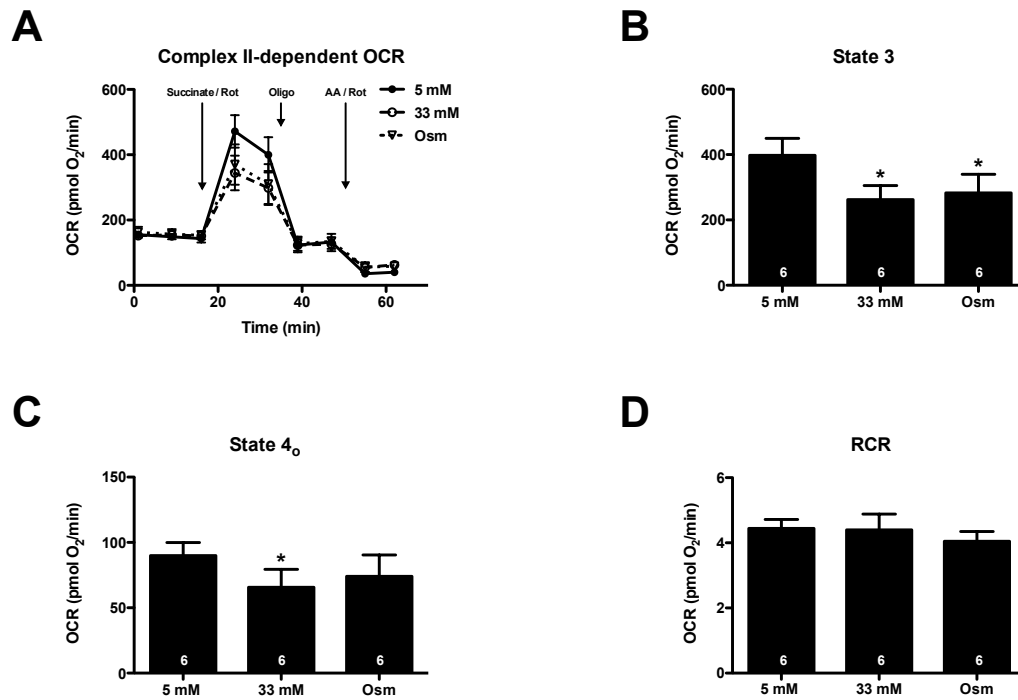


Figure 23. High glucose depresses Complex II-dependent State 3 and 4_o respiration

NRCMs were treated for 48 h with 5 mM, 33 mM glucose, or an osmotic control. During XF analysis NRCMs were permeabilized and provided with succinate (to support Complex II-dependent respiration) as well as Rot (to inhibit Complex I activity). A) XF assay of Complex II-dependent respiration: following three baseline OCR measurements in MAS buffer, the permeabilization agent, saponin, and succinate+Rot were injected. After two measurements, oligomycin (Oligo), then AA + Rot (AA/Rot) were injected sequentially, with measurements recorded after each injection. B) State 3 OCR: The AA + Rot rate was subtracted from the succinate-stimulated rate to determine the State 3 rates. C) State 4_o OCR: The AA + Rot rate was subtracted from the oligomycin rate to obtain State 4_o rates. D) RCR: State 3 / State 4_o. As indicated in bars n=6 independent experiments, * indicates p < 0.05 vs. 5 mM glucose.

OGA overexpression does not rescue the high glucose-induced bioenergetic defect

Because our data suggest that protein O-GlcNAcylation is an unlikely culprit in high glucose-induced mitochondrial dysfunction, we reasoned that if enhanced protein O-GlcNAcylation is necessary (though clearly insufficient) for the high glucose-induced depression in bioenergetic reserve capacity, then decreasing protein O-GlcNAcylation should rescue this defect. To this end, we overexpressed OGA, which as expected decreased O-GlcNAcylation (Figure 24A,B) and produced detectable OGA in mitochondrial fractions; however, there was not a significant difference in O-GlcNAcylation in the mitochondrial fraction (Figure 24C,D). OGA overexpression did not rescue suppression of mitochondrial reserve capacity induced by high glucose ($p < 0.05$; Figure 5H). In fact, in cells incubated with high glucose, overexpression of OGA depressed both maximal respiration ($p < 0.05$; Figure 24G) and reserve capacity ($p < 0.05$; Figure 24H). Overexpression of OGA did not affect ATP-linked respiration or proton leak (Figure 24I,J). These results suggest that an elevated level of O-GlcNAcylation is neither necessary nor sufficient to explain high glucose-induced suppression of mitochondrial bioenergetics.

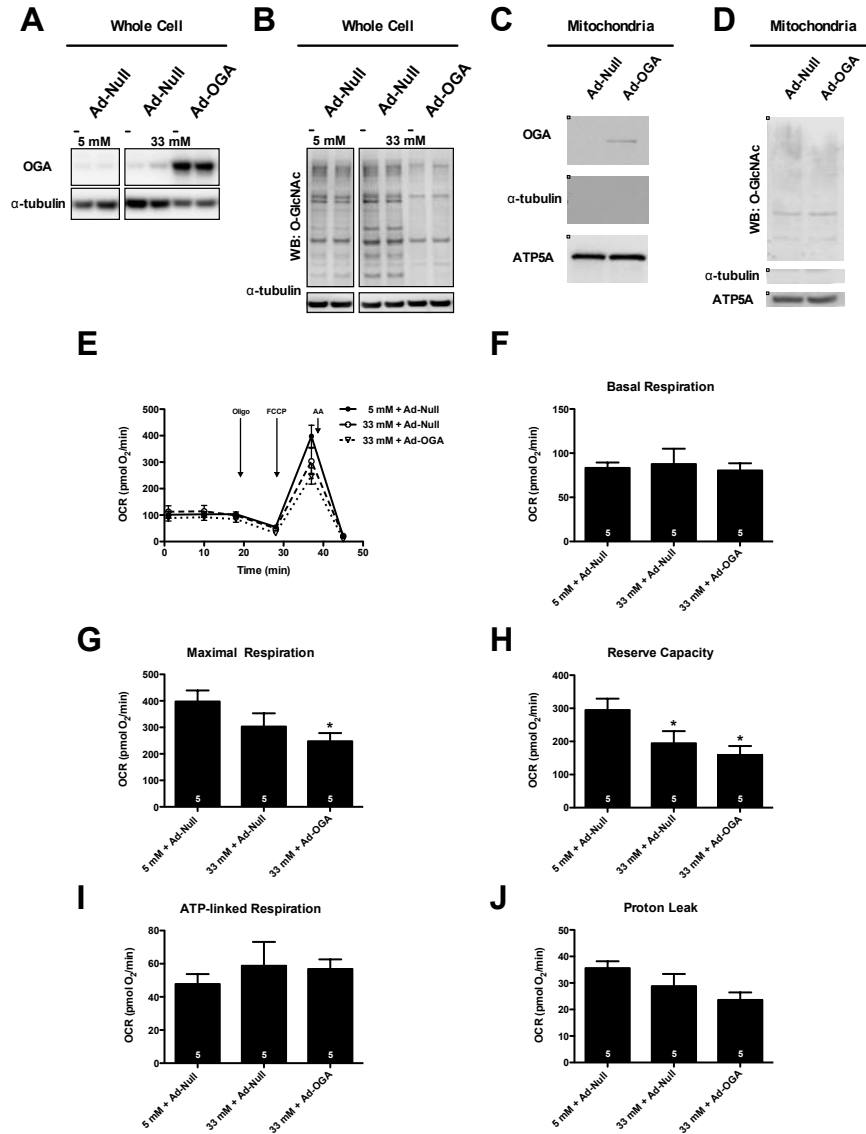


Figure 24: Overexpression of OGA does not rescue high glucose-induced suppression of bioenergetic reserve. NRCMs were transduced with virus to overexpress OGA prior to treatment with hyperglycemia. Ad-Null virus was used as a vector control. A) Immunoblot for whole cell OGA protein expression following viral transduction. B) Whole cell protein O-GlcNAcylation levels following adenoviral transduction. C) Immunoblot for mitochondrial OGA following adenoviral overexpression. D) Immunoblot for mitochondrial protein O-GlcNAcylation following adenoviral overexpression of OGA. E) Mitochondrial function assay following 48 h of hyperglycemic treatment. From assay in part E) parameters of mitochondrial function were measured; F) Basal respiration; G) Maximal respiration; H) Reserve capacity; I) ATP-linked respiration; and J) Proton leak. As indicated in bars n=5 independent experiments, * indicates $p < 0.05$ vs. 5 mM glucose + Ad-Null.

CHAPTER V

DISCUSSION

Since the discovery of O-GlcNAc in 1984, roughly 1,000 nuclear and cytoplasmic proteins have been identified to be O-GlcNAcylated. These targets are involved in a host of cellular processes such as transcription, translation, signal transduction, and cell cycle control^{55, 107-109}. O-GlcNAcylation occurs on serine and threonine residues, which are potential sites for phosphorylation. Thus, protein O-GlcNAcylation may alter protein function and affect downstream signaling in a manner similar to protein phosphorylation. Augmented protein O-GlcNAcylation has been implicated to be cytoprotective in response to a myriad of stressors including ischemia-reperfusion, myocardial infarction, and oxidative stress. Several studies indicate that this protective effect could be mediated through maintaining mitochondrial membrane stability. Nevertheless, dysregulation of protein O-GlcNAcylation is associated with pathology and highlights the importance of understanding the regulation of this phenomenon.

The enzymes that regulate protein O-GlcNAcylation, OGT and OGA, are ubiquitously expressed. OGT catalyzes the addition of O-GlcNAc to protein serine residues while OGA catalyzes their removal. Elevation of OGT precedes augmentation of O-GlcNAcylation and favors cell survival. Ablation of OGT in

cardiomyocytes exacerbates MI-induced cardiac dysfunction and enhances myocardial apoptosis; however, the role of OGA in HF was not as clear. Hence, the purpose of this thesis was to elucidate the role of OGA in HF. We hypothesized that ablation of OGA would favor O-GlcNAcylation and attenuate infarcted-induced cardiac dysfunction through preserving mitochondrial function.

Our findings indicate that downregulation of OGA contributes to the augmentation of O-GlcNAcylation in non-reperfused myocardial infarction. Suppression of OGA expression can be posttranscriptionally regulated. In addition the timely suppression of OGA is necessary for the development of HF. Lastly, acute alterations in O-GlcNAc levels alone do not contribute to mitochondrial dysfunction manifested in HF. These findings emphasize that the regulation of OGA expression is an important facet of HF whose mechanism of action may be independent of mitochondrial function.

In our first aim (Figure 25), we identified the temporal and spatial changes of OGA expression following HF. Within 5 d of MI, OGA protein expression decreased, while OGT expression and protein O-GlcNAcylation increased. This elevation in O-GlcNAcylation persisted despite normalization of OGT expression by 28 d post MI – though at this time point OGA expression remained suppressed. Chronically, OGA suppression is the likely arbiter of augmented protein O-GlcNAcylation in HF. Additionally, we discovered a negative regulator of OGA expression in HF, miR-539, which is elevated at both 5 d and 28 d post MI. In a series of molecular studies, we found that miR-539 binds to the 3'UTR of OGA mRNA and inhibits OGA expression. In additional experiments, we found

that miR-539 may mediate reduction in OGA expression in response to hypoxia-reoxygenation. This is the first miRNA identified to regulate expression of the O-GlcNAcylation machinery (i.e. OGT or OGA).

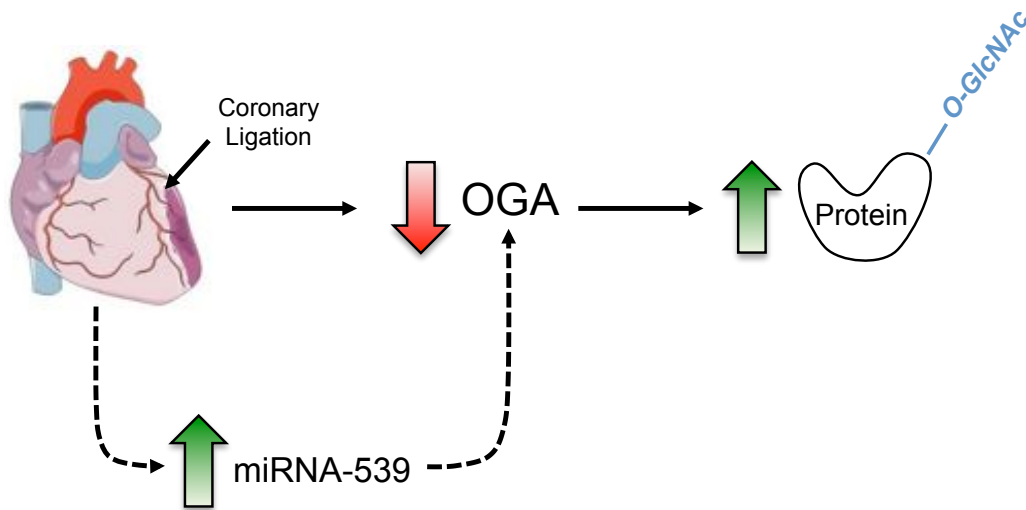


Figure 25. Aim 1 summary. In response to myocardial stress, such as MI, miRNA-539 is upregulated, OGA is suppressed, and protein O-GlcNAcylation is augmented. miRNA-539 is a negative posttranslational regulator of OGA mRNA. miRNA-539 can suppresses OGA expression and which may contribute to elevated protein O-GlcNAcylation observed in HF. Image of ligated heart from <https://www.unil.ch/caf/en/home/menuinst/services/micro-surgery.html>.

The majority of studies regarding miRNAs have focused on ones that play a prominent role in cardiovascular disorders such as MI, cardiac hypertrophy, HF, fibrosis, and pressure overload-induced cardiac remodeling¹¹⁰⁻¹¹³. Relatively few studies have focused on miRNAs involved in metabolic disorders^{114, 115}. Moreover, there are no prior studies implicating miRNAs in the regulation of OGA of OGT expression. Here, for the first time we report a novel paradigm of miRNA-mediated down-regulation of OGA with concomitant augmentation of O-

GlcNAcylation in the failing heart. Examination of miR-539 by both miRNA microarray followed by qRT-PCR demonstrated its upregulation in the failing heart.

OGA may be a potential conserved target of miR-539 since we demonstrated significant downregulation of OGA in both miR-539 overexpressing NRCMs (rat) and HEK293 (human) cells. Furthermore, inhibition of miRNA-539 in both NRCMs and HEK293 cells overexpressing miR-539 resulted in augmented OGA expression and concomitant reduction in O-GlcNAcylation. These data indicate that miR-539 may be a potential marker/target of disease.

Interestingly, miR-539 could have several other targets in addition to simply regulating OGA. Although OGT does not have target sites for miR-539 binding, reduction of the OGT protein level by miR-539 overexpression reveals that there could be indirect mechanisms involved in the regulation of OGT by OGA or other targets of miR-539. A recent study indicates that miR-539 regulates mitochondrial fission and apoptosis by targeting prohibitin 2 (PHB2) in cardiomyocytes¹¹⁶. In mast cells, CD117 represses miR-539 expression, thereby de-repressing microphthalmia-associated transcription factor expression and promoting proliferation¹¹⁷. In other cell types, miR-539 expression may be biotin-sensitive, and miR-539 targets the mRNA of holocarboxylase synthase, which participates in genetic stability¹¹⁸. Such collective findings create interesting implications for a more detailed understanding of the molecular interactions governing O-GlcNAc-dependent cell function; however, there is no evidence, at present to directly link the aforementioned observations to one another, at least

at the level of O-GlcNAcylation.

Understanding the regulation of O-GlcNAcylation holds critical importance not only in HF but also in multiple diseases; no disease exemplifies the potential impact better than diabetes. Several studies suggest that elevated O-GlcNAc levels contribute to diabetic cardiomyopathy⁸². In humans, the OGA/MGEA5 chromosome locus 10q24.1 is associated with late-onset Alzheimer disease¹¹⁹. Experimental observations demonstrated that inhibition of OGA decreases phosphorylation of Tau and protects against Tau-mediated neurodegeneration as well as prevents amyloid- β load by increasing the amount of secreted amyloid precursor protein (sAPP α)^{52, 120}. This line of evidences suggests that increased O-GlcNAcylation by OGA inhibition improves neuronal outcome.

In addition, numerous studies showed hyper O-GlcNAcylation, increased expression of OGT, and decreased OGA expression in various cancers^{121, 122}. In part, hyper O-GlcNAcylation was also observed as a mechanism that promotes cancer cell survival and stress resistance. Similar to the approach of targeting kinases, targeting OGA and OGT could be a valuable approach in many cancer therapies. Thus, the implications for our findings with miR-539 could be broad and manifold. Moreover, it is imperative to more carefully investigate the transcriptional and post-transcriptional regulation of OGT and OGA in relevant disease models.

Suppression of OGA appears to be a necessary protective response to enhance protein O-GlcNAcylation in response to stress. In our second aim (Figure 26) we hypothesized that ablating OGA prior to myocardial infarction

would attenuate cardiac dysfunction exhibited after MI. To do so, we generated an inducible cardiac specific OGA knockout mouse. Induction of tamoxifen only induced ablation of OGA in the heart. OGA remained present in skeletal muscle, kidney, liver, and lungs. Cardiac function was assessed from 5 d and up to 8 wk post tamoxifen. No differences were observed in parameters of cardiac function; EF, CO, and FS. When cohorts were subjected to MI 5 d post tamoxifen, EF was suppressed in the OGA KO at 1 wk post infarction. At 4 wk no difference in EF between OGA KO and WT MI groups was observed.

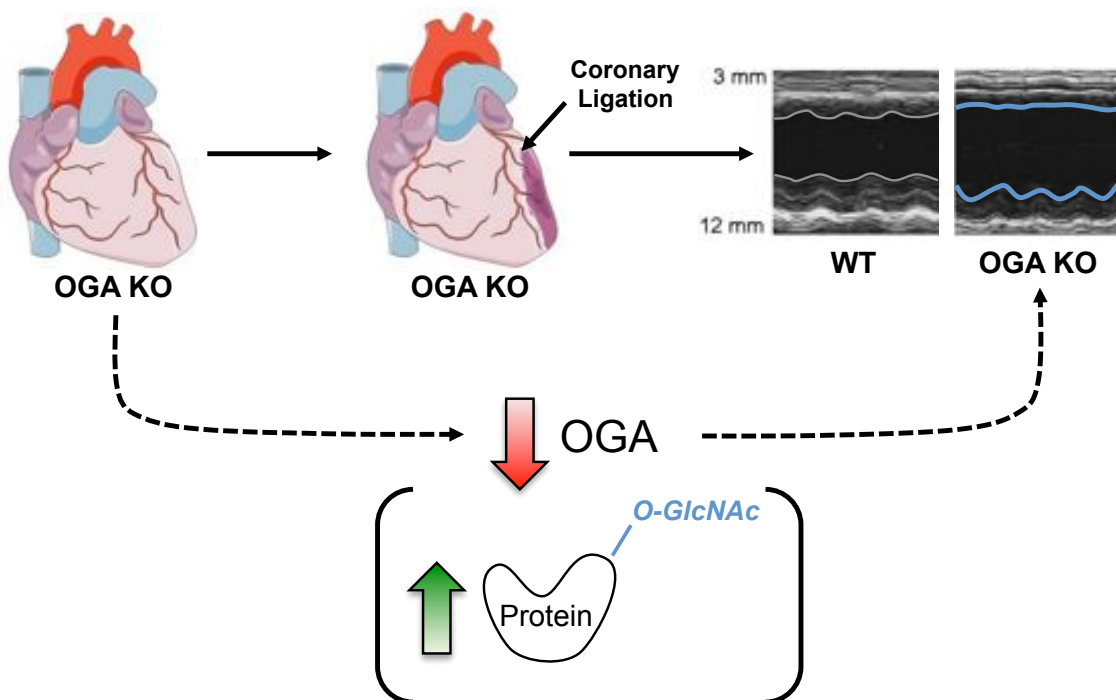


Figure 26. Aim 2 summary. Cardiomyocyte-specific ablation of OGA suppresses OGA expression and augments protein O-GlcNAcylation. Ablation of OGA prior to MI exacerbates cardiac dysfunction within 1 wk. M-mode image adapted from *Watson et al. 2010*. Image of normal and ligated heart from <https://www.unil.ch/caf/en/home/menuinst/services/micro-surgery.html>.

It was surprising to find that OGA ablation actually hastened HF at 1 wk post infarction. When we examined cardiac function 4 wk post MI we saw no difference in EF between WT and KO groups despite augmentation of O-

GlcNAcylation in KO cohort. We verified that OGA deletion did not affect infarct area 24 h post MI. However there is evidence that OGA gene mutation may be detrimental. The OGA gene has been identified as a diabetes susceptibility locus¹²³. Multiple single nucleotide polymorphism sites of OGA have been associated with increased onset of diabetes among Mexican Americans^{124, 125}. Similarly “Goto Kakizaki” rats, which have a deletion at exon 8 in the OGA gene, demonstrate spontaneous diabetes. Perturbations in O-GlcNAc cycling have been often attributed to be maladaptive in chronic metabolic diseases such as diabetes and cancer. Augmented O-GlcNAc has been implicated in affecting mitochondrial function thereby altering cardiac function.

Even though we saw no differences in genes involved in metabolism between WT and KO, loss of OGA may impact transcriptional machinery and other aspects of infarct healing. Alterations in O-GlcNAc signaling may impact the O-GlcNAcylation status of transcription factors, histones, and even RNA polymerase II thereby affecting their function. The Hanover group demonstrated notable deregulation of genes involved in immunity, cell proliferation, and metabolism in a conditional whole body OGA KO model. These could be other possible avenues of interest to pursue as potential mediators of the observed cardiac dysfunction.

In our third aim (Figure 27) we addressed the contribution of protein O-GlcNAcylation to mitochondrial dysfunction. Recent studies have implicated perturbations in O-GlcNAc cycling may be complicit in mediating cardiomyocyte mitochondrial dysfunction in the context of diabetes. We directly addressed

whether O-GlcNAcylation alone could mediate mitochondrial dysfunction. Increasing O-GlcNAcylation through either OGA inhibition or OGT overexpression was insufficient to induce mitochondrial dysfunction. Surprisingly, inhibition of OGA enhanced Complex II state 3 and 4_o mediated OCR. Most evidence of O-GlcNAc-mediated mitochondrial dysfunction was conducted in the context of hyperglycemia or diabetes. Hence, we addressed the relationship among high glucose, mitochondrial dysfunction, and O-GlcNAcylation. We confirmed that high glucose increased protein O-GlcNAcylation and induced mitochondrial dysfunction. However our osmotic control exerted a similar suppressive effect on bioenergetic reserve without augmenting O-GlcNAcylation. We went a step further to see if rescuing high glucose-induced O-GlcNAcylation via OGA overexpression would revert the depression in mitochondrial reserve capacity. The suppressive effect remained despite our manipulation of O-GlcNAcylation. Thus, increased O-GlcNAcylation is neither sufficient nor necessary for high glucose-induced mitochondrial dysfunction in isolated cardiomyocytes.

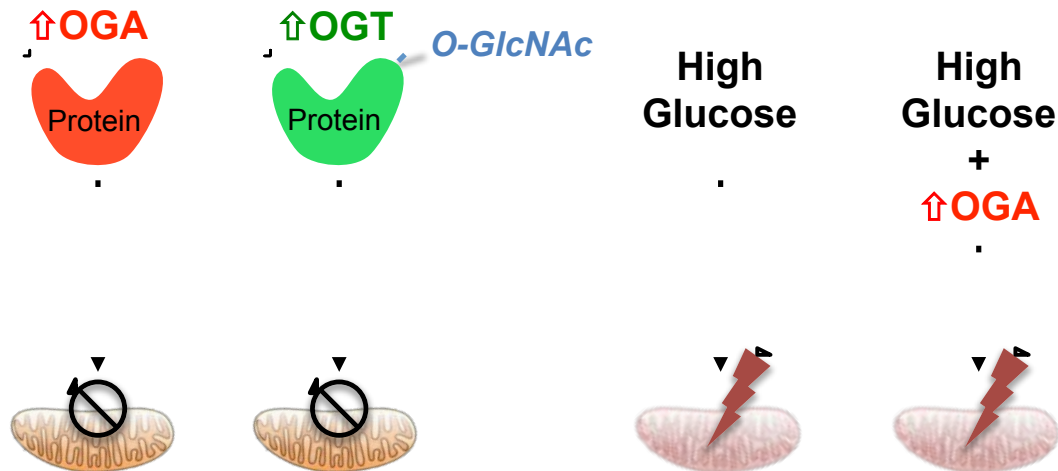


Figure 27. Aim 3 summary. Modulation of cardiomyocyte O-GlcNAcylation through overexpression of OGA or OGT resulted in no substantial changes in mitochondrial function. Decreasing (overexpression of OGA) or increasing O-GlcNAcylation (overexpression of OGT) does not mediate mitochondrial dysfunction. However hyperglycemia augmented O-GlcNAcylation and suppressed mitochondrial reserve capacity. Removing O-GlcNAc by overexpression of OGA does not rescue hyperglycemia-induced mitochondrial dysfunction. O-GlcNAcylation alone is not sufficient to cause mitochondrial dysfunction.

Consenting studies demonstrate that reliance on fatty acid oxidation decreases during HF. However there is debate as to whether glycolysis is altered. Nevertheless, flux through the HBP is increased and is demonstrated through increased protein O-GlcNAcylation. Similarly in diabetes elevated extracellular glucose floods accessory pathways of glucose metabolism and induces perturbations in O-GlcNAc levels. As such, protein O-GlcNAcylation has received growing attention as a candidate component of diabetic pathophysiology¹²⁶. Indeed, elevated extracellular glucose concentration enhances OGT activity, and promotes protein O-GlcNAcylation^{58, 77, 82, 106}. Moreover, O-GlcNAcylation is enhanced in patients with diabetes. Animal models of diabetes – such as streptozotocin-treated mice, Zucker rats, and *db/db* mice – all demonstrate elevated O-GlcNAcylation of at least some proteins in the

heart^{60, 106}. Thus, the coincident observations of increased O-GlcNAcylation and cardiac dysfunction during diabetes is consistent with the notion that O-GlcNAc plays a role in diabetic cardiac dysfunction.

Given that mitochondria play a critical role in metabolism and preservation of their function is pivotal to cardiac function, several groups have investigated the potential role of hyperglycemia/high glucose in mitochondrial dysfunction¹²⁷. Specifically, some have attempted to identify a connection between O-GlcNAcylation and mitochondrial dysfunction^{106, 128}. Hu et al identified high glucose-induced O-GlcNAcylation of cardiac mitochondrial Complexes I, III, and IV, and associated it with impaired mitochondrial function in permeabilized NRCMs. Overexpression of OGA (to reverse the high glucose-induced increase in O-GlcNAcylation) largely rescued the observed defects in mitochondrial Complex activities. Despite our differences in observed outcomes there were several similarities between our work and the Dillmann group :1) both focused on mitochondrial function in NRCMs, and assessed it, in part, via oxygen consumption rates; 2) both used mannitol as an osmotic control; 3) both attempted adenoviral-mediated rescue of high glucose-induced mitochondrial dysfunction; 4) both studies (at least in part) assessed cell function in permeabilized cells. Nevertheless, there were key differences in methodology between the two studies: 1) we evaluated mitochondrial function in adherent cardiomyocytes (intact and permeabilized); 2) we recapitulated the increase in O-GlcNAcylation via genetic overexpression of OGT and pharmacologic inhibition of OGA (in the absence of high glucose); and 3) we maintained the intact cells in

the respective glucose conditions (i.e. the high glucose cells were subjected to the XF assay in high glucose conditions). Ultimately, any of a number of these relatively subtle study differences may partially explain the discrepancies in our findings.

In a related and recent study, Tan et al used¹²⁸ a proteomic approach to study the effect of altering O-GlcNAc on mitochondrial protein expression, morphology, and function in neuroblastoma cells. They observed that overexpression of either OGT or OGA resulted in altered mitochondrial expression of proteins involved in transport, translation, and respiratory activity. Furthermore, these changes resulted in alterations in mitochondrial morphology and function. On face value, it may appear that the results of Tan et al also disagree with our present results; however, the differences may be fewer than they appear. We, too, found that overexpression of either OGT or OGA reduced OCR (including maximal OCR) in the context of high glucose. Yet, when we overexpressed OGT or OGA in euglycemic conditions, only basal respiration was slightly depressed. Interestingly, TMG, which remarkably increased O-GlcNAc levels, did not negatively affect OCR. Thus, these data indicate that there is not a clear and deleterious relationship between O-GlcNAcylation and mitochondrial dysfunction.

The fact that modulation of O-GlcNAcylation in the context of hyperglycemia had little effect on mitochondrial energetics suggests an alternative mechanism by which hyperglycemia impairs mitochondrial function. Interestingly, the defect in reserve capacity caused by the hyperglycemic

condition was recapitulated with the osmotic control, mannitol. Although we did not study the mechanism by which osmotic stress may have mediated changes in mitochondrial function, this observation could be relevant for response of myocytes to stress. For example, elevated by-products of anaerobic metabolism occurring during ischemia create an osmotic load that has been estimated to be ~60 mOsM. This acute change in osmolality regulates cell volume, cation/anion transport and other phenomena such as ischemic preconditioning. Hence, because cell volume is tightly linked with cation/anion transport, and cation transport is a key regulator of ATP demand and mitochondrial activity, it is possible that the osmotic stress induced by high glucose reduces reserve capacity in a manner dependent on changes in these critical processes. Further studies are required to assess the full significance of osmotic stress to hyperglycemia-induced myocyte stress.

Whether a mitochondrial O-GlcNAcylation system exists remains unclear. There is evidence of a mitochondrial (m)OGT¹²⁹. This would suggest that a mitochondrial (m)OGA should exist as well. However, our studies demonstrate that under normal conditions cardiomyocyte mitochondria have little, if any, detectable OGA. We only detected mitochondrial OGA when we overexpressed OGA using adenovirus. Because this is an overexpression system and fractionation procedures do not yield 100% pure subcellular fractions, it is possible that the OGA we found in the mitochondrial fraction was a contaminant from the cytoplasm. More importantly, the transport mechanism for the essential substrate required for O-GlcNAcylation, UDP-GlcNAc, has never been identified

in the mitochondrion. Hence, the nature of how mitochondrial O-GlcNAcylation occurs and whether it is due to a veritable mitochondrial O-GlcNAc-modification system, comprising a UDP-GlcNAc transporter, (m)OGA and (m)OGT, is still uncertain. Though, It it is possible that O-GlcNAcylation of mitochondrial proteins predominately occurs in the cytosol prior to mitochondrial protein targeting.

Interestingly, we demonstrated that Complex II state 3 and 4_o OCR was enhanced in response to inhibition of OGA and increased protein O-GlcNAcylation. Though the acute enhancement of Complex II function did not result in mitochondrial dysfunction enhanced Complex II activity may lead to reactive oxygen species (ROS) production in a chronic setting. Mitochondrial studies have documented that both the forward and backward reactions of Complex II can generate ROS¹³⁰. In fact ROS production is increased in the failing myocardium^{131, 132} and may contribute to structural and functional changes observed during the progression of HF. It is possible that under chronic conditions, elevated O-GlcNAcylation may affect mitochondrial function through augmented ROS production through Complex II.

In conclusion, several approaches, including overexpression of OGA or OGT, exposure to high glucose, and pharmacological manipulation, were used to assess the role of O-GlcNAc in regulating cardiomyocyte bioenergetics. We demonstrate that O-GlcNAcylation is likely not responsible for mitochondrial dysfunction occurring during hyperglycemic conditions, and that osmotic stress due to high glucose appears to underlie depression of mitochondrial reserve capacity. Although these findings do not entirely rule out the involvement of O-

GlcNAc in modulating bioenergetics in diabetes, they show that increasing O-GlcNAc levels is not sufficient or necessary to cause high glucose-induced bioenergetic dysfunction.

CHAPTER VI

SUMMARY AND FUTURE DIRECTIONS

Acute global augmentation of protein O-GlcNAcylation occurs in response to a myriad of stressors and confers a survival advantage at the cellular level. Several *in vitro* and *in vivo* studies have demonstrated O-GlcNAc-mediated cardioprotection against ischemia-reperfusion, myocardial infarction, and oxidative stress. Recent studies have investigated the two antagonistic enzymes that regulate protein O-GlcNAcylation. In the context of HF, ablation of OGT, the enzyme that catalyzes the addition of O-GlcNAc to proteins, in cardiomyocytes exacerbates cardiac dysfunction. However, in the context of HF little is known of the enzyme involved in removing the O-GlcNAc modification namely, OGA. The present study focused on the role of OGA in HF.

First we characterized the temporal expression of OGA following myocardial infarction. After MI, OGA expression is decreased and remains suppressed for 4 wk post MI. Despite the reduction in OGA expression, protein O-GlcNAcylation remains elevated compared to sham hearts. Chronically, OGA suppression may be the likely mediator of O-GlcNAcylation. We probed further into the regulation of OGA and discovered a novel regulator of OGA suppression

in HF, miRNA-539. Augmented expression of miRNA-539 coincided with OGA suppression after 5 d and 28 d of MI. Furthermore, *in vitro* studies confirmed induction of miRNA-539 negatively regulated OGA expression. These data indicate that chronic suppression of OGA may in part contribute to the augmentation of O-GlcNAcylation in HF. Furthermore, we developed a genetic model of cardiomyocyte specific OGA ablation, which did not induce cardiac dysfunction, to test whether ablation of OGA would attenuate HF. However when we genetically ablated OGA prior to coronary ligation we observed a hastening of cardiac dysfunction within 1 wk. The OGA KO hearts were more dysfunctional, contrary to our hypothesis.

Augmented cardiomyocyte O-GlcNAcylation has been identified as a possible culprit involved in diabetic cardiomyopathy. As such, we assessed the contribution of OGA to mitochondrial function to explain the exacerbation of cardiac dysfunction we observed at 1 wk. We found little evidence to support this implication. Neither OGA nor OGT mediated mitochondrial dysfunction. Though induction of O-GlcNAcylation through hyperglycemia did suppress mitochondrial reserve capacity. However this effect was recapitulated with an osmotic control. Modulation of O-GlcNAc alone did not cause mitochondrial dysfunction.

According to our data regulation of OGA is imperative for the progression of HF. We identified a novel regulator of OGA expression, miR-539, which is up regulated in HF. Future studies could identify additional roles of miR-539 in the development of HF. Recent studies have indicated that it may regulate mitochondrial fission in cardiomyocytes. Mitochondrial fission and fusion appear

to be critical to the maintenance of normal mitochondrial function. Moreover miRNA-539 could play roles in cardiovascular diseases where altered O-GlcNAcylation occurs such as hypertension and ischemia reperfusion. In light of results from this study, it will be interesting to see whether miR-539 expression is altered in these diseases and the use of miR-539 mimic or inhibitor may contribute a new and broad therapeutic approach to modulate O-GlcNAc signaling.

Along the lines of regulation of OGA, we could more specifically interrogate the timing effect of OGA suppression on HF. We see that suppression of OGA occurs within 5 days of MI. Future studies will assess the temporal effect of OGA in HF more clearly. Specifically, we will identify when OGA suppression is most imperative for the progression of HF. Since we have an inducible model of OGA deletion we could ablate OGA after MI instead of prior to MI.

In addition to regulating protein O-GlcNAcylation, OGA has other potential function that we have yet to explore. OGA has a HAT domain, which has both active and inactive states. It is possible that OGA could activate gene expression through acetylation of histones. Ablation of OGA may induce alterations in histone acetylation thereby causing altered gene expression necessary to attenuate cardiac dysfunction seen in MI.

Lastly, there is potential for a role of O-GlcNAcylation in the development of fibrosis. The death of cardiomyocytes immediately following MI triggers an inflammatory/repairative response that removes necrotic tissue and heals the heart with a collagen scar. Much of this healing process is mediated by resident

cardiac fibroblasts. Fibroblasts function to maintain the integrity of the cardiac matrix. Indeed they play prominent roles in the different phases of post-infarct repair: the inflammatory, proliferative, and maturation. During these phases the cardiac fibroblasts initiate inflammatory responses¹³³, proliferate, activate, and transdifferentiate into myofibroblasts to heal infarcted myocardium. The inflammatory and proliferative phases are transient and last only up to a week¹³⁴.¹³⁵ Coincidentally we see an exacerbation in cardiac dysfunction in OGA KO hearts following one week of MI. This period of time is critical for post-infarct healing. It is possible that loss of cardiomyocyte OGA may alter cardiac remodeling through altering fibroblast activity or activation. Thus, altered O-GlcNAcylation may affect these primary mediators of fibrosis. We have previously shown that abrogation of OGT enhanced cardiac fibrosis 4 wk post MI⁷¹. In addition, preliminary data from our lab from cardiac fibroblasts isolated after MI demonstrate altered protein O-GlcNAcylation (Data not shown). In addition, OGT mRNA was significantly suppressed 5 d post MI (Data not shown) in these fibroblasts. Therefore, it is plausible that alterations in OGA expression could affect them. Furthermore we have the tools to specifically assess the question *in vitro* through the use of OGA and OGT floxed fibroblasts isolated from our OGA^{F/W} and OGT^{F/F} mice. Adenoviral overexpression of Cre Recombinase in these fibroblasts should ablate OGA or OGT expression and alter O-GlcNAcylation. Thus, we can specifically assess the contribution of O-GlcNAcylation to fibroblast activation and function. These future studies may

provide further insight into more prominent roles of OGA in heart failure (Figure 28).

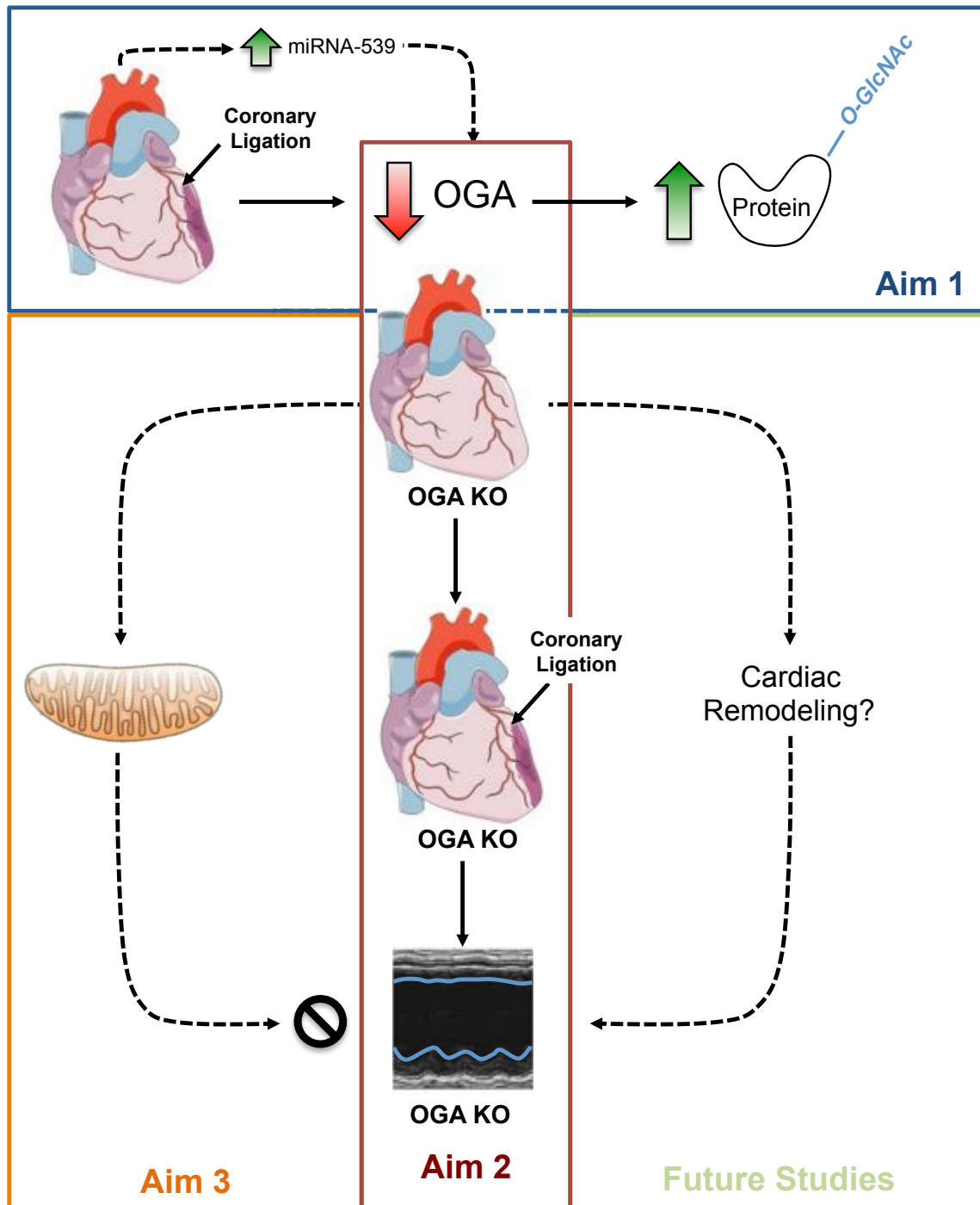


Figure 28. Summary of findings. Suppression of OGA and augmentation of O-GlcNAcylation occurs following MI. This suppression of OGA could be due to upregulation of miRNA-539, a negative posttranscriptional regulator of OGA expression (Aim 1). We hypothesized that ablation of OGA prior to infarction may be proadaptive. We generated a cardiomyocyte-specific OGA deficient mouse. Ablation of OGA prior to MI hastens cardiac dysfunction (Aim2). We hypothesized that OGA ablation may mediate mitochondrial dysfunction. We assessed the contribution of O-GlcNAcylation to induce mitochondrial dysfunction. O-GlcNAcylation alone was insufficient to cause mitochondrial dysfunction (Aim 3). We propose that OGA may contribute to post-infarct remodeling (Future Studies). M-mode image adapted from *Watson et al. 2010*. Image of normal and ligated heart from <https://www.unil.ch/caf/en/home/menuinst/services/micro-surgery.html>.

REFERENCES

1. Mozaffarian D, Benjamin EJ, Go AS, Arnett DK, Blaha MJ, Cushman M, Das SR, de Ferranti S, Despres JP, Fullerton HJ, Howard VJ, Huffman MD, Isasi CR, Jimenez MC, Judd SE, Kissela BM, Lichtman JH, Lisabeth LD, Liu S, Mackey RH, Magid DJ, McGuire DK, Mohler ER, 3rd, Moy CS, Muntner P, Mussolino ME, Nasir K, Neumar RW, Nichol G, Palaniappan L, Pandey DK, Reeves MJ, Rodriguez CJ, Rosamond W, Sorlie PD, Stein J, Towfighi A, Turan TN, Virani SS, Woo D, Yeh RW, Turner MB, American Heart Association Statistics C and Stroke Statistics S. Heart Disease and Stroke Statistics-2016 Update: A Report From the American Heart Association. *Circulation*. 2016;133:e38-e360.
2. Doenst T, Nguyen TD and Abel ED. Cardiac metabolism in heart failure: implications beyond ATP production. *Circ Res*. 2013;113:709-24.
3. Neubauer S, Horn M, Cramer M, Harre K, Newell JB, Peters W, Pabst T, Ertl G, Hahn D, Ingwall JS and Kochsiek K. Myocardial phosphocreatine-to-ATP ratio is a predictor of mortality in patients with dilated cardiomyopathy. *Circulation*. 1997;96:2190-6.
4. Ashrafian H, Frenneaux MP and Opie LH. Metabolic mechanisms in heart failure. *Circulation*. 2007;116:434-48.
5. Ventura-Clapier R, Garnier A and Veksler V. Energy metabolism in heart failure. *J Physiol*. 2004;555:1-13.
6. Ventura-Clapier R, Garnier A, Veksler V and Joubert F. Bioenergetics of the failing heart. *Biochim Biophys Acta*. 2011;1813:1360-72.
7. Rosenblatt-Velin N, Montessuit C, Papageorgiou I, Terrand J and Lerch R. Postinfarction heart failure in rats is associated with upregulation of GLUT-1 and downregulation of genes of fatty acid metabolism. *Cardiovasc Res*. 2001;52:407-16.
8. Doenst T, Pytel G, Schreppe A, Amorim P, Farber G, Shingu Y, Mohr FW and Schwarzer M. Decreased rates of substrate oxidation ex vivo predict the

onset of heart failure and contractile dysfunction in rats with pressure overload. *Cardiovasc Res.* 2010;86:461-70.

9. Kato T, Niizuma S, Inuzuka Y, Kawashima T, Okuda J, Tamaki Y, Iwanaga Y, Narazaki M, Matsuda T, Soga T, Kita T, Kimura T and Shioi T. Analysis of metabolic remodeling in compensated left ventricular hypertrophy and heart failure. *Circ Heart Fail.* 2010;3:420-30.

10. Marshall S, Bacote V and Traxinger RR. Discovery of a metabolic pathway mediating glucose-induced desensitization of the glucose transport system. Role of hexosamine biosynthesis in the induction of insulin resistance. *J Biol Chem.* 1991;266:4706-12.

11. Broschat KO, Gorka C, Page JD, Martin-Berger CL, Davies MS, Huang Hc HC, Gulve EA, Salsgiver WJ and Kasten TP. Kinetic characterization of human glutamine-fructose-6-phosphate amidotransferase I: potent feedback inhibition by glucosamine 6-phosphate. *J Biol Chem.* 2002;277:14764-70.

12. Boehmelt G, Wakeham A, Elia A, Sasaki T, Plyte S, Potter J, Yang Y, Tsang E, Ruland J, Iscove NN, Dennis JW and Mak TW. Decreased UDP-GlcNAc levels abrogate proliferation control in EMeg32-deficient cells. *EMBO J.* 2000;19:5092-104.

13. Greig KT, Antonchuk J, Metcalf D, Morgan PO, Krebs DL, Zhang JG, Hacking DF, Bode L, Robb L, Kranz C, de Graaf C, Bahlo M, Nicola NA, Nutt SL, Freeze HH, Alexander WS, Hilton DJ and Kile BT. Agm1/Pgm3-mediated sugar nucleotide synthesis is essential for hematopoiesis and development. *Mol Cell Biol.* 2007;27:5849-59.

14. Dassanayaka S and Jones SP. O-GlcNAc and the cardiovascular system. *Pharmacol Ther.* 2014;142:62-71.

15. Wells L, Vosseller K and Hart GW. A role for N-acetylglucosamine as a nutrient sensor and mediator of insulin resistance. *Cell Mol Life Sci.* 2003;60:222-8.

16. Bond MR and Hanover JA. O-GlcNAc Cycling: A Link Between Metabolism and Chronic Disease. *Annu Rev Nutr.* 2013.

17. McClain DA. Hexosamines as mediators of nutrient sensing and regulation in diabetes. *J Diabetes Complications.* 2002;16:72-80.

18. McClain DA, Lubas WA, Cooksey RC, Hazel M, Parker GJ, Love DC and Hanover JA. Altered glycan-dependent signaling induces insulin resistance and hyperleptinemia. *Proc Natl Acad Sci U S A.* 2002;99:10695-9.

19. Rossetti L. Perspective: Hexosamines and nutrient sensing. *Endocrinology.* 2000;141:1922-5.

20. Oki T, Yamazaki K, Kuromitsu J, Okada M and Tanaka I. cDNA cloning and mapping of a novel subtype of glutamine:fructose-6-phosphate amidotransferase (GFAT2) in human and mouse. *Genomics*. 1999;57:227-34.
21. DeHaven JE, Robinson KA, Nelson BA and Buse MG. A novel variant of glutamine: fructose-6-phosphate amidotransferase-1 (GFAT1) mRNA is selectively expressed in striated muscle. *Diabetes*. 2001;50:2419-24.
22. Niimi M, Ogawara T, Yamashita T, Yamamoto Y, Ueyama A, Kambe T, Okamoto T, Ban T, Tamanoi H, Ozaki K, Fujiwara T, Fukui H, Takahashi EI, Kyushiki H and Tanigami A. Identification of GFAT1-L, a novel splice variant of human glutamine: fructose-6-phosphate amidotransferase (GFAT1) that is expressed abundantly in skeletal muscle. *J Hum Genet*. 2001;46:566-71.
23. Chang Q, Su K, Baker JR, Yang X, Paterson AJ and Kudlow JE. Phosphorylation of human glutamine:fructose-6-phosphate amidotransferase by cAMP-dependent protein kinase at serine 205 blocks the enzyme activity. *J Biol Chem*. 2000;275:21981-7.
24. Hu Y, Riesland L, Paterson AJ and Kudlow JE. Phosphorylation of mouse glutamine-fructose-6-phosphate amidotransferase 2 (GFAT2) by cAMP-dependent protein kinase increases the enzyme activity. *J Biol Chem*. 2004;279:29988-93.
25. Paterson AJ and Kudlow JE. Regulation of glutamine:fructose-6-phosphate amidotransferase gene transcription by epidermal growth factor and glucose. *Endocrinology*. 1995;136:2809-16.
26. Kreppel LK, Blomberg MA and Hart GW. Dynamic glycosylation of nuclear and cytosolic proteins. Cloning and characterization of a unique O-GlcNAc transferase with multiple tetratricopeptide repeats. *J Biol Chem*. 1997;272:9308-15.
27. Haltiwanger RS, Blomberg MA and Hart GW. Glycosylation of nuclear and cytoplasmic proteins. Purification and characterization of a uridine diphospho-N-acetylglucosamine:polypeptide beta-N-acetylglucosaminyltransferase. *J Biol Chem*. 1992;267:9005-13.
28. Haltiwanger RS, Holt GD and Hart GW. Enzymatic addition of O-GlcNAc to nuclear and cytoplasmic proteins. Identification of a uridine diphospho-N-acetylglucosamine:peptide beta-N-acetylglucosaminyltransferase. *J Biol Chem*. 1990;265:2563-8.
29. Lubas WA and Hanover JA. Functional expression of O-linked GlcNAc transferase. Domain structure and substrate specificity. *J Biol Chem*. 2000;275:10983-8.

30. Muller R, Jenny A and Stanley P. The EGF repeat-specific O-GlcNAc-transferase Eogt interacts with notch signaling and pyrimidine metabolism pathways in *Drosophila*. *PLoS One*. 2013;8:e62835.
31. Sakaidani Y, Ichiyanagi N, Saito C, Nomura T, Ito M, Nishio Y, Nadano D, Matsuda T, Furukawa K and Okajima T. O-linked-N-acetylglucosamine modification of mammalian Notch receptors by an atypical O-GlcNAc transferase Eogt1. *Biochem Biophys Res Commun*. 2012;419:14-9.
32. Gao Y, Wells L, Comer FI, Parker GJ and Hart GW. Dynamic O-glycosylation of nuclear and cytosolic proteins: cloning and characterization of a neutral, cytosolic beta-N-acetylglucosaminidase from human brain. *J Biol Chem*. 2001;276:9838-45.
33. Lubas WA, Frank DW, Krause M and Hanover JA. O-Linked GlcNAc transferase is a conserved nucleocytoplasmic protein containing tetratricopeptide repeats. *J Biol Chem*. 1997;272:9316-24.
34. Blatch GL and Lassle M. The tetratricopeptide repeat: a structural motif mediating protein-protein interactions. *Bioessays*. 1999;21:932-9.
35. Groves MR and Barford D. Topological characteristics of helical repeat proteins. *Curr Opin Struct Biol*. 1999;9:383-9.
36. Jinek M, Rehwinkel J, Lazarus BD, Izaurralde E, Hanover JA and Conti E. The superhelical TPR-repeat domain of O-linked GlcNAc transferase exhibits structural similarities to importin alpha. *Nat Struct Mol Biol*. 2004;11:1001-7.
37. Clarke AJ, Hurtado-Guerrero R, Pathak S, Schuttelkopf AW, Borodkin V, Shepherd SM, Ibrahim AF and van Aalten DM. Structural insights into mechanism and specificity of O-GlcNAc transferase. *EMBO J*. 2008;27:2780-8.
38. Martinez-Fleites C, Macauley MS, He Y, Shen DL, Vocadlo DJ and Davies GJ. Structure of an O-GlcNAc transferase homolog provides insight into intracellular glycosylation. *Nat Struct Mol Biol*. 2008;15:764-5.
39. Vocadlo DJ. O-GlcNAc processing enzymes: catalytic mechanisms, substrate specificity, and enzyme regulation. *Curr Opin Chem Biol*. 2012;16:488-97.
40. Kreppel LK and Hart GW. Regulation of a cytosolic and nuclear O-GlcNAc transferase. Role of the tetratricopeptide repeats. *J Biol Chem*. 1999;274:32015-22.
41. Lazarus MB, Nam Y, Jiang J, Sliz P and Walker S. Structure of human O-GlcNAc transferase and its complex with a peptide substrate. *Nature*. 2011;469:564-7.

42. Gross BJ, Kraybill BC and Walker S. Discovery of O-GlcNAc transferase inhibitors. *J Am Chem Soc.* 2005;127:14588-9.
43. Jiang J, Lazarus MB, Pasquina L, Sliz P and Walker S. A neutral diphosphate mimic crosslinks the active site of human O-GlcNAc transferase. *Nat Chem Biol.* 2012;8:72-7.
44. Banerjee PS, Hart GW and Cho JW. Chemical approaches to study O-GlcNAcylation. *Chem Soc Rev.* 2013;42:4345-57.
45. Ngoh GA, Watson LJ, Facundo HT, Dillmann W and Jones SP. Non-canonical glycosyltransferase modulates post-hypoxic cardiac myocyte death and mitochondrial permeability transition. *J Mol Cell Cardiol.* 2008;45:313-25.
46. Gloster TM, Zandberg WF, Heinonen JE, Shen DL, Deng L and Vocadlo DJ. Hijacking a biosynthetic pathway yields a glycosyltransferase inhibitor within cells. *Nat Chem Biol.* 2011;7:174-81.
47. Butkinaree C, Cheung WD, Park S, Park K, Barber M and Hart GW. Characterization of beta-N-acetylglucosaminidase cleavage by caspase-3 during apoptosis. *J Biol Chem.* 2008;283:23557-66.
48. Comtesse N, Maldener E and Meese E. Identification of a nuclear variant of MGEA5, a cytoplasmic hyaluronidase and a beta-N-acetylglucosaminidase. *Biochem Biophys Res Commun.* 2001;283:634-40.
49. Lameira J, Alves CN, Moliner V, Marti S, Kanaan N and Tunon I. A quantum mechanics/molecular mechanics study of the protein-ligand interaction of two potent inhibitors of human O-GlcNAcase: PUGNAc and NAG-thiazoline. *J Phys Chem B.* 2008;112:14260-6.
50. Schimpl M, Borodkin VS, Gray LJ and van Aalten DM. Synergy of peptide and sugar in O-GlcNAcase substrate recognition. *Chem Biol.* 2012;19:173-8.
51. Dorfmueller HC, Borodkin VS, Schimpl M, Zheng X, Kime R, Read KD and van Aalten DM. Cell-penetrant, nanomolar O-GlcNAcase inhibitors selective against lysosomal hexosaminidases. *Chem Biol.* 2010;17:1250-5.
52. Yuzwa SA, Macauley MS, Heinonen JE, Shan X, Dennis RJ, He Y, Whitworth GE, Stubbs KA, McEachern EJ, Davies GJ and Vocadlo DJ. A potent mechanism-inspired O-GlcNAcase inhibitor that blocks phosphorylation of tau in vivo. *Nat Chem Biol.* 2008;4:483-90.
53. Ngoh GA, Hamid T, Prabhu SD and Jones SP. O-GlcNAc signaling attenuates ER stress-induced cardiomyocyte death. *Am J Physiol Heart Circ Physiol.* 2009;297:H1711-9.

54. Hart GW, Kreppel LK, Comer FI, Arnold CS, Snow DM, Ye Z, Cheng X, DellaManna D, Caine DS, Earles BJ, Akimoto Y, Cole RN and Hayes BK. O-GlcNAcylation of key nuclear and cytoskeletal proteins: reciprocity with O-phosphorylation and putative roles in protein multimerization. *Glycobiology*. 1996;6:711-6.
55. Hart GW, Housley MP and Slawson C. Cycling of O-linked beta-N-acetylglucosamine on nucleocytoplasmic proteins. *Nature*. 2007;446:1017-22.
56. Cheng X, Cole RN, Zaia J and Hart GW. Alternative O-glycosylation/O-phosphorylation of the murine estrogen receptor beta. *Biochemistry*. 2000;39:11609-20.
57. Hart GW, Greis KD, Dong LY, Blomberg MA, Chou TY, Jiang MS, Roquemore EP, Snow DM, Kreppel LK, Cole RN and et al. O-linked N-acetylglucosamine: the "yin-yang" of Ser/Thr phosphorylation? Nuclear and cytoplasmic glycosylation. *Adv Exp Med Biol*. 1995;376:115-23.
58. Akimoto Y, Kreppel LK, Hirano H and Hart GW. Increased O-GlcNAc transferase in pancreas of rats with streptozotocin-induced diabetes. *Diabetologia*. 2000;43:1239-47.
59. Zachara NE and Hart GW. O-GlcNAc a sensor of cellular state: the role of nucleocytoplasmic glycosylation in modulating cellular function in response to nutrition and stress. *Biochim Biophys Acta*. 2004;1673:13-28.
60. Fulop N, Mason MM, Dutta K, Wang P, Davidoff AJ, Marchase RB and Chatham JC. Impact of Type 2 diabetes and aging on cardiomyocyte function and O-linked N-acetylglucosamine levels in the heart. *Am J Physiol Cell Physiol*. 2007;292:C1370-8.
61. Ngoh GA and Jones SP. New insights into metabolic signaling and cell survival: the role of beta-O-linkage of N-acetylglucosamine. *J Pharmacol Exp Ther*. 2008;327:602-9.
62. Jones SP, Zachara NE, Ngoh GA, Hill BG, Teshima Y, Bhatnagar A, Hart GW and Marban E. Cardioprotection by N-acetylglucosamine linkage to cellular proteins. *Circulation*. 2008;117:1172-82.
63. Lima VV, Giachini FR, Choi H, Carneiro FS, Carneiro ZN, Fortes ZB, Carvalho MH, Webb RC and Tostes RC. Impaired vasodilator activity in deoxycorticosterone acetate-salt hypertension is associated with increased protein O-GlcNAcylation. *Hypertension*. 2009;53:166-74.
64. Lima VV, Rigsby CS, Hardy DM, Webb RC and Tostes RC. O-GlcNAcylation: a novel post-translational mechanism to alter vascular cellular signaling in health and disease: focus on hypertension. *J Am Soc Hypertens*. 2009;3:374-87.

65. Lima VV, Giachini FR, Hardy DM, Webb RC and Tostes RC. O-GlcNAcylation: a novel pathway contributing to the effects of endothelin in the vasculature. *Am J Physiol Regul Integr Comp Physiol*. 2011;300:R236-50.
66. Xing D, Feng W, Not LG, Miller AP, Zhang Y, Chen YF, Majid-Hassan E, Chatham JC and Oparil S. Increased protein O-GlcNAc modification inhibits inflammatory and neointimal responses to acute endoluminal arterial injury. *Am J Physiol Heart Circ Physiol*. 2008;295:H335-42.
67. Hilgers RH, Xing D, Gong K, Chen YF, Chatham JC and Oparil S. Acute O-GlcNAcylation prevents inflammation-induced vascular dysfunction. *Am J Physiol Heart Circ Physiol*. 2012;303:H513-22.
68. Xing D, Gong K, Feng W, Nozell SE, Chen YF, Chatham JC and Oparil S. O-GlcNAc modification of NFkappaB p65 inhibits TNF-alpha-induced inflammatory mediator expression in rat aortic smooth muscle cells. *PLoS One*. 2011;6:e24021.
69. Allard MF, Schonekess BO, Henning SL, English DR and Lopaschuk GD. Contribution of oxidative metabolism and glycolysis to ATP production in hypertrophied hearts. *Am J Physiol*. 1994;267:H742-50.
70. Chatham JC and Young ME. Metabolic remodeling in the hypertrophic heart: fuel for thought. *Circ Res*. 2012;111:666-8.
71. Watson LJ, Facundo HT, Ngoh GA, Ameen M, Brainard RE, Lemma KM, Long BW, Prabhu SD, Xuan YT and Jones SP. O-linked beta-N-acetylglucosamine transferase is indispensable in the failing heart. *Proc Natl Acad Sci U S A*. 2010;107:17797-802.
72. Young ME, Yan J, Razeghi P, Cooksey RC, Guthrie PH, Stepkowski SM, McClain DA, Tian R and Taegtmeyer H. Proposed regulation of gene expression by glucose in rodent heart. *Gene Regul Syst Bio*. 2007;1:251-62.
73. Fulop N, Feng W, Xing D, He K, Not LG, Brocks CA, Marchase RB, Miller AP and Chatham JC. Aging leads to increased levels of protein O-linked N-acetylglucosamine in heart, aorta, brain and skeletal muscle in Brown-Norway rats. *Biogerontology*. 2008;9:139-51.
74. Facundo HT, Brainard RE, Watson LJ, Ngoh GA, Hamid T, Prabhu SD and Jones SP. O-GlcNAc signaling is essential for NFAT-mediated transcriptional reprogramming during cardiomyocyte hypertrophy. *Am J Physiol Heart Circ Physiol*. 2012;302:H2122-30.
75. Golks A, Tran TT, Goetschy JF and Guerini D. Requirement for O-linked N-acetylglucosaminyltransferase in lymphocytes activation. *EMBO J*. 2007;26:4368-79.

76. Molkentin JD, Lu JR, Antos CL, Markham B, Richardson J, Robbins J, Grant SR and Olson EN. A calcineurin-dependent transcriptional pathway for cardiac hypertrophy. *Cell*. 1998;93:215-28.
77. Akimoto Y, Kreppel LK, Hirano H and Hart GW. Hyperglycemia and the O-GlcNAc transferase in rat aortic smooth muscle cells: elevated expression and altered patterns of O-GlcNAcylation. *Arch Biochem Biophys*. 2001;389:166-75.
78. Buse MG, Robinson KA, Marshall BA, Hresko RC and Mueckler MM. Enhanced O-GlcNAc protein modification is associated with insulin resistance in GLUT1-overexpressing muscles. *Am J Physiol Endocrinol Metab*. 2002;283:E241-50.
79. Clark RJ, McDonough PM, Swanson E, Trost SU, Suzuki M, Fukuda M and Dillmann WH. Diabetes and the accompanying hyperglycemia impairs cardiomyocyte calcium cycling through increased nuclear O-GlcNAcylation. *J Biol Chem*. 2003;278:44230-7.
80. Hu Y, Belke D, Suarez J, Swanson E, Clark R, Hoshijima M and Dillmann WH. Adenovirus-mediated overexpression of O-GlcNAcase improves contractile function in the diabetic heart. *Circ Res*. 2005;96:1006-13.
81. Wang Z, Park K, Comer F, Hsieh-Wilson LC, Saudek CD and Hart GW. Site-specific GlcNAcylation of human erythrocyte proteins: potential biomarker(s) for diabetes. *Diabetes*. 2009;58:309-17.
82. Marsh SA, Dell'Italia LJ and Chatham JC. Activation of the hexosamine biosynthesis pathway and protein O-GlcNAcylation modulate hypertrophic and cell signaling pathways in cardiomyocytes from diabetic mice. *Amino Acids*. 2011;40:819-28.
83. McLarty JL, Marsh SA and Chatham JC. Post-translational protein modification by O-linked N-acetyl-glucosamine: Its role in mediating the adverse effects of diabetes on the heart. *Life Sci*. 2012.
84. Crook ED, Daniels MC, Smith TM and McClain DA. Regulation of insulin-stimulated glycogen synthase activity by overexpression of glutamine: fructose-6-phosphate amidotransferase in rat-1 fibroblasts. *Diabetes*. 1993;42:1289-96.
85. Hebert LF, Jr., Daniels MC, Zhou J, Crook ED, Turner RL, Simmons ST, Neidigh JL, Zhu JS, Baron AD and McClain DA. Overexpression of glutamine:fructose-6-phosphate amidotransferase in transgenic mice leads to insulin resistance. *J Clin Invest*. 1996;98:930-6.
86. Arias EB, Kim J and Cartee GD. Prolonged incubation in PUGNAc results in increased protein O-Linked glycosylation and insulin resistance in rat skeletal muscle. *Diabetes*. 2004;53:921-30.

87. Dehennaut V and Lefebvre T. Proteomics and PUGNAcity will overcome questioning of insulin resistance induction by non-selective inhibition of O-GlcNAcase. *Proteomics*. 2013.
88. Lee JE, Park JH, Moon PG and Baek MC. Identification of differentially expressed proteins by treatment with PUGNAc in 3T3-L1 adipocytes through analysis of ATP-binding proteome. *Proteomics*. 2013.
89. Nelson BA, Robinson KA and Buse MG. High glucose and glucosamine induce insulin resistance via different mechanisms in 3T3-L1 adipocytes. *Diabetes*. 2000;49:981-91.
90. Nelson BA, Robinson KA and Buse MG. Defective Akt activation is associated with glucose- but not glucosamine-induced insulin resistance. *Am J Physiol Endocrinol Metab*. 2002;282:E497-506.
91. Macauley MS, Bubb AK, Martinez-Fleites C, Davies GJ and Vocadlo DJ. Elevation of global O-GlcNAc levels in 3T3-L1 adipocytes by selective inhibition of O-GlcNAcase does not induce insulin resistance. *J Biol Chem*. 2008;283:34687-95.
92. Robinson KA, Ball LE and Buse MG. Reduction of O-GlcNAc protein modification does not prevent insulin resistance in 3T3-L1 adipocytes. *Am J Physiol Endocrinol Metab*. 2007;292:E884-90.
93. Dentin R, Hedrick S, Xie J, Yates J, 3rd and Montminy M. Hepatic glucose sensing via the CREB coactivator CRTC2. *Science*. 2008;319:1402-5.
94. Ngho GA, Watson LJ, Facundo HT and Jones SP. Augmented O-GlcNAc signaling attenuates oxidative stress and calcium overload in cardiomyocytes. *Amino Acids*. 2011;40:895-911.
95. Yokoe S, Asahi M, Takeda T, Otsu K, Taniguchi N, Miyoshi E and Suzuki K. Inhibition of phospholamban phosphorylation by O-GlcNAcylation: implications for diabetic cardiomyopathy. *Glycobiology*. 2010;20:1217-26.
96. Taegtmeyer H, Beauloye C, Harmancey R and Hue L. Insulin Resistance Protects the Heart from Fuel Overload in Dysregulated Metabolic States. *Am J Physiol Heart Circ Physiol*. 2013.
97. Condorelli G, Roncarati R, Ross J, Jr., Pisani A, Stassi G, Todaro M, Trocha S, Drusco A, Gu Y, Russo MA, Frati G, Jones SP, Lefer DJ, Napoli C and Croce CM. Heart-targeted overexpression of caspase3 in mice increases infarct size and depresses cardiac function. *Proc Natl Acad Sci U S A*. 2001;98:9977-82.

98. Greer JJ, Kakkar AK, Elrod JW, Watson LJ, Jones SP and Lefer DJ. Low-dose simvastatin improves survival and ventricular function via eNOS in congestive heart failure. *Am J Physiol Heart Circ Physiol*. 2006;291:H2743-51.
99. Jones SP, Greer JJ, van Haperen R, Duncker DJ, de Crom R and Lefer DJ. Endothelial nitric oxide synthase overexpression attenuates congestive heart failure in mice. *Proc Natl Acad Sci U S A*. 2003;100:4891-6.
100. Jones SP, Greer JJ, Ware PD, Yang J, Walsh K and Lefer DJ. Deficiency of iNOS does not attenuate severe congestive heart failure in mice. *Am J Physiol Heart Circ Physiol*. 2005;288:H365-70.
101. Wang J, Wang Q, Watson LJ, Jones SP and Epstein PN. Cardiac overexpression of 8-oxoguanine DNA glycosylase 1 protects mitochondrial DNA and reduces cardiac fibrosis following transaortic constriction. *Am J Physiol Heart Circ Physiol*. 2011;301:H2073-80.
102. Wang J, Xu J, Wang Q, Brainard RE, Watson LJ, Jones SP and Epstein PN. Reduced Cardiac Fructose 2,6 Bisphosphate Increases Hypertrophy and Decreases Glycolysis following Aortic Constriction. *PLoS One*. 2013;8:e53951.
103. Wang Q, Donthi RV, Wang J, Lange AJ, Watson LJ, Jones SP and Epstein PN. Cardiac phosphatase-deficient 6-phosphofructo-2-kinase/fructose-2,6-bisphosphatase increases glycolysis, hypertrophy, and myocyte resistance to hypoxia. *Am J Physiol Heart Circ Physiol*. 2008;294:H2889-97.
104. Obernosterer G, Martinez J and Alenius M. Locked nucleic acid-based in situ detection of microRNAs in mouse tissue sections. *Nat Protoc*. 2007;2:1508-14.
105. Dassanayaka S, Readnower RD, Salabei JK, Long BW, Aird AL, Zheng YT, Muthusamy S, Facundo HT, Hill BG and Jones SP. High glucose induces mitochondrial dysfunction independently of protein O-GlcNAcylation. *Biochem J*. 2015;467:115-26.
106. Hu Y, Suarez J, Fricovsky E, Wang H, Scott BT, Trauger SA, Han W, Hu Y, Oyeleye MO and Dillmann WH. Increased enzymatic O-GlcNAcylation of mitochondrial proteins impairs mitochondrial function in cardiac myocytes exposed to high glucose. *J Biol Chem*. 2009;284:547-55.
107. Housley MP, Rodgers JT, Udeshi ND, Kelly TJ, Shabanowitz J, Hunt DF, Puigserver P and Hart GW. O-GlcNAc regulates FoxO activation in response to glucose. *J Biol Chem*. 2008;283:16283-92.
108. Ozcan S, Andrali SS and Cantrell JE. Modulation of transcription factor function by O-GlcNAc modification. *Biochim Biophys Acta*. 2010;1799:353-64.

109. Slawson C, Zachara NE, Vosseller K, Cheung WD, Lane MD and Hart GW. Perturbations in O-linked beta-N-acetylglucosamine protein modification cause severe defects in mitotic progression and cytokinesis. *J Biol Chem*. 2005;280:32944-56.
110. Callis TE, Pandya K, Seok HY, Tang RH, Tatsuguchi M, Huang ZP, Chen JF, Deng Z, Gunn B, Shumate J, Willis MS, Selzman CH and Wang DZ. MicroRNA-208a is a regulator of cardiac hypertrophy and conduction in mice. *J Clin Invest*. 2009;119:2772-86.
111. Thum T, Gross C, Fiedler J, Fischer T, Kissler S, Bussen M, Galuppo P, Just S, Rottbauer W, Frantz S, Castoldi M, Soutschek J, Koteliansky V, Rosenwald A, Basson MA, Licht JD, Pena JT, Rouhanifard SH, Muckenthaler MU, Tuschl T, Martin GR, Bauersachs J and Engelhardt S. MicroRNA-21 contributes to myocardial disease by stimulating MAP kinase signalling in fibroblasts. *Nature*. 2008;456:980-4.
112. van Rooij E, Sutherland LB, Qi X, Richardson JA, Hill J and Olson EN. Control of stress-dependent cardiac growth and gene expression by a microRNA. *Science*. 2007;316:575-9.
113. van Rooij E, Sutherland LB, Thatcher JE, DiMaio JM, Naseem RH, Marshall WS, Hill JA and Olson EN. Dysregulation of microRNAs after myocardial infarction reveals a role of miR-29 in cardiac fibrosis. *Proc Natl Acad Sci U S A*. 2008;105:13027-32.
114. Esau C, Davis S, Murray SF, Yu XX, Pandey SK, Pear M, Watts L, Booten SL, Graham M, McKay R, Subramaniam A, Propp S, Lollo BA, Freier S, Bennett CF, Bhanot S and Monia BP. miR-122 regulation of lipid metabolism revealed by in vivo antisense targeting. *Cell Metab*. 2006;3:87-98.
115. Najafi-Shoushtari SH, Kristo F, Li Y, Shioda T, Cohen DE, Gerszten RE and Naar AM. MicroRNA-33 and the SREBP host genes cooperate to control cholesterol homeostasis. *Science*. 2010;328:1566-9.
116. Wang K, Long B, Zhou LY, Liu F, Zhou QY, Liu CY, Fan YY and Li PF. CARL lncRNA inhibits anoxia-induced mitochondrial fission and apoptosis in cardiomyocytes by impairing miR-539-dependent PHB2 downregulation. *Nat Commun*. 2014;5:3596.
117. Lee YN, Brandal S, Noel P, Wentzel E, Mendell JT, McDevitt MA, Kapur R, Carter M, Metcalfe DD and Takemoto CM. KIT signaling regulates MITF expression through miRNAs in normal and malignant mast cell proliferation. *Blood*. 2011;117:3629-40.
118. Rodriguez-Melendez R, Cano S, Mendez ST and Velazquez A. Biotin regulates the genetic expression of holocarboxylase synthetase and mitochondrial carboxylases in rats. *J Nutr*. 2001;131:1909-13.

119. Deng Y, Li B, Liu Y, Iqbal K, Grundke-Iqbal I and Gong CX. Dysregulation of insulin signaling, glucose transporters, O-GlcNAcylation, and phosphorylation of tau and neurofilaments in the brain: Implication for Alzheimer's disease. *Am J Pathol.* 2009;175:2089-98.
120. Jacobsen KT and Iverfeldt K. O-GlcNAcylation increases non-amyloidogenic processing of the amyloid-beta precursor protein (APP). *Biochem Biophys Res Commun.* 2011;404:882-6.
121. Ma Z and Vosseller K. O-GlcNAc in cancer biology. *Amino Acids.* 2013;45:719-33.
122. Mi W, Gu Y, Han C, Liu H, Fan Q, Zhang X, Cong Q and Yu W. O-GlcNAcylation is a novel regulator of lung and colon cancer malignancy. *Biochim Biophys Acta.* 2011;1812:514-9.
123. Kudlow JE. The O-GlcNAcase theory of diabetes: commentary on a candidate gene for diabetes. *Mol Genet Metab.* 2002;77:1-2.
124. Duggirala R, Blangero J, Almasy L, Dyer TD, Williams KL, Leach RJ, O'Connell P and Stern MP. Linkage of type 2 diabetes mellitus and of age at onset to a genetic location on chromosome 10q in Mexican Americans. *Am J Hum Genet.* 1999;64:1127-40.
125. Farook VS, Bogardus C and Prochazka M. Analysis of MGEA5 on 10q24.1-q24.3 encoding the beta-O-linked N-acetylglucosaminidase as a candidate gene for type 2 diabetes mellitus in Pima Indians. *Mol Genet Metab.* 2002;77:189-93.
126. Erickson JR, Pereira L, Wang L, Han G, Ferguson A, Dao K, Copeland RJ, Despa F, Hart GW, Ripplinger CM and Bers DM. Diabetic hyperglycaemia activates CaMKII and arrhythmias by O-linked glycosylation. *Nature.* 2013;502:372-6.
127. Bugger H and Abel ED. Mitochondria in the diabetic heart. *Cardiovasc Res.* 2010;88:229-40.
128. Tan EP, Villar MT, E L, Lu J, Selfridge JE, Artigues A, Swerdlow RH and Slawson C. Altering O-Linked beta-N-Acetylglucosamine Cycling Disrupts Mitochondrial Function. *J Biol Chem.* 2014;289:14719-30.
129. Love DC, Kochan J, Cathey RL, Shin SH and Hanover JA. Mitochondrial and nucleocytoplasmic targeting of O-linked GlcNAc transferase. *J Cell Sci.* 2003;116:647-54.
130. Quinlan CL, Orr AL, Perevoshchikova IV, Treberg JR, Ackrell BA and Brand MD. Mitochondrial complex II can generate reactive oxygen species at

high rates in both the forward and reverse reactions. *J Biol Chem.* 2012;287:27255-64.

131. Ide T, Tsutsui H, Kinugawa S, Suematsu N, Hayashidani S, Ichikawa K, Utsumi H, Machida Y, Egashira K and Takeshita A. Direct evidence for increased hydroxyl radicals originating from superoxide in the failing myocardium. *Circ Res.* 2000;86:152-7.

132. Sawyer DB and Colucci WS. Mitochondrial oxidative stress in heart failure: "oxygen wastage" revisited. *Circ Res.* 2000;86:119-20.

133. Kawaguchi M, Takahashi M, Hata T, Kashima Y, Usui F, Morimoto H, Izawa A, Takahashi Y, Masumoto J, Koyama J, Hongo M, Noda T, Nakayama J, Sagara J, Taniguchi S and Ikeda U. Inflammasome activation of cardiac fibroblasts is essential for myocardial ischemia/reperfusion injury. *Circulation.* 2011;123:594-604.

134. Dewald O, Ren G, Duerr GD, Zoerlein M, Klemm C, Gersch C, Tincey S, Michael LH, Entman ML and Frangogiannis NG. Of mice and dogs: species-specific differences in the inflammatory response following myocardial infarction. *Am J Pathol.* 2004;164:665-77.

135. Dobaczewski M, Gonzalez-Quesada C and Frangogiannis NG. The extracellular matrix as a modulator of the inflammatory and reparative response following myocardial infarction. *J Mol Cell Cardiol.* 2010;48:504-11.

CURRICULUM VITAE

Sujith Dassanayaka, MS

Predoctoral Student

ADDRESS

Institute of Molecular Cardiology; Diabetes and Obesity Center
Department of Medicine – Division of Cardiovascular Medicine
Department of Physiology and Biophysics
University of Louisville School of Medicine
580 South Preston Street – 326
Louisville, KY, 40202

PLACE OF BIRTH

State College, PA, USA

EDUCATION

University of Louisville School of Medicine

Ph.D. in Physiology and Biophysics (Anticipated) 2016

M.S. in Physiology and Biophysics 2010

Transylvania University

B.A. in Biology, and, B.A. in Spanish 2006

PROFESSIONAL SOCIETY MEMBERSHIPS

American Physiological Society 2013 – present

American Society for Pharmacology and
Experimental Therapeutics 2013 – present

HONORS AND AWARDS

- 1st Place, Engineering Collaboration Award, Research! Louisville 2011
- APS KY Meritorious Abstract Award 2014

GRANTS AND FUNDING

- American Heart Association – Predoctoral Fellowship 2014 – 2016
Award # 14PRE19710015
“The Role of OGA in Heart Failure”
Role: Principal Investigator
Sponsor: Steven P. Jones, Ph.D.

ABSTRACTS

1. Roberts AM, Lominadze D, **Dassanayaka S**, Sachleben LR Jr, Juniel CL, Gozal E. Pulmonary microvascular constriction and oxidative stress in the intact-ventilated mouse lung during acute inhibition of nitric oxide synthase. *Experimental Biology* 2010.
2. **Dassanayaka S**, Sobieski MA, Koenig SC, D’Souza SE, Bartoli CR. Novel *in vitro* model to elucidate mechanisms of acquired von Willebrand’s disease with LVAD support. *Biomedical Engineering Society* 2011. – *Selected for Oral Presentation*
3. **Dassanayaka S**, Sobieski MA, Koenig SC, D’Souza SE, Bartoli CR. Potential mechanistic pathways of acquired von Willebrand’s disease in patients with a continuous flow LVAD: *in vitro* findings. *Research! Louisville* 2011. – *Award Winner; 1st Place Best Abstract – Engineering Collaboration Award*
4. **Dassanayaka S**, Readnower RD, Long BW, Aird AL, Salabei JK, Hill BG, Jones SP. Hyperglycemia suppresses cardiomyocyte bioenergetic reserve independent of O-GlcNAcylation. 2014. *FASEB J.* 28:1155.5 – *Selected for Oral Presentation, Award Winner; APS KY Meritorious Abstract Award*
5. **Dassanayaka S**, Brainard RE, Watson LJ, Long BW, Brittan, KR, DeMartino AM, Aird AL, Muthusamy S, Hamid T, Prabhu SD, and Jones

SP. Cardiomyocyte *Ogt* limits ventricular dysfunction following pressure overload without affecting hypertrophy. 2016. Experimental Biology.

6. **Dassanayaka S**, Long BW, Zafir A, Ghafghazi S, Hunt GN, Noble CT, DeMartino AM, Brittian KR, Jones SP, and Wysoczynski M. A streamlined technique to stabilize c-kit expression in cardiac mesenchymal cells. 2016. BCVS.

PEER REVIEWED PUBLICATIONS

1. Bartoli CR, **Dassanayaka S**, Brittian K, Nadar AC, Ismahil MA, Koenig SC, Prabhu SD. Direct measurement of blood flow in microvessels grown in matrigel *in vivo*. J Surg Res. 2012 Jan;172(1):e55-60.
2. **Dassanayaka S**, Slaughter MS, Bartoli CR. Mechanistic pathway(s) of acquired von Willebrand's disease in patients with a continuous-flow left ventricular assist device: *in vitro* findings. ASAIO J. 2013 Mar-Apr;59(2):123-9.
3. Bartoli CR, **Dassanayaka S**, Brittian KR, Lockett A, Sithu S, Siess T, Raess DH, Spence PA, Koenig SC, Dowling RD, D'Souza SE. Insights into the mechanism(s) of von Willebrand factor degradation during mechanical circulatory support. J Thorac Cardiovasc Surg. 2014 May;147(5):1634-43.
4. **Dassanayaka S**, Jones SP. O-GlcNAc and the cardiovascular system. Journal of Pharmacol Ther. 2014 Apr;142(1):62-71.
5. Muthusamy S, DeMartino AM, Watson LJ, Brittian KR, Zafir A, **Dassanayaka S**, Hong KU, Jones SP. MicroRNA-539 is up-regulated in failing heart, and suppresses O-GlcNAcase expression. J Biol Chem. 2014 Oct 24;289(43):29665-76.
6. **Dassanayaka S**, Readnower RD, Salabei JK, Long BW, Aird AL, Zheng YT, Muthusamy S, Facundo HT, Hill BG, Jones SP. High glucose induces mitochondrial dysfunction independently of protein O-GlcNAcylation. Biochem J. 2015 Apr 1;467(1):115-26.
7. **Dassanayaka S** and Jones SP. Recent developments in heart failure. Circ Res. 2015 Sep 11;117(7):e58-63.
8. Muthusamy S, Hong KU, **Dassanayaka S**, Hamid T, and Jones SP. E2F1 transcription factor regulates O-linked N-acetylglucosamine (O-GlcNAc) transferase and O-GlcNAcase expression. J Biol Chem. 2015 Dec 25;290(52):31013-24.

9. Wysoczynski M, **Dassanayaka S**, Long BW, Zafir A, Ghafghazi S, Hunt G, Noble C, DeMartino AM, Brittian KR, Hong KU, and Jones SP. Front Cell Dev Biol. A streamlined technique to stabilize c-kit expression in cardiac mesenchymal stromal cells. Front Cell Dev Biol. 2016. (**Accepted**)
10. **Dassanayaka S**, Brainard RE, Watson LJ, Long BW, Brittian, KR, DeMartino AM, Aird AL, Muthusamy S, Hamid T, Prabhu SD, and Jones SP. Cardiomyocyte *Ogt* limits ventricular dysfunction following pressure overload without affecting hypertrophy. 2016. (**in revision**)